2014

MULTI – MODALITY MOLECULAR IMAGING OF ADOPTIVE IMMUNE CELL THERAPY IN BREAST CANCER

Fatma Youniss
Virginia Commonwealth University

MULTI – MODALITY MOLECULAR IMAGING OF ADOPTIVE IMMUNE CELL THERAPY IN BREAST CANCER

A dissertation submitted in partial fulfillment of the requirements for the degree of Doctor of Philosophy at Virginia Commonwealth University.

by

FATMA MOUSA YOUNISS, Ms

Advisor: Jamal Zweit, PhD, DSc

Professor, Department of Radiology& Director of Center for Molecular Imaging

Virginia Commonwealth University

School of Medicine

Richmond, Virginia

March 28th 2014

DEDICATION

This thesis is dedicated to someone special who influenced my life and made me the way I am today, my parents. They were the reason for this accomplishment, they are my super HEROS. It was their dream for me to get a much better education than they received; I believe, today their dream has come true.

ACKNOWLEDGEMENTS

I am deeply grateful to everyone who has provided support and guidance throughout my dissertation project. Primarily, I am thankful to prof. Jamal Zweit, my advisor, for his guidance. He continually supported me by providing priceless, imminent feedback to help me see the bigger picture and achieve this success. It is a great honor for me to be a student of such a committed and passionate researcher. I would like to thank my mentor for years of support, careful attention and, most importantly, kindness.

I am grateful to the members of my thesis committee, Dr. Harry Bear, Dr. Masoud Manjili, and Dr. Darrell Irvine for their time and dedication. Your guidance from our first meeting to this thesis has been critical to my growth as a researcher. Special thanks to Drs. Harry Bear and Laura Graham who allowed me to use their lab and for their expertise in T-cells culturing and growing.

Special thanks to Dr. Sundaresan Gobalakreshnan, Dr. Purnima Jose for their guidance, assistance, advice and intellectual input throughout the struggling time during this dissertation. Special thanks to Ekaterine Goliadze, Shanaz for their support, advice and help.

Special thanks to Dr. Gajanan K Dewkar and Celina M Thadigiri for their help in the radiosynthesis and analysis of [^{124}I] –FIAU

Special thanks to the all members of the Center for Molecular Imaging (CMI) who all made the lab an enjoyable place to work. The mice were not pleasant conversationalist like you all.

Special thanks to my sister Rabha and my husband Fakhri who understanding me, even when the whole world didn't and for their motivation, enthusiasm, and pushing me to achieve this success.

I would also like to extend my sincerest thanks to my family, especially my dearest mother, Karima and my father Mousa and all of my brothers and sisters for their prayers and encouragement to finish this project.

Also, I would like to thank Phillip Vaughan of VCU Writing Center for editing my thesis. Truly, your eyes are magic in correcting the slightest error. I am also grateful to my country, Libya, for giving me the scholarship.

Lastly and mostly, I'd like to thank God for giving me all that I am grateful for.

Table of Content

Dedication 2
Acknowledgements 3
Table of contents 4
List of Tables 7
List of Figures 8
List of Schemes 14
List of abbreviations 15
Abstract 19
Chapter One Statement of Aims 23
1.1Objectives 23
1.2. Specific aims 23
1.3. Significant and impact 24
1.4. Innovation 24
Chapter Two Breast Cancer 25
2.1 Biology of Breast Cancer 25
2.2. Subtypes of breast cancer 26
2.3. Treatment of breast cancer 28
2.4. Adoptive Immune cell Therapy (AIT) 29
2.5. Adoptive Immune Cell Therapy (AIT) of breast cancer 31
Chapter Three Molecular Imaging of Breast Cancer 34
3.1. Introduction 34
3.2. Labeling approaches 37
3.3. PET imaging 41
3.3.1. Decay and annihilation 41
3.3.2. Coincidence events 42
3.3.3 PET Radionuclides used for imaging in AIT 44
3.4. Optical Imaging 44
3.4.1. Introduction 44
3.4.2 Multi-spectral fluorescence imaging (theory and concepts) 45
3.4.2.1. Florescence (definition, emission and excitation spectrum) 45
3.4.2.2 Autofluorescence (definition and multispectral analysis solution) 46
3.4.2.3. Multi-spectral imaging system (Maestro2) 47
3.5. Labeling and imaging of T lymphocytes (literature review) 48
Chapter Four Materials and Methods 51
4.1. Animals 52
4.2. Cell lines 52
4.3. Isolation, activation and *in vitro* expansion of 4T1 tumor specific T lymphocytes..... 53
4.4. Labeling methods of T- lymphocytes 54
4.4.1 Direct labeling with NIR-fluorescent probe 54
4.4.1.1. Cell proliferation assessment 55
4.4.1.2. Cell Viability assays 55
4.4.1.3 Cell function assessment (Interferon- γ release assay) 56
4.4.1.4. Animal model and T lymphocyte trafficking 57
4.4.1.5. Multi-spectral fluorescence imaging 58
4.4.1.6. Immunohistochemistry analysis 58

4.4.2. Indirect labeling method using PET Reporter Gene (PRG) 59
4.4.2.1. Transient transfection..... 59
4.4.2.1.1. HSV1tk vector isolation..... 59
4.4.2.1.2. Transfection of Jurkat cells using polymer-based transfection reagent 61
4.4.2.1.3. Confirmation of the presence of HSV1-tk gene in the isolated vector 61
4.4.2.1.4. Cell lysate preparation 62
4.4.2.1.5. Protein concentration determination in cell lysate..... 62
4.4.2.1.6. Determination of the HSV1tk expression by western blots 63
4.4.2.2. Stable transduction of Jurkat, HEK 293, 4T1 and T cells using HSV1tk lentiviral Vector..... 65
4.4.2.2.1. Purification of HSV1TK protein..... 66
4.4.2.2.2. HSV1tk Lentivirus construction 67
4.4.2.2.3. Creating stable transduced cell line 69
4.4.2.2.4. Transduction procedure 69
4.4.2.2.5. Selection of stable transduced cells using Blasticidin 69
4.4.2.2.6. Confirmation of the presence of HSV1tk in the stable transduced cells by RT-PCR 70
4.4.2.2.7. Detection of the HSV1tk expression in the stable transduced cell lines western blot 71
4.4.2.2.8. Radiosynthesis of [^{124}I]-FIAU (synthesis, mechanism of trapping by cells and characterizations) 71
4.4.2.2.9. ^{124}I- [FIAU] uptake by Jurkat, 4T1 and HEK cells 75
4.4.2.2.10 T lymphocytes transduction..... 75
4.4.2.2.11. Detection of HSV1tk expression in transduced T lymphocytes 76
4.4.2.2.12. Transduced T lymphocytes proliferation and viability..... 76
4.4.2.2.13. Transduced T lymphocytes phenotyping 77
4.4.2.2.14 Interferon- γ production pre and post transduction..... 77
4.4.2.2.15. ^{124}I- [FIAU] uptake by T lymphocytes 78
4.4.2.2.16. Multi-labeled T lymphocytes trafficking and imaging (Optical & PET) 78
4.4.2.2.17. Biodistribution study..... 79
4.4.2.2.18. Detection of HSV1TK at some organs in vivo 80
4.5. Studying the trafficking pattern of T lymphocytes to 4T1 metastasis 80
4.6. Statistical analysis..... 81
Chapter Five Results 82
5.1. Direct labeling of T lymphocytes using DiR probe..... 82
5.1.1. DiR signal detection and labeling efficiency 82
5.1.2. DiR labels T cells with negligible transfer to tumor cells 83
5.1.3. Cell proliferation pre and post labeling was comparable..... 84
5.1.4. DiR labeled cells showed 80-90 % viability when labeled using 320µg/ml of labeling solution 85
5.1.5. Interferon-γ production in *vitro* and *in vivo* 89
5.1.6. Multi-spectral fluorescent imaging of T cell trafficking 90
5.1.7. Localization of labeled T-lymphocytes at tumor and non-tumor tissues..... 96
5.1.8. T cells specificity and their AIT function with or without DiR labeling in vivo 99
5.1.9. Immunohistochemistry confirms localization of activated T cells at the tumor site..... 101

5.1.10. Confirmation of immunehistochemistry results by flow cytometry 103
5.1.11. Verification of DiR labeled cells localization at tumor site..... 104
5.2. Indirect labeling of T lymphocytes by PRG (HSV1tk) 105
5.2.1. Transient transfection by transfection reagent..... 105
5.2.2. Stable transduction by HSV1tk lentivirus 107
5.2.2.1. Confirmation of the presence of HSV1tk gene in pMOD-HSV1tk plasmid 107
5.2.2.2. Selection of stable transduced Jurkat, HEK 293 and 4T1 cells 109
5.2.2.3. Verfication of HSV1tk gene expression by RT-PCR and westren blot..... 114
5.2.2.4. ^{124}I [FIAU] uptake by transduced Jurkat, HEK 293 and 4T1 cells 115
5.2.2.5. PET imaging of 4T1 tumor 117
5.2.2.6. T-lymphocytes transduction..... 117
5.2.2.6.1. T lymphocytes proliferation and viability before and after transduction 117
5.2.2.6.2. Confirmation of HSV1tk gene expression in transduced T cells 119
5.2.2.6.3. Interferon- γ protein release before and after T cell transduction 122
5.2.2.6.4. Cell phenotype before and after T cells transduction 123
5.2.2.6.5. [^{124}I] FIAU uptake by T lymphocytes 125
5.2.2.6.6 Biodistribution study..... 127
5.2.2.6.7 Detection of HSV1TK at different organs by western blot 129
5.2.2.6.8 4T1 tumor metastasis and T cells trafficking study..... 129
Chapter Six: Discussions 129
Chapter Seven Conclusion and Future Work..... 137
Appendix..... 139
References..... 140
Vita 146

List of Tables

Table 1 demonstrated some characteristics of each modality regarding to their use in cell therapy monitoring and imaging. ……36

Table 2 RGs classifications based on their products and their corresponding probes [46]. ……..40

Table 3 Isotopes and examples of their radiotracers used to track immune cells for PET imaging. …….44

Table 4 Serial dilution of BSA in RIPA lysis buffer…… 62

List of Figures

Figure 1 normal anatomy of the breast. Shows the normal structure of lobes, lobules and ducts. Lymph nodes are shown in the axilla region. Adopted from [2] ……. 26

Figure 2 breast cancer (DCIS-MI) developments. Ductal hyperplasia develops to Atypical ductal hyperplasia then ductal carcinoma in situ. With microinnovation at late stages become ductal carcinoma in situ with microinvasion (DCIS-MI).adopted from [2]……..29

Figure 3 direct and indirect labeling strategies. Direct labeling (1- immune cells harvested from donor animal and ex vivo activated and expanded, 2- cells labeled with radio or optical probe, 3- cell reinfused to same strain host animal bearing same tumor, 4- serial imaging over specific period of time preformed). Indirect labeling (1- immune cells harvested from donor animal and ex vivo activated and expanded, 2- cells transduced with reporter gene (RG) using viral vector carrying RG, waiting few days for gene expression and RG enzyme production, 3- transduced cells reinfused to same strain host animal bearing same tumor, 4- a substrate of the RG enzyme injected and serial imaging over specific period of time preformed) [43]……..38

Figure 4 the indirect labeling method from cell transduction to imaging. Viral vectors are used to transduce cells with specific reporter gene (RG), once the transduction is established and the RG is integrated into cell genome, transcription and translation controlled by specific promoter occur. The product of RG translation is an enzyme which will phosphorlate specific probe to be trapped in the transduced cells [44]……..39

Figure 5 demonstrations of the positron emission and annihilation. 5a An unstable nuclide with an extra proton which decays into neutron, positron and neutrino. 5b positron travels a certain distance depends on its energy then annihilates with an electron and the result 2 gamma rays (511Kev each) emitted in opposite direction about 180^0 away from each other……43

Figure 6 A true coincidence detection occurs when the two gamma rays are detected from one annihilation event in the time window. B if at least one of the gamma photons under goes Compton scattering, and both photons still detected in the time window, scattered coincidence has occurred. C random coincidence occurs when both photons detect in the time window and are from deferent annihilation events……43

Figure 7 Multispectral fluorescence imaging system (Maestro2 at CMI/VCU). Wavelength range = 500-950 nm; FOV = Max 3 mice; Spectral Unmixing and Dynamic Contrast Enhancement (DyCE™) allows quantitation of temporal biodistribution of fluorescent markers at much earlier time points (first few seconds following injection)……47

Figure 8 the pMOD-HSV1tk was cloned to pLenti6/UbC/V5/DEST and the result is pLenti6-UBC-V5-DEST/pDONR221/HSV1tk (HSV1tk-Lentiviral vector)……67

Figure 9, Radio-TLC of [^{124}I]-FIAU before purification (panel A) and Radio-TLC of [^{124}I]-FIAU after purification (panel B)……..72

Figure 10, HPLC profile of [^{124}F]-FIAU (panel A) spiked with standard cold FIAU (panel B)…73

Figure 11, HPLC profile of [^{124}F]-FIAU (A) before Sep-Pak purification, and after Sep-Pak purification (B)……73

Figure12 DiR labeled T cells were imaged at different time points up to day 9 (Panel A). DiR labeled T cells showed detectable signal for more than one week. On days 7 and 9 only few cells were left, that's why only half million of cells were plated. Even on day 9 the DiR signal looks stronger than previous days, because of the fluorescence quenching phenomenon. This means decrease of the fluorescence signal given from too much intense fluorescence material. In our case, as cells divided the DiR is diluted with each division and the DiR become more and more diluted (less intense) leading to prevent fluorescence quenching and increase DiR fluorescent signal. Panel B is flow cytometry data showed that the mean fluorescent intensity (MFI) is increasing with DiR labeled CD3 T cells and the labeling efficiency with DiR is94 %.....……
…..81

Figure 13 DiR labeled T cells incubated with 4T1 tumor cells for 24hrs, showed negligible to no transfer between both cells……..82

Figure 14 T cell proliferation based on viable cell counts on each day compared to the number of cells on day 1 of ex vivo expansion. Showed that, cells proliferation was higher on day 6 that is why this was the chosen time for labeling. Furthermore, no significant differences between labeled and unlabeled cell proliferation post-labeling. (Fold increase in cell number is the number of cells at each day pre or post labeling compared to the cell number on day 1 directly after the activation in I/B)…….83

Figure 15 Percent viability of T cells labeled with various concentrations of DiR measured using Cell TiterGlo assay. Bryostatin/Ionomycin (B/I) activated 4T1-cells grown in IL-2 were labeled on day 6 of their *ex vivo* expansion. Viability of T-cells 1, 4 and 7 days post-labeling was compared with unlabeled cells and expressed as percent viability. * and # means there is a significant differences in the cell viability between day 1 to day 7 and day 4 to day 7 respectively. These differences were more observable with IL2 cells than IL7/15 cells. Cells showed 80 to 90 % viability on days 1 and 4 post-labeling. On day 7 post-labeling which id day-13 post-labeling, cell viability was 60% or below because these are primary cells and their viability decreases beyond day 10 of *ex vivo* expansion. Average ±S.D from three different experiments are shown in the graph……..84

Figure 16 T cells % of viability tested by flow cytometry (apoptosis kit). DiR labeled cells were tested on days 2 and 7 post labeling. All results showed that, the viability of DiR labeled cells is somehow higher than unlabeled cells, indicating that, DiR probe does not affect cell viability…86

Figure 17 The amount of interferon-γ released in the cells supernatant and in the mice serum showed higher amount of this cytokine in both cases, when the 4T1 specific T cells or in the mice injected with 4T1 specific T-cells compared to other groups as shown in panel A, B and C……88

Figure 18**.** Fluorescence imaging of T cell trafficking. Homing of 4T1 sensitized DiR labeled T cells to (Panel A) 4T1 tumor site, (Panel **B)** Meth-A carcinoma tumor site (used as negative control tumor) 4 days after the tumors have been implanted. Red color indicates the signal from the NIR DiR Dye used to label the T cells. (**C)** Tumor/ Background ratios graph showed that, cells localized at the tumor site on day 1 peaked on day 6 and persisted up to 21 days in the animal. While in case of Meth A tumor, there was no localization of 4T1 specific T cells at the tumor site…….89

Figure 19**.** Fluorescence imaging of T cell trafficking **(A)** Adoptive of 4T1 sensitized T cells expanded in IL-2 media, injected one week prior to 4T1 challenge. The labeled 4T1 specific T cells were able to leave the lymphoid compartment and localized at the tumor site in 2 hours. Green color denotes Autofluorescence and the Red color denotes the signal from DiR labeled lymphocytes. **(B)** Tumor/ Background ratios obtained from mice injected with T cells and inoculated with 4T1 cells a week later. The graph showed the signal appeared on day 1 (on the 2 hours image) peaked on day 3 and persisted 21 days in the mice……...90

Figure 20 Tumor/ Background ratios graph of animals bearing 3 days 4T1 tumor and injected with IL7/15 cells. The graph showed that, cells localized at the tumor site on day 1 peaked on day 8 then decreased sharply with time up to 21 days in the animal…….91

Figure 21 Fluorescence imaging of IL2 cell trafficking. Homing of 4T1 sensitized DiR labeled cells to 4T1 tumor site 7 days after the tumors have been implanted (panel A), Panel B fluorescent imaging of animals injected with the IL2 cell lysate supernatant. Red color indicates the signal from the NIR DiR Dye used to label the T cells. (**C)** Tumor/ Background ratios graph showed that, cells localized at the tumor site on day 1(on 2hrs) peaked on day 3 and persisted up to 14 days in the animal. While in case of IL2 lysate, there was no localization of 4T1 specific T cells at the tumor site……...92

Figure 22 Fluorescence imaging of IL7/15 cell trafficking. Homing of 4T1 sensitized DiR labeled cells to 4T1 tumor site 7 days after the tumors have been implanted (panel A), Panel B fluorescent imaging of animals injected with the IL7/15 cell lysate. Red color indicates the signal from the NIR DiR Dye used to label the T cells. (**C)** Tumor/ Background ratios graph showed that, cells localized at the tumor site on day peaked on day 3 and persisted up to 14 days in the animal. While in case of IL7/15 lysate , there was no localization of 4T1 specific T cells at the tumor site. …….93

Figure 23 panels A,B,C and D Fluorescence imaging of tumor, liver, lungs, spleen, and bone marrow *ex vivo.* (E,F**)** Quantification of the signal from labeled T-lymphocytes at the tumor site and other organs on days 3 and 10 post T-cells administration……..95

Figure 24 T cells with and without DiR labeling function in vivo against 4T1 and Meth A tumors. Panel A T cells activity against 4T1 tumor, tumor volume was zero starting from day 6 after AIT (T cells with or without DiR labeling) administrations. Control and CYP groups showed an increase in the tumor volume as time increases. Panel B T cells activity against Meth A tumor, no decrease or regression in the tumor volume with time and no differences compared to other groups (control and CYP), indicating that T cells are antigen specific against 4T1 tumor……97

Figure 25 (A-B) Mouse bearing 4T1 tumor was injected with activated T-cells and the tumor sections were stained for CD69 activated T-cells (red color) marker and F4/80 macrophage (green color) marker. (C-D) Images of 4T1 tumor sections obtained from mouse bearing 4T1 tumor but not injected with activated T cells, stained for CD69 and F4/80 markers. (E) Spleen section stained for CD69 (used as positive control for activated T-cells) and (F) Liver section stained F4/80 (used as positive control of macrophages)……99

Figure 26 assessment of immunohistochemistry result by flow cytometry. Panel A tissues were stained for macrophages (F4/80), panel B tissues were stained for immune cell marker CD45. Both confirm that DiR is linked to T cells and no transfer of DiR to other cells……..101

Figure 27 fluorescent images of liver, heart and 4T1 tumor sections of animal injected with DiR only. From the ex vivo imaging higher signal was detected in the liver and no signal was in the heart, that is why liver was used as positive and heart negative controls. 4T1 tumor section showed no signal of DiR indicating that, the signal detected at the tumor site is correlated to DiR labeled cells……...101

Figure 28 Gel electrophoresis result (panel A) confirmed the presence of HSV1tk gene.1 and 5 DNA ladder, 2= plasmid intact DNA move as coils can't calculate its size, 3= single cut Using NcoI restriction enzyme (linearized plasmid) (first band= 4580bp), 4= double cut using 2 restriction enzymes NcoI, and NheI (first band = 4580bp- (2148bp-561bp) = 2993bp)(Second band = 2148bp-561bp = 1587bp). Panel B showed pROF9-HSV1tk-sh plasmid map……102

Figure 29 western blot result of transfected jurkat cell exhibit HSV1 tk expression in jurkat cells at different time points post transfection……...103

Figure 30 panel A gel electrophoresis result, panel B pMOD-HSV1tk map. According to the standard size of DNA ladder and the pMOD-HSV1tk plasmid map, HSV1tk gene showed the exact size as shown in the map .The size of linearized plasmid DNA is 3280bp, size of DNA fragments from digested DNA with Nco-I and Nhe-I are 1255-116=1139 (single cut), 3280-1139=2141 (double cut)……104

Figure 31 western blot result of pMOD-HSV1tk Ecoli lysate showed HSV1TK enzyme of different masses from total protein of Ecoli lysate……...….104

Figure 32 western blot result of purified HSV1TK enzyme, panel A 2µg of HSV1TK enzyme was tested against different concentrations of primary antibody. To obtain single band without

non specific binding 1:10,000 concentration was selected for the following western blot assays (panel A). Panel B different masses of HSV1TK enzyme were tested against the chosen primary antibody concentration. Panel C showed HSV1TK signal quantization at different masses. Based on these findings 0.5 µg was selected for following western blot assays…….105

Figure 33 Panel A bright field images taken by fluorescent microscope of Jurkat cells at different concentrations of Blasticidin, cells are not able to proliferate and produce colonies in Blasticidin compared to 0 concentration. Panel B the % of viability of jurkat cells at different concentrations of Blasticidin on days 3 and 14 of incubation. At 2µg/ml on day 14 of incubation cells were at 0% of viability…….107

Figure 34 panel A bright field images of HEK 293 cells. The % of viability of HEK 293 cells at different concentrations of Blasticidin on days 7 and 14 of incubation (panel B), even at 8µg/ml of Blasticidin concentration on day 14 of incubation, cells showed about 11% viable cells. Panel C, cells were incubated with 0 and 10 µg/ml of Blasticidin and the viability was tested on days 3,7,10 and 14 post incubation. The 0% of viability for HEK cells was at 10µg/ml on day 14 of incubation……..108

Figure 35 panel A bright field images of 4T1 cells at different concentrations of Blasticidin. Panel B the % of viability of 4T1 cells at different concentrations of Blasticidin on days 1, 7 and 14 of incubation. At 8µg/ml on day 14 of incubation cells were at 0% of viability……...109

Figure 36 Panel A RT-PCR result showed HSV1tk gene in the transduced cells. Lane 1 and 2 used as positive controls. Lane 1 is the pMOD-HSV1tk DNA (bacterial vector), lane 2 is pLenti6-UBC-V5-HSV1tk (viral vector). Acording to the DNA ladder both lanes are between 1.6 and 1 kb and the expected size is 1.2 kb. Lane 3 Jurkat cell cDNA control, Lane 4 Jurkat cell cDNA transduced with HSV1tk lentivirus. Lane 5 HEK cell cDNA control. Lane 6 HEK cell cDNA transduced with HSV1tk lentivirus. Lane 7 4T1 cell cDNA control. Lane 8 4T1 cellcDNA transduced with HSV1tk lentivirus. Panel B the expression ratio of HSV1tk/Beta Actin, JC= Jurkat cells, C= control, TD=transduced. 4T1 cells exhibit the higher ratio compared to jurkat and HEK cells. There is significant differenc between transduced 4T1 and both Jurkat and HEK ($p < 0.05$) but no significant difference between Jurkat and HEK cells……...110

Figure 37 western blot result showed HSV1-TK enzyme expressed in the transduced cells.
1 = the purified HSV1TK protein, 2 = untransduced jurkat cells, 3 = transduced jurkat cells, 4 = untransduced HEK cells, 5 = transduced HEK cells, 6 = untransduced 4T1 cells, and 7 = thransduced 4T1 cells (300µg of total protein of cell lysate was loaded) (panel A).Panel B showed the normalized signal of HSV1TK to beta-actin……...111

Figure 38 [^{124} I] FIAU uptake in transduced Jurkat cells (panel A), HEK cells (panel B) and 4T1 cells (panel C). 4T1 cells showed the maximum uptake among the three cell lines at the different time points…….112

Figure 39 4T1 wild type tumor (A, B) on the left flank of a mouse imaged 1 hour (A) and 24 hours (B) post injection of ^{124}I-FIAU, shows the radiotracer completely clearing from the tumor (2.87 %ID/g to 0 %ID/g). Whereas, the HSV1-tk stably transduced 4T1 tumor (C,D) in the left flank of another mouse shows the tumor activity to retain the radiotracer from 2.54 %ID/g at 1 hour (C) to 1.05 %ID/g after 24 hours (D). Also seen are the stomach (3.83 %ID/g) and the thyroid (21.2 %ID/g)…….113

Figure 40 the % of viability of IL2 or IL7/15 at MOI of 2 and 5 (panel A), cell viability at MOI of 2 decreases to less than 60% on day 3, 6 and become about 20% on day 9 post transduction.While at MOI of 5 at days 3, 6 and 9 decreases to be less that 30%. At MOI of 1, 0.2 and 0.03 the average viability about 80% (panel B)…….....114

Figure 41 fold increase in cell number for transduced (TD) and untransduced (UNTD) IL2 or IL7/15 cells at MOI of 1(transduction was done on day 3 post ex vivo expansion). No significant differences between TD and UNTD cells…….115

Figure 42 the expression ration of HSV1TK to Beta actin in IL2 or IL7/15 cells at different MOIs. At MOI of 1 IL2 cells shwed the higher expresion ratio. While IL7/15 cells shwed almost same ratio for all MOIs……..116

Figure 43 western blot results of transduced IL2 or IL7/15 cells at MOI of 1, 0.2 and 0.03. Based on the linear relationship of the purified HSV1TK (panel C) the HSV1TK mass was calculated as illustrated in panel D. IL2 cells at MOI of 1 showed the highest expression of HSV1TK and this result is consistent with RT-PCR result……117

Figure 44 the expression ratio of HSV1tk to Beta Actin at days 1, 3, 5 and 7 post transduction. IL2 cells showed higher expression than IL7/15 cells. Moreover day 1 and day 3 showed the higher expression for both cells. Based on this result transduced cells were used for the in vivo and ex vivo studies on day 3 post transduction…….118

Figure 45 the production of interferon γ protein from transduced and untransduced cells.
Nil is stated for cells that were incubated alone. Other cells were incubated with 4T1 tumor cells to stimulate cell to release interferon γ in their supernatant. No significant differences ($p<0.05$) were observed before and after transduction for both cell groups……....119

Figure 46 flow cytometry of IL2 and IL7/15 cells phenotype before and after transduction stained for CD8/CD69 or CD8/CD62L. No significant difference between transduced and untransduced cells for both cell groups (the % population of positive staining for CD8/CD69 or CD8/CD62L indicated in blue color)……..121

Figure 47 the % uptake of [^{124}I] FIAU by transduced T cells along with stable transduced jurkat cells. the transduction effecency of Jurkat cells is 100 % while T cells compared with Jurkat cells shwoed less the 40% of cells are transduced……122

Figure 48 transduced cells protein concentration post [^{124}I] FIAU uptake. Jurkat cells (TDJC) showed higher protein concentration than T cells especially at 18 hours. There is significant differences ($p<0.05$) between protein concentration of Jurkat compared to T cells at 18 hours. ……..122

Figure 49 biodistribution study of transduced IL2 and IL7/15 animals on day 3 post ^{124}I [FIAU] injections (panel A). Both groups show similar %ID/tissue in all tissues. Panel B and C both groups were compared to DiR group. There are significant differences between TD groups and DiR groups ($p< 0.05$) in %ID/tissue in all tissues. Values expressed as %ID/gm ± SEM (n=3). ……..124

Figure 50 the western blot result of organs post transduced T cell injections. 1= lymph nodes, 2= 4T1 tumor, 3= lungs, 4= liver, 5= spleen and 6= control tumor (from animals not injected with untransduced T cell). HSV1TK enzyme is clearly showed at these organs beside the tumor which is consistent with the fluorescent data and Biodistribution study result. (Green color is Beta Actin, and red is Viral Thymidin Kinase (VTK))…….125

Figure 51 tumor volume measurements at different time post transduced and untransduced 4T1 tumor implantation. Abdominal mammary fat pad (MFP) did not grow well compared to left and right flank tumors……126

Figure 52 Biodistribution studies at 24 hours post ^{124}I FIAU injections. Panel A Biodistribution study from animals that has MFT tumors in the abdominal region. High % ID/gm was detected at the intestine, liver, stomach and tumor. Panel B Biodistribution study from animals implanted with flank tumors. The right flank tumor (transduced tumor) showed higher %ID/gm than the left flank tumor (wild type tumor). Values expressed in %ID± SEM…….127

Figure 53 western blot result of tissues after 4 weeks of transduced 4T1 tumor implantation in the abdominal mammary fat pad. 1 is the purified HSV1TK protein, 2 is wild type 4T1 tumor, 3 is transduced 4T1 tumor, 4 to 8 are lungs, brain, lymph nodes, liver and spleen…….128

List of Schemes

Scheme 1 The chemical structure of the fluorescent probe (DiR)…….55

Scheme 2 Radiosynthesis of [^{124}I] FIAU …….71

Scheme 3 Mechanism of [^{124}I] FIAU trapping by cell**.** Viral Thymidine kinase enzyme (HSV-1TK) transfers a γ phosphate group from ATP to the 5' hydroxyl group of pyrimidine deoxynucleosides. The lipophilic tracer diffuses into the cell and is phosphorylated by HSV1-TK enzyme activity, and trapped within the cell…….....71

List of abbreviations

AIT	Adoptive immune cell therapy
ACI	Adoptive cellular immunotherapy
ACT	Adoptive cell transfer
IL2	Interleukin 2
IL7	Interleukin 7
IL15	Interleukin 15
IL10	Interleukin 10
HSV1tk	Herpes simplex virus type 1 thymidine kinase
FIAU	2-fluoro-2-deoxy-1 β- D- arabinofuranosyl-5-iodouracil
MOI	Multiplicity of infectious
NIR	Near-infrared
DiR	1,1- dioctadecyltetramethyl indotricarbocyanine iodide
MSFI	Multi-Spectral Fluorescence Imaging
PET	Positron Emission Tomography
SPECT	Single Photon Emission Tomography
MRI	Magnetic resonance Imaging
RG	Reporter Gene
PRG	PET Reporter Gene
%ID/gm	Percentage Injected Dose per gram of tissue

IGF-1 &IGF-2	Insulin and Insulin-like Growth Factors
FGF	Fibroblast Growth Factors
EGF	Epidermal Growth Factor
TGF-α	Transforming Growth Factor Alpha
DCIS-MI	Ductal Carcinoma in Situ with Microinvasion
PR	Progestin Receptors
ER	Estrogen Receptors
HER-2	Human Epidermal Growth Factor Receptor-2
CD8	Cytotoxic T cells
CD4	Helper T cells
F4/80	Macrophages
CD45	general immune cell marker
CD62L	L-Selectin migration marker for effective T cells
CD69	Activated T cells marker
CIK	Cytokine-Induced Killer
γð cells	Gamma-Delta T cells
NK cells	Natural killer T cells
T-reg	Regulatory T cells
TGF-ß	Tumor Growth Factor-beta
Th-1	Type 1 helper T cells
CTL	Cytotoxic T lymphocytes
DLN	Draining Lymph Nodes
TCR	T Cell Receptor

PCR	Protein Kinase C
B/I	Bryostatin 1/ Ionomycin
NFAT	Nuclear Factor of Activated T cells
NF Kβ	Nuclear Factor Kaba-beta
MHC	Major Histocompatibility Complex
DCs	Dendritic Cells
MSOT	Multi Spectral Optoacoustic Tomography
MF	Magnetic Field
RF	Radiofrequency
[^{18}F]-FDG	[^{18}F] fluoro-2-deoxy-d-glucose,
[^{18}F]-FHBG	[4-^{18}F- fluoro-3- (hydroxymethyl) butyl] guanine,
^{18}F-FEAU	2$^{'}$- ^{18}F- fluoro-2$^{'}$-deoxy-1-beta-d-arabinofuranosyl-5-ethyluracil,
^{124}I-FIAU	2$^{'}$-fluoro-2$^{'}$- deoxy- 1-beta-D-arabinofuranosyl-5- ^{124}I- iodouracil,
^{64}Cu-PTSM	^{64}Cu-pyruvaldehyde-bis (N^4- methylthiosemicarbazone),
^{99m}Tc-HMPAO	^{99m}Tc- hexamethylpropyleneamine oxin
SSTrs	Specific Membrane Receptors
NIS	Sodium Iodide Symporter
NET	Norepinephrine Ttransporter
CCD	Charged Coupled Device
RLuc	Renilla Luciferase
FLuc	Firefly Luciferase
LC	Luquid Crystal
IACUC	Institutional Animal Care and Use Committee

DMEM	Modified Eagle Medium
PBS	Phosphate Buffer Saline
CYP	Cychlophosphamide
INF-γ	Interferon-gamma protein
HEK 293	Human Embryonic kidney cells
TD	Transduced cells
UNTD	Untransduced cells
RT-PCR	Real Time Polymerase Chain Reaction
ELISA	Enzyme-linked Immunosorbent Assay
MDSCs	Splenocyte Myeloid-Derived Suppressor Cells

Abstract

Cancer treatment by adoptive immune cell therapy (AIT) is a form of immunotherapy that relies on the *in vitro* activation and/or expansion of immune cells. In this approach, immune cells, particularly CD8+ T lymphocytes, can potentially be harvested from a tumor-bearing patient, then activated and/or expanded *in vitro* in the presence of cytokines and other growth factors, and then transferred back into the same patient to induce tumor regression. AIT allows the *in vitro* generation and activation of T-lymphocytes away from the immunosuppressive tumor microenvironment, thereby providing optimum conditions for potent anti-tumor activity.

The overall objective of this study is to: a) develop multi-modality (optical- and radionuclide-based) molecular imaging approaches to study the overall kinetics of labeled adoptively transferred T- lymphocytes *in vivo*, b) to non-invasively image and assess *in-vivo*, targeting and retention of adoptively transferred labeled T-lymphocytes at the tumor site.

T-lymphocytes obtained from draining lymph nodes of 4T1 (murine breast cancer cell) sensitized BALB/C mice were activated *in vitro* with Bryostatin/ Ionomycin for 18 hours, and were grown in either Interleukin-2 (IL-2) or combination of Interleukin-7 and Interleukin-15 (IL-7/IL-15) for 13 days, (cells grown in IL-2 called IL2 cells, and cells grown in IL7/15 called IL7/15 cells). In order to validate the methodology and to offer future clinical translation, both direct and indirect cell labeling methods were expanded and employed. The first method was based on direct *in vitro* cell labeling by lipophilic near-infrared (NIR) fluorescent probe, 1,1-dioctadecyltetramethyl indotricarbocyanine iodide, (DiR), followed by intravenous (i.v.) injection into BALB/C mice for multi-spectral fluorescence imaging (MSFI). The second method was based on indirect labeling of T- lymphocytes through transduction of a reporter gene (cell cytoplasm labeling Herpes Simplex Virus type 1- thymidine kinase (HSV-1 tk). The product of

this reporter gene is an enzyme (HSV-1TK) which phosphorylates a radio labeled substrate 2-fluoro-2-deoxy-1 β- D- arabinofuranosyl-5-iodouracil ([^{124}I]-FIAU) for Positron Emission tomography (PET) imaging.

ATP based cell viability assay, flow cytometry and interferon-γ (IFN-γ) ELISA were used to investigate if there are any changes in cell viability, proliferation and function respectively, before and after direct and indirect labeling. The results showed that cell viability, proliferation, and function of labeled 4T1 specific T-lymphocytes were not affected by labeling for direct labeling methods at DiR concentration of 320μg/ml. For the indirect labeling method, the viability and proliferation results showed that cell viability decreases as multiplicity of infectious (MOI) increases. In particular, at MOI of 10 almost all cells die 3 days post transduction. At MOI of 5, cells viability was ≤ 30% and at MOI of 2 was ≤ 60%. Cell viability was 80% at MOI of 1.

The results of optical imaging were as follows: when the recipient mice with established 4T1 tumors were injected with DiR labeled 4T1 specific T-lymphocytes, the 4T1 specific T-lymphocytes (IL2 cells) infused into tumor-bearing mice showed high tumor retention, which peaked 3 or 6 days post infusion depending on the tumor size and persisted at the tumor site for 3 weeks. In contrast, IL7/15 cells showed lower signal at the tumor site and this peaked on day 8. On the other case when 4T1 tumor cells were implanted 1-week post-infusion of labeled T-lymphocytes. IL2 T-lymphocytes moved out of lymphoid compartments to the site of subsequent 4T1 inoculation within two hours and peaked on day 3 and the signal persisted for 2 more weeks. In contrast with infusion of IL7/15 cells, the signal was barely detected and did not show a similar trafficking pattern as with IL2 cells.

The results of the indirect labeling method, PET reporter gene (PRG) system (HSV-1tk / [^{124}I] FIAU) showed that both IL2 and IL7/15 cells were successfully transduced as verified *ex*

vivo by real time PCR and western blot. T Cells transduction efficiency was assessed from cell uptake study in comparison to stable transduced Jurkat cells which have transduction efficiency of 100 %. Both IL2 and IL7/15 cells showed lower transduction efficiency (≤ 30%) compared to Jurkat cells. Consequently, PET imaging did not show a detectable signal of transduced T cells *in vivo*. Biodistribution study was carried out on day 3 post [^{124}I]-FIAU injections. Results were consistent with the optical imaging results, except for IL7/15 cells. Transduced and untransduced IL2 and IL7/15 cells were labeled with DiR and injected (i.v.) into Balb / C mice and then imaged by both imaging modalities (MSFI and PET) at the same time. MSFI images of transduced IL2 cell showed detectable signal starting from 2 hours, peaked at 72 hours and persisted up to 2 weeks, while IL7/15 cells were detectable at the tumor site starting at 24 hours, peaked at 72 hours and persisted up to 2 weeks. By the end of this study animals were dissected and tissue activities were counted using gamma counting and expressed as % Injected dose/gram of tissue (%ID/gm). Transduced IL2 and IL7/15 cells showed higher %ID/gm than other organs at lungs, liver, spleen, tumor, lymph nodes and bone/bone marrow. IL7/15 cells compared to IL2 cells showed higher %ID/gm at same organs. Neither IL2 nor IL7/15 untransduced DiR labeled cells showed any activity at tumor site, and their activities at other organs was very low compared to transduced cells.

To investigate whether labeled T-lymphocytes will localize at tumor metastases or not, and to study the difference in their migration patterns to the tumor site versus tumor metastases, 4T1 tumor cells were successfully transduced with HSV-1tk as confirmed by RT-PCR , western blot and cell uptake study. Transduced 4T1 cells were implanted in the right flank or in the mammary fat pad of the mouse. Serial PET imaging was carried out in the third and fourth week

post tumor implantation to know when the tumor will metastasizes. PET imaging showed only signal at the tumor site and no metastasis were detected.

Chapter One: Statement of Aims

1.1Objectives

The overall objective of this project is to develop multi-modality in vivo imaging to study the kinetics of labeled immune cells particularly T-lymphocytes sensitized specifically to inhibit 4T1 breast carcinoma tumor growth using Optical and PET imaging. This project intends to address the following questions:

- What are the differences between T-lymphocytes grown in IL-2 versus IL7/15 in their migration patterns? (Where do they localize, when do they localize at tumor site, how long they persist, and do they retain their proliferation and functional abilities?)

- What are the differences between direct and indirect labeling methods in terms of their specificity and sensitivity?

- Do T-lymphocytes localize at the tumor metastases? What are the differences in T-cell homing between primary tumor and metastases?

1.2. Specific aims

1) To compare direct and indirect T-cell labeling methods, in terms of their specificity and sensitivity.

2) Using quantitative multi-modality (optical and PET) imaging the proliferation, trafficking and persistence of immune cells at various time points in vivo will be studied.

3) To compare the trafficking and homing of T-cells grown in IL-2 versus cells grown in the combination of IL-7 and IL-15.

4) To investigate the differences in trafficking and homing capabilities of labeled T-lymphocytes at primary tumor versus tumor metastases.

1.3. Significant and impact

Information from this project could provide direct in vivo data on delivery, localization, retention, and function of labeled immune cells within the context of adoptive immune cell therapy. This information is vital to understand the *in vivo* trafficking behavior to guide translation of immune cell therapy in the clinical setting.

1.4. Innovation

This work is novel in two important aspects:

1) Employing two different imaging modalities to study the trafficking and homing of T-lymphocytes grown in different cytokines (IL-2 versus the combination of IL7and IL-15).

2) Applying two different imaging modalities to image labeled T-lymphocytes and labeled 4T1 tumor in the same animal at the same time to know the difference in their migration pattern between primary tumor and metastases.

Chapter Two: Breast Cancer

2.1 Biology of Breast Cancer

Breast cancer is the most common form of cancer in women, affecting one in every eight women in the United States [1]. Normal breast has six to nine overlapping sections, called lobes. Within each lobe there are many smaller lobules, which end in dozens of tiny bulbs that can produce milk. The lobes, lobules and bulbs are all linked by thin tubes called ducts. These ducts lead to the nipple in the center of a dark area of skin called the areola (figure 1). Fat fills the spaces around the lobules and ducts. There are no muscles in the breast, but muscles lie under each breast and cover the ribs. Each breast also contains blood and lymph vessels. The lymph vessels lead to small bean-shaped structures called lymph nodes. Clusters of lymph nodes are found in the axilla (under the arm), above the collarbone and in the chest [2].

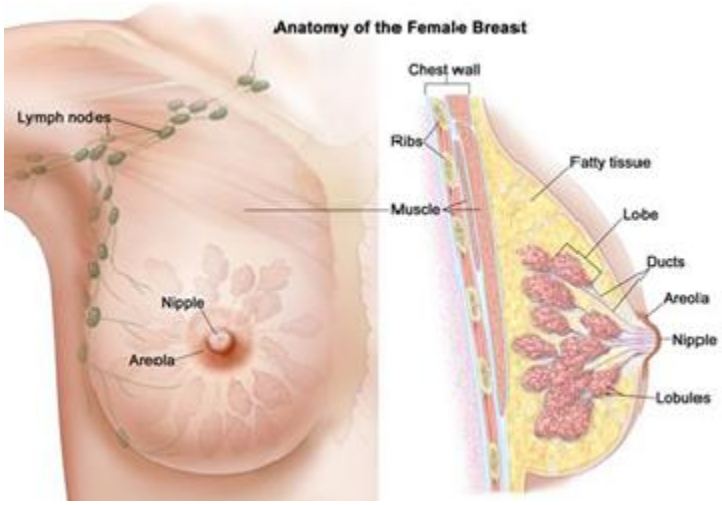

Figure 1 normal anatomy of the breast. Shows the normal structure of lobes, lobules and ducts. Lymph nodes are shown in the axilla region. Adopted from [2]

Normal breast growth and development are regulated by the complex interaction of many hormones and growth factors include estrogens, progesterone, androgens, glucocorticoids, prolactin, thyroid hormone, insulin and insulin-like growth factors (IGF-1 and IGF-2), fibroblast

growth factors (FGF), and epidermal growth factor (EGF)/transforming growth factor alpha (TGF-α) [3]. The interaction of growth factors, cytokines, and hormones with specific membrane receptors triggers a cascade of intracellular biochemical signals, resulting in the activation and repression of various subsets of genes. Several of these hormones have been shown to play an active role in the development of breast cancer. For example, estrogen stimulates breast cell division, which can increase the risk of breast cancer. Furthermore, breast cells are not fully mature in girls and young women who have not had their first full-term pregnancy [2]. Breast cells which are not fully mature bind carcinogens more strongly and they are not as efficient at repair DNA damage as mature breast cells. Breast cancer, like any other cancer, takes years to develop, and it can take place at any part of the breast anatomy. In terms of histology, breast cancers are heterogeneous, they are mainly ductal, but also lobular, mixed ductal and lobular, cribriform, mucinous and tubular carcinomas [4]. Figure 2 illustrates the stages of breast cancer development at the ductal part. For some reason mostly DNA mutations in any of breast genes, normal cells divide rapidly and causes ductal hyperplasia, which with time develop to atypical ductal hyperplasia then ductal carcinoma in situ (DCIS) and in then becomes DCIS with microinvasion (DCIS-MI).

2.2. Subtypes of breast cancer

Based on the hormones and growth factor regulations, breast cancer has several subtypes, the most commons are:

Basal (Triple Negative) Breast Cancer

The basal subtype is also called “triple negative” cancer, because the cells are negative for three common markers: estrogen receptors (ER), progestin receptors (PR), and human epidermal

growth factor receptor-2 (HER-2). Although the basal subtype is only found in about 15% of breast cancers, it has been shown to be aggressive, unresponsive to treatment and, ultimately, indicative of a poor prognosis [5]. Basal-type breast cancer is diagnosed more often in African American women than in Caucasian women in the United States [6]. Compared to other subtypes, it is poorly defined by mammography and best detected by MRI. It is also often detected as grade III, tumors, resulting in more aggressive and poor overall prognosis [7].

HER-2 Over-expression Breast Cancer

As the name suggests, HER-2 over-expressing tumors have extra copies of the HER-2 gene and over-produce the resulting growth-enhancing protein. This protein is overexpressed in about 20% of breast cancers [8]. Biologically, the up-regulation of HER2 gene is associated with increased proliferation, angiogenesis, and invasiveness [9].

These tumors tend to grow quickly but are responsive to targeted drug treatment with compounds like, Trastuzumab and more recently other drugs such Lapatinib and Pertuzumab which have shown specific activity against HER2 positive breast cancer and an increase in the median survival up to 2 years [10].

Luminal A and B Breast Cancers

Luminal A and B subtypes are both estrogen-receptor-positive (ER+) and low-grade, with luminal A tumors growing very slowly and luminal B tumors growing more quickly. Luminal A tumors have the best prognosis. Several studies have been conducted using microarray technology, to study breast cancer subtypes showed that, for different gene expression profiles, prognosis and treatment response vary for different subtypes [11]. Luminal B compared to luminal A shows lower expression levels of ER or estrogen-regulated genes, lower or no progesterone receptor (PR) expression, higher tumor grade, higher expression of proliferation-related genes and

activation of growth factor receptor signaling pathways. Also luminal B tumors have lower sensitivity to endocrine treatment and higher sensitivity to chemotherapy than luminal A tumors [12].

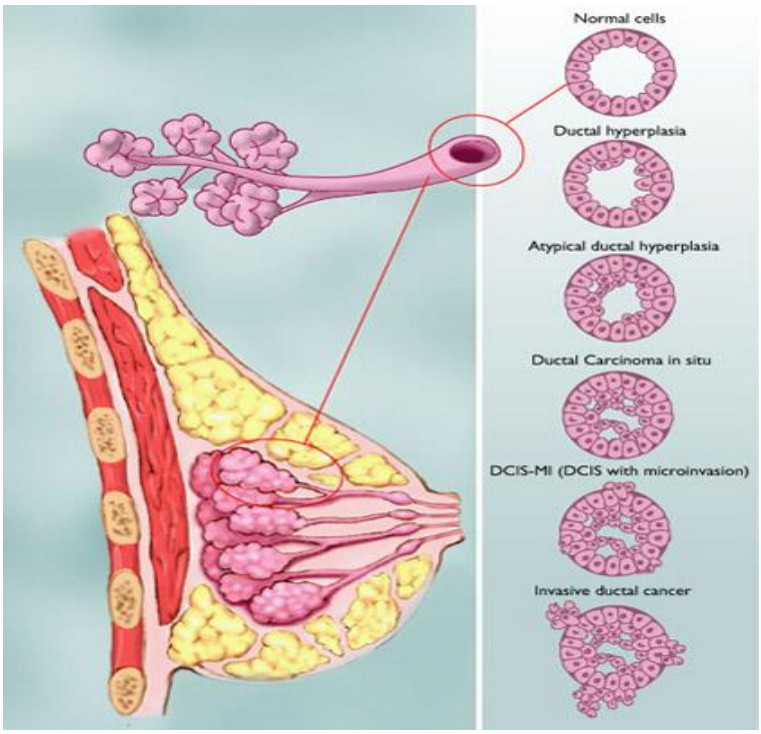

Figure 2 breast cancer (DCIS-MI) developments. Ductal hyperplasia develops to Atypical ductal hyperplasia then ductal carcinoma in situ. With microinnovation at late stages become ductal carcinoma in situ with microinvasion (DCIS-MI).adopted from [2]

2.3. Treatment of breast cancer

Treatment options of breast cancer include; surgery, chemotherapy, radiotherapy, hormone therapy and immunotherapy. The choice of treatment is based on the tumor subtype and stage of the disease. Several studies showed that, combination of treatment options (adjuvant therapy) is more effective than single agent therapy. Radical mastectomy (local surgery) followed by radiotherapy produce local control. Chemotherapy is preferred in cases of receptor-negative tumors, acquired resistance to hormonal therapy and aggressive visceral metastatic diseases. Primary chemotherapy is increasingly used in the treatment of locally advanced tumors with

increased rates of breast-conservative surgery. In case of hormone receptor positively and absent of visceral, life-threading disease, endocrine manipulation is the treatment of choice [13]. Endocrine manipulation usually done, using Tamoxifen or ovarian ablation or both (both are more effective), for postmenopausal patients [13]. Immunotherapy of breast cancer as an adjuvant therapy, based on active immunizations or passive therapy has in some instances been shown to prevent tumor recurrence and improve patient survival [14]. The rationale behind immunotherapy for breast cancer can be highlighted in two points: i) Breast screening provides an opportunity to employ immunotherapy in early stage of tumor development, when the immunosuppressive effects of the tumor are relatively low, ii) Breast cancer expresses specific tumor antigens which can be utilized to ex vivo engineer T-lymphocytes to yield tumor specificity [15].

2.4. Adoptive Immune cell Therapy (AIT)

The first observations that the immune system has antitumor effects against sarcoma tumors were noticed in 1890s by William Coley [16]. After years later, researchers noticed that, the major mediators inducing this effect are T cells [17] and based on this rationale the concept of Adoptive cellular immunotherapy (ACI) or Adoptive cell transfer (ACT) or Adoptive immune cell therapy (AIT) was introduced [18]. The immune response to genetic changes in transformed tumor cells appears from the accumulation of antigen-specific T cells within the tumor and draining lymph nodes [19]. T-cells function as part of the adaptive immune system, to attack and kill tumor cells; unfortunately tumors keep growing because the anti-tumor immune response is either not sufficiently strong to eliminate tumor cells or the anti-tumor immunity is suppressed by regulatory cells or other factors secreted by the tumor. In the past, the immune system has been thought to play a role in the recognition and elimination of nascent malignancies through so called

immunosurveillance [20]. However, because of a lack of concrete evidence, the hypothesis of immunosurveillance had been abandoned and recently a new concept called immunoediting which is comprised of three phases; elimination, equilibrium and escape phase, has been demonstrated:

1. Elimination phase: during the elimination phase, T cells (CD4, CD8, NK and γð cells) appear to recognize transformed cells early in the development of tumors; the mechanism of this recognition is not fully understood but sufficient to kill some tumors.
2. Equilibrium phase: in the equilibrium phase, tumors that are not completely eliminated undergo a selection process termed immunoediting whereby tumor cells " hide" their antigens by weak expression or endocytosis, thereby allowing tumor cells to escape immune response, survive and accumulate mutations.
3. Escape phase: in the escape phase, when tumors are fully developed and can be detected, they can promote immune suppression through recruitment of suppressive cells such as regulatoray T cells (T-reg) and production of suppressive cytokines as IL-10 and TGFß [21- 23].

AIT could overcome the limitations described above, because it relies on enhancing the patient's immune system *ex vivo* isolated from the suppressive environment of tumor cells. It is based on isolation, expansion, and re-infusion of large numbers of tumor specific patient's own immune cells, particularly cytotoxic T lymphocytes, to induce tumor regression. Potentially, AIT could be an effective treatment strategy, because it facilitates direct interaction between immune cells and tumor cells without adverse effects on normal cells.

In order to understand the dynamics and the process of AIT and to monitor the migration, localization and retention of labeled immune cells, in vivo studies, in live subjects and within the intact physiological environment, are needed.

2.5. Adoptive Immune Cell Therapy (AIT) of breast cancer

Breast cancer is a systemic disease with primary local tumor and disseminated metastatic disease. The aim of Surgery, chemotherapy and radiotherapy is to induce primary tumor regression over the specific treatment regimen. Clinically in breast cancer, micrometastatic tumor can be eliminated using hormone therapy, chemotherapy and AIT [24]. In wide variety of breast cancer, the tumor-infiltrating T lymphocytes, particularly type-1 helper T cells (Th1) and cytotoxic T lymphocytes cells (CTL) are correlated with the absence of metastatic invasion and increased overall survival rates [25]

Several studies in AIT of breast cancer highlighted that, the success of AIT is based on the *ex vivo* activation of T cells. It occurs through two stages: an *ex vivo* stage involves incubating T-lymphocytes with appropriate antigens or non-specific activators (either antibodies or chemicals) and growth factors that mimic the *in vivo* activation environment. One such environment has been achieved by pulsing T-lymphocytes in Bryostatin 1 and Ionomycin, which mimic TCR signaling to trigger the T-cell activation pathway. Bryostatin 1 activates Protein kinase C (PKC) and Ionomycin increases intracellular calcium, and together they lead to activation of transcription factors: nuclear factor Kβ (NF Kβ) and nuclear factor of activated T cells (NFAT) respectively. These transcription factors move to the nucleus and initiate the transcription of IL-2 and other genes which are essential for T-cell proliferation [26-28]. The *in vivo* stage through the interaction

between MHC–peptide (Major Histocompatibility Complex) expressed on antigen- presenting cells e.g. dendritic cells (DCs) to initiate T-cell activation [28].

The success of AIT relies on manipulation of tumor specific T-lymphocytes to produce large numbers of these cells as well as optimization of effector functions. AIT allows the generation and activation of T-lymphocytes away from the suppressive tumor environment providing the optimal environment for anti-tumor responses [29]. One example of AIT success in the treatment of advanced metastasized breast cancer patients was shown by Christoph Domschke and his colleagues [30]. They demonstrated that, adoptively transferred T-cell clones (tumor antigen-reactive type-1 T cells) persist *in vivo* and preferentially localize to tumor sites and mediate an antigen-specific immune response characterized by metastases regression and significantly longer overall survival in 7 of 16 patients. Another study showed that the re-infusion of T lymphocytes, engineered to express Tumor- specific TCR, induce regression in 13% of patients [31]. The question is; why some patients respond to the therapy and some do not? Tracking the movement, proliferation and viability of re-infused tumor specific T-lymphocytes by multi-modality imaging in serial images at different time points during the treatment could define the parameters that lead to successful AIT. Therefore, In order to understand the dynamics and the process of AIT, noninvasive and repetitive multimodality imaging of labeled immune cells provides the opportunity to study in vivo trafficking, homing, tumor targeting, activation, proliferation and persistence of transferred labeled cells [32].

This thesis aims to contribute new knowledge in this context, by direct in vivo imaging of pathways associated with the process of AIT.

Chapter Three: Molecular Imaging of AIT

3.1. Introduction

Molecular imaging is the visualization, characterization, and measurement of biological processes at the molecular and cellular levels in humans and other living systems [33]. The main advantage of *in vivo* molecular imaging is its ability to characterize diseased tissues without invasive biopsies or surgical procedures and with this information in hand; more personalized treatment planning can be applied [34]. Different imaging modalities are used for molecular imaging, including optical (fluorescence and bioluminescence), positron emission tomography (PET), single photon emission computed tomography (SPECT), magnetic resonance imaging (MRI) [35] and more recently the development of Multi Spectral Optoacoustic Tomography (MSOT) imaging [36]. Optical imaging utilizes light photons at different wavelengths at visible and infrared ranges resulting from fluorescent and biolumencent events. The application of optical imaging is limited in humans because the wavelength of the probes emitted in the biolumencent or fluorescent processes are too weak to penetrate deep and thick layers of tissues that are blood-rich tissues. In optical imaging, low noise images require acquisition times of about 5-10 minutes, which may increase the thermal noise, but this can be reduced with thermo-electric cooler. However, this technique is widely used in molecular imaging due to its simplicity and cost effectiveness [37]. Radionuclide-based imaging methods (PET and SPECT) are based on gamma (γ)-positron and single photon emitting radionuclides used to radiolabel probes specific for the process under study. Clinical PET has spatial resolution of about 5mm, while animal micro-PET resolution is about 1.5 mm [38]. PET compared to SPECT has higher sensitivity and both are independent of tissue depth.

MRI is widely used for soft tissue imaging. The physics of MRI is based on the alignment of the protons to magnetic field (MF) when they are placed in strong MF and form longitudinal

magnetization. Radio frequency (RF) pulses are used to alter the protons alignment and tilts the longitudinal magnetization to be transversal magnetization , when the RF is turned off, the protons realign with magnetic field again and generate an electromagnetic flux that provide information about tissues under study. Due to this, the image acquisition time is long but high spatial resolution and good image contrast is achievable [39].

Table-1 summarizes the advantages and limitations for each imaging modality and their application in cell-based imaging and trafficking. The role of molecular imaging in AIT is to optimize and maximize the chance of AIT success for each individual patient as the cells are the patient's own cells [40]. A number of variables need to be optimized for each individual patient to obtain the desired outcome of AIT. As an example of these variables, is the number of cells to effectively treat a certain tumor. Measuring tumor size and injecting different numbers of cells will provide information about the effective number that has to be injected for each individual patient.

Table: 1 demonstrated some characteristics of each modality regarding to their use in cell therapy monitoring and imaging.

Modality	Imaging probe Used to track cells	Advantages	Limitations	Application in AIT
PET	^{18}F-FDG, ^{18}F- FHBG ^{18}F-FEAU, ^{124}I-FIAU ^{64}Cu-PTSM ^{89}Zr- Oxine	Unlimited depth penetration, Whole-body imaging, quantitative data, anatomical and physiological information when combined with CT	Radiation exposure Expensive, long acquisition time (minutes to hours), low spatial resolution when used alone	Has been used to label directly or indirectly T cells, DC and other immune cells for monitoring cell localization trafficking And persistence *in vivo* in animals and human.
SPECT	^{111}In-Oxine, ^{99m}Tc-HMPAO, $^{123/125/131}$I- FIAU	Unlimited depth penetration, Whole-body imaging, quantitative data, anatomical and physiological information when combined with CT	Quantitative, unlimited depth penetration, Low spatial resolution and ionizing radiation.	
MRI	Iron oxide nanoparticles (SPIO), Gadolinium-chelates	High spatial resolution, Unlimited depth penetration, no ionizing radiation, Whole-body imaging, Excellent soft-tissue contrast	Expensive, Limited sensitivity (require large amount of the probe which might be toxic to the subject under study) and long acquisition time	
Optical Imaging	Organic dyes, fluorescent proteins, quantum dots and luciferase in bioluminescence imaging	Fast, simple ,inexpensive, quantitative, high sensitivity, and no ionizing radiation	Limited depth penetration ($\leq$ 1cm)	

[^{18}F]-FDG =[^{18}F] fluoro-2-deoxy-d-glucose, [^{18}F]-FHBG= [4-^{18}F- fluoro-3- (hydroxymethyl) butyl] guanine, ^{18}F-FEAU= 2$^{'}$- ^{18}F- fluoro-2$^{'}$-deoxy-1-beta-d-arabinofuranosyl-5-ethyluracil, ^{124}I-FIAU = 2$^{'}$-fluoro-2$^{'}$- deoxy- 1-beta-D-arabinofuranosyl-5- ^{124}I- iodouracil, ^{64}Cu-PTSM= ^{64}Cu-pyruvaldehyde-bis (N^4- methylthiosemicarbazone), ^{99m}Tc-HMPAO= ^{99m}Tc-hexamethylpropyleneamine oxin

3.2. Labeling approaches

Molecular imaging of immune cells requires labeling of these cells directly or indirectly. Direct labeling is based on the incubation of activated and *in vitro* expanded immune cells in the labeling probe for a few minutes (10-30 minutes) followed by washing then reinfusion into a subject under examination, followed by serial images at different time points. This method depends on the ability of a cell to retain the label. The advantages of direct labeling approach are relatively easy, low expenses, and well established methods. However, this method does not allow Long term monitoring of labeled cells because the label is lost or diluted as a result of apoptosis or mitosis respectively [41,42].

Indirect labeling is achieved through transduction of immune cells with a reporter gene, for example; Herpes Simplex Virus type 1-thymidine kinase (HSV-1 tk, cell cytoplasm labeling). The product of this reporter gene is an enzyme that phosphorylates a radio-labeled substrate 2-fluoro-2-deoxy-1 β- D- arabinofuranosyl-5- ^{124}I iodouracil [^{124}I]-FIAU for PET imaging. Figure 3 demonstrates the strategies of direct and indirect labeling approaches. Figure 4 showed schematic representation of the indirect labeling mechanism and trapping of the labeled probe by the cell.

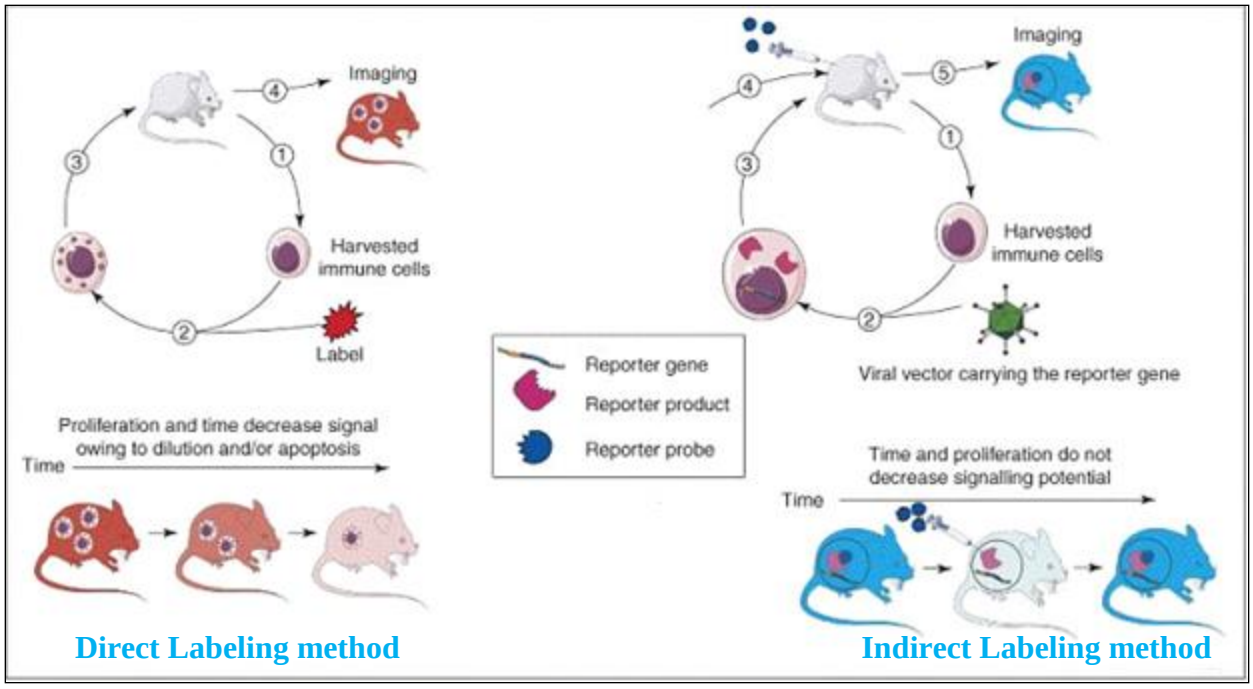

Figure 3 direct and indirect labeling strategies. Direct labeling (1- immune cells harvested from donor animal and ex vivo activated and expanded, 2- cells labeled with radio or optical probe, 3- cell reinfused to same strain host animal bearing same tumor, 4- serial imaging over specific period of time preformed). Indirect labeling (1- immune cells harvested from donor animal and ex vivo activated and expanded, 2- cells transduced with reporter gene (RG) using viral vector carrying RG, waiting few days for gene expression and RG enzyme production, 3- transduced cells reinfused to same strain host animal bearing same tumor, 4- a substrate of the RG enzyme injected and serial imaging over specific period of time preformed) [43].

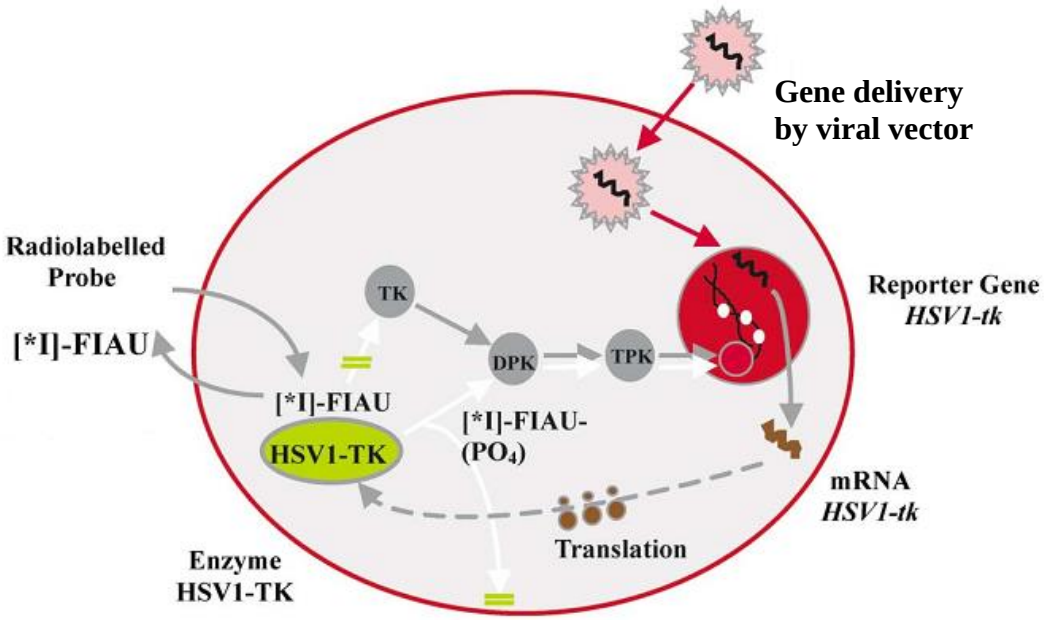

Figure 4 the indirect labeling method from cell transduction to imaging. Viral vectors are used to transduce cells with specific reporter gene (RG), once the transduction is established and the RG is integrated into cell genome, transcription and translation controlled by specific promoter occur. The product of RG translation is an enzyme which will phosphorylate specific probe to be trapped in the transduced cells [44].

Indirect labeling method allows for reliable, stable and harmless visualization of cellular trafficking, persistence, proliferation and function at target site. Furthermore, it permits long-term cell monitoring (months) if the RG is integrated into target cell genome [45]. However, this approach is limited by targeting or delivery of the RG to cell under transduction, integration, activation, amount or level of RG (transduction efficiency), RG expression and persistence over time and immune response problems.

A number of RGs have been developed for radio and non radiotracer (Bioluminescence) imaging, (listed in table 2). Three categories are identified based on the RG product: transporter, enzyme and receptor. The transporter group includes the sodium iodide symporter (NIS) and the norepinephrine transporter (NET). The enzyme classification includes herpes simplex virus 1 thymidine kinase (HSV1-tk) gene and the HSV1-tk mutant (HSV1-sr39tk). The receptor group

includes Specific membrane receptors (SSTrs), which mediate the various actions of somatostatin, which is a peptide that inhibits the release of growth hormone. RG applications initially were in gene therapy and adoptive cell-based therapies. Recently, noninvasive *in vivo* reporter gene imaging is likely to include: (a) quantitative monitoring of gene therapy vectors for targeting and transduction efficacy in clinical protocols by imaging the location, extent and duration of transgene expression; (b) monitoring of cell trafficking, targeting, replication and activation in adoptive T-cell and stem/progenitor cell therapies; and (c) assessments of endogenous molecular events using different inducible reporter gene imaging systems [46].

Table 2 RGs classifications based on their products and their corresponding probes [46].

Class	RG	RG probe (RGP)	Imaging modality
Receptor	SSTr2	[^{111}In] DTPA-Octerotide [^{99m}Tc] P829 [^{99m}Tc] P2045	SPECT
Transporter	NIS NET	[^{99m}Tc] Demotate1 [^{124}I] Iodine [^{99m}Tc] Pertechnetate [^{131}I] Iodine [^{123}I] MIBG	SPECT PET SPECT

Enzyme	HSV1tk HSV1-sr39tk Firefly luciferase Renilla Luciferase	[^{123,124,125,131}I]-FIAU [^{18}F]-FIAU [^{123,124,125,131}I]-IVDU [^{123,124,125,131}I]-VFAU [^{123,124,125,131}I]-IVFRU [^{18}F]-FEAU [^{18}F]-FHBG [^{18}F]-FHPG [^{18}F]-FIRU [^{18}F]-FUdR luciferin coelenterazine	PET and SPECT PET PET and SPECT PET and SPECT PET PET PET PET Bioluminescence Bioluminescence

3.3. PET imaging

3.3.1. Decay and annihilation

PET imaging was developed several decades ago. Currently, it is playing an important role in the diagnosis, staging and therapy monitoring of different types of cancer [47]. PET probes or tracers are radiopharmaceutical compounds labeled with a positron-emitting radionuclide. The most widely used PET tracer is the fluorinated analogue of glucose fluorodeoxyglucose (FDG) labeled with ^{18}F due to the increased utilization of glucose by brain and heart normal cells and also malignant cells. Positron emitting radionuclides are neutron- deficient isotopes which reach stability through nuclear transformation of proton to neutron (figure 5a) with emission of positron (positive electron e^{+}) and neutrino. The maximum energy of emitted positron depends on the isotope, it ranges from 0.6 MeV of ^{18}F to 3.4 MeV of ^{82}Rb [51]. The emitted positron travels a certain range depending on its energy, which will be lost through interactions with surrounding tissues until it annihilates with an electron (figure 5b). The result is 2 annihilation gamma rays, 0.511 MeV energy each emitted in opposite directions (about 180^{0} from each other) and detected

in coincidence within time window of 2τ ns. The distance traveled by the positron from the decay event to the annihilation event (positron range) and the non-linearity of the annihilation gamma rays cause loss of spatial resolution that cannot be recovered during image reconstruction.

3.3.2. Coincidence events

Three coincidence events in PET are identified as: true, scattered, and random (figure 6). True coincidence occurs when both photons from an annihilation event are detected by detectors in coincidences and no other event is detected within the time window. A scattered coincidence occurs when at least one of the detected photons undergoes Compton scattering prior to detection. Scattered coincidences add background to the true coincidence, decreases image contrast and cause overestimating of the isotope concentration. Random coincidences occur when two photons are not arising from the same annihilation event and detected within the convenience time window [48].

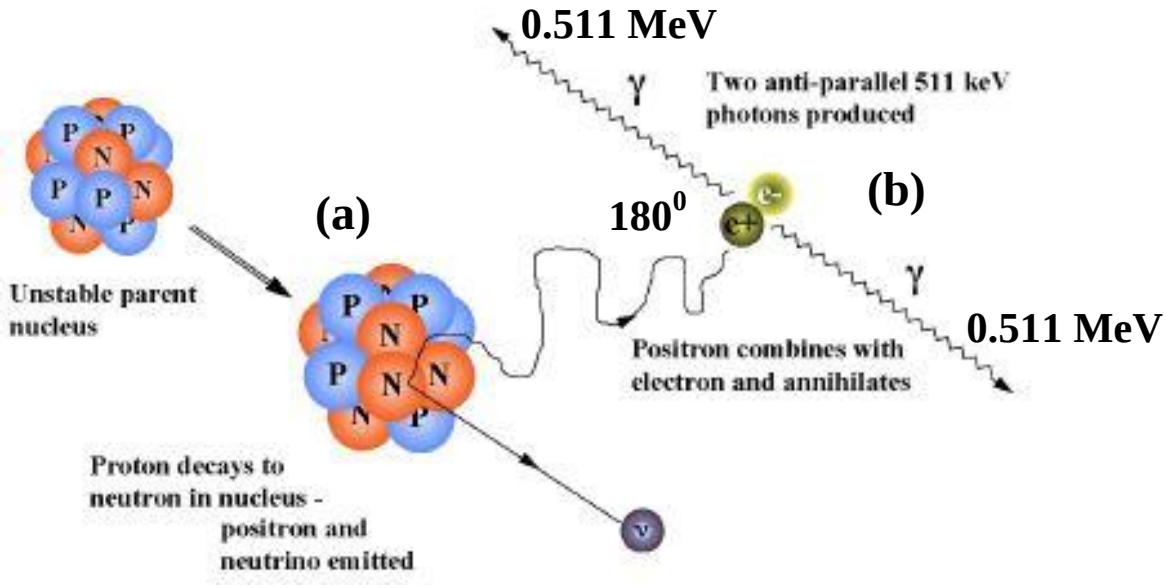

Figure 5 demonstrations of the positron emission and annihilation. 5a An unstable nuclide with an extra proton which decays into neutron, positron and neutrino. 5b positron travels a certain distance depends on its energy then annihilates with an electron and the result 2 gamma rays (511Kev each) emitted in opposite direction about 180^0 away from each other.

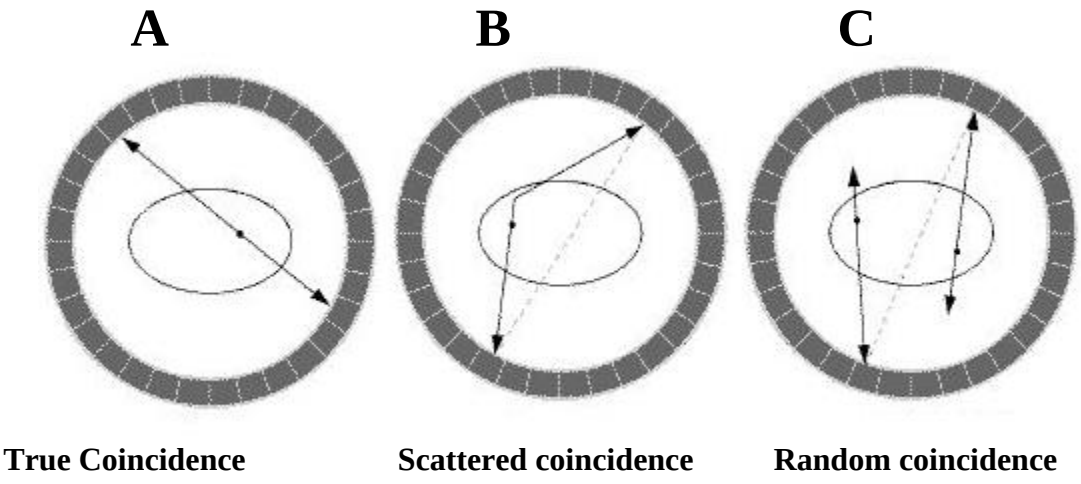

Figure 6 A true coincidence detection occurs when the two gamma rays are detected from one annihilation event in the time window. B if at least one of the gamma photons under goes Compton scattering, and both photons still detected in the time window, scattered coincidence has occurred. C random coincidence occurs when both photons detect in the time window and are from deferent annihilation events.

3.3.3 PET Radionuclides used for imaging in AIT

Avariety of radionuclides has been used to track and monitor labeled cells in vivo. The common radionuclides are listed in table 3. ^{18}F is widely used as PET radionuclide in many applications due to its short half-life and fast clearance from subject under study. However, it requires rapid radiochemistry and immediate delivery. ^{64}Cu and ^{124}I have relatively longer half-lives making them more acceptable for long term tracking and monitoring of labeled cells.

Table 3 Isotopes and examples of their radiotracers used to track immune cells for PET imaging.

Nuclide & Radiotracer	Mechanism of cell labeling	Half-life	Decay modes	Maximum positron energy (MeV) and yield (%)	production
^{18}F-FDG	Cross cell membrane by transporters	109.8 minutes	EC, ß$^{+}$	0.634 (96.7 %)	^{18}O (p ,n) ^{18}F ^{20}Ne (d, α) ^{18}F
^{64}Cu-PTSM	Lipophilic cross cell membrane through passive diffusion	12.7 hours	EC, ß$^{+}$, ß$^{-}$	0.653 (17.4%)	^{62}Ni (p, n) ^{64}Cu
^{124}I- FIAU	Trapped by cell through phosphorylation by viral thymidine kinase produced by transduced cells	4.18 days	EC, ß$^{+}$	2.138 (23.0%)	^{126}Te (p,3n) ^{124}I
^{89}Zr-Oxine	Lipophilic cross cell membrane through passive diffusion	3.26 days	ß$^{+}$	1.74 (12%)	^{89}Y(p, n) ^{89}Zr

3.4. Optical Imaging

3.4.1. Introduction

Optical imaging is noninvasive *in vivo* imaging with light photons detected by charged coupled device (CCD) detectors made from silicon crystals which have high sensitivity to light. Two common types of optical imaging are well-known in the realm of molecular imaging; fluorescence and bioluminescence imaging. In the Fluorescence imaging an excitation light of one

wavelength in the range between 395-600 nm illuminates the subject under study and an emission light with wavelength higher than the excitation wavelength detected by CCD detector [49]. The use of near-infrared probes (spectrum range 700-1000nm) for optical imaging maximizes tissue penetration because hemoglobin and water which are the major absorbers of light have lowest absorption coefficients in the infrared range. In bioluminescence imaging only the emission light is detected by CCD detectors and no excitation light is used in this technique. The most commonly used bioluminescence probes are reporter genes, Firefly or Renilla Luciferase (FLuc or RLuc respectively). Their substrates are Luciferin for FLuc and Coelenterazin for RLuc. In case of using FLuc, cells transfected by FLuc gene and express the Luciferase enzyme that will oxidize the Luciferin (given as i.v. injection at different time points) in the presence of oxygen, ATP and magnesium (Mg^{2+}) to produce Oxyluciferin and light which will be detected by CCD camera to be quantified and process image reconstruction. The main advantage of bioluminescence imaging is that it can detect very low signal and the background signal is very low. But the efficiency of the transmission light is limited and depends on the tissue type. Skin and muscle have highest transmission, whereas highly vascular organs such as liver and spleen have lowest transmission because of the absorption of the light by oxyhemoglobin and deoxyhemoglobin [50].

3.4.2 Multi-spectral fluorescence imaging (theory and concepts)

3.4.2.1. Florescence (definition, emission and excitation spectrum)

Fluorescence is the emission of light that occurs rapidly (around one million of a second) after illumination. When the light emission takes longer time is called phosphorescence. Two major problems are encountered with fluorescence measurement: first, fluorescence is emitted by the fluorescent molecule such as dyes in all directions and most imaging systems are designed to

capture light coming from particular direction. Second, it is difficult to obtain identical excitation of the total fluorescent molecules in the subject under study [51]. Fluorescent materials always emitted light with longer wavelength than the exciting light. The differences between wavelengths of emission and excitation lights is called Stoke's shift. The range of the excitation wavelengths known as absorption spectrum, while the emitted light covers range of wavelengths known as emission spectrum. In most cases there is overlap between the excitation and the emission spectrum.

3.4.2.2. Autofluorescence (definition and multispectral analysis solution)

Some biological materials such as vitamins, hormones, and enzymes are naturally fluorescent. Resulting strong fluorescent signals interfere with the signal of specific labeling probe and cause unwanted background which known as autofluorescence. Animal skin, fur and food, particularly if the food contained Chlorophyll, are strong sources of the autofluorescence signals [52]. Excitation and emission filters are used to reduce this problem. Both filters should be chosen to match the maximum excitation and emission wavelengths of a specific probe. Multispectral imaging systems provide a unique solution to the autofluorescence problem using multispectral analysis. It is based on the fact that all fluorescent materials produce specific emission spectra. Multispectral analysis generates spectral curves for the various fluorescent materials and autofluorscence curves in the subject under study. Based on this technique a series of images are captured called image cube taken at specific wavelength. Using sophisticated algorithms, the contribution of autoflourscence to the image can be removed, and specific fluorescence spectra for specific probe are separated.

3.4.2.3. Multi-spectral imaging system (Maestro2)

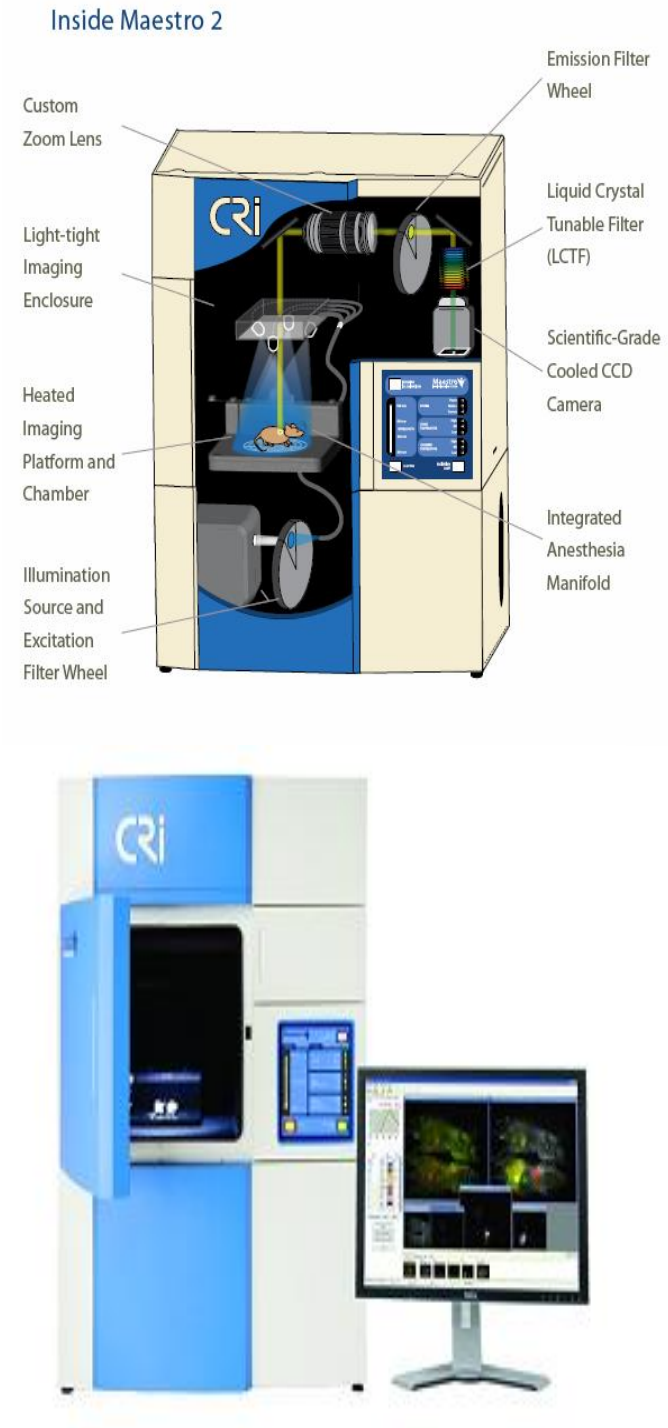

The multi-spectral imaging system used in this project is shown in figure 7. The various components of the system include, high-resolution, scientific- grade CCD imaging sensor, solid-state liquid crystal (LC) wavelength tuning element, spectrally optimized lens and internal optics, an excitation light source and emission filter assembly. The system has a control panel with switches for the excitation lamp, shutter, and white interior lights. It also displays the system statues such as the interior temperature and current filter wavelength.

Figure 7 Multispectral fluorescence imaging system (Maestro2 at CMI/VCU). Wavelength range = 500-950 nm; FOV = Max 3 mice; Spectral Unmixing and Dynamic Contrast Enhancement (DyCE™) allows quantitation of temporal biodistribution of fluorescent markers at much earlier time points (first few seconds following injection).

3.5. Labeling and imaging of T lymphocytes (literature review)

Noninvasive *in vivo* imaging of adoptively transferred T-lymphocytes requires an effective and mild labeling methodology and the right imaging technology direct labeling enables the imaging of cells labeled *ex vivo* and reinfused into the patient or subject who is being examined. Radionuclide based direct labeling probes for SPECT/PET imaging includes include, [^{111}In]-Oxine, [^{18}F-]FDG,[^{99m}Tc]-HMPAO, and[^{64}Cu]-PTSM. These have been used to monitor the migration of T-lymphocytes *in vivo* [53, 54]. However, these techniques do not permit long term monitoring due to the short physical half-life of the radionuclides, relatively low level of radioactivity per cell, and in certain instances, are limited by significant cell toxicity [55]. On the other hand, indirect labeling utilizes imageable reporter protein/probe combinations and rely on the *ex vivo* transduction of a relevant reporter gene into the immune-competent cells. Following reinfusion of the transduced cells into the subject, the product of the reporter gene can be imaged by injecting a suitable radiolabeled substrate. Herpes Simplex Virus Type-1 Thymidine Kinase (HSV1-tk) is such a PET reporter gene (PRG) and is one of the most commonly used indirect methods to image adoptively transferred T-lymphocytes in animals and patients, and it can be imaged with various substrates such as[^{124}I]-FIAU, [^{131}I]-FIAU, [^{18}F]-FEAU and [^{18}F]-FHBG [58,59]. The sodium iodide symporter (NIS) is another reporter gene that has also been evaluated for imaging cells of the immune system in immortalized macrophage cell lines genetically engineered to express NIS and GFP (RAW264.7/hNIS-GFP) [56]. Using [^{124}I-NaI PET imaging, these investigators monitored macrophage migration towards inflamed tissue. In addition to ^{124}I, $^{99m}Tc0_4$, ^{123}I, ^{125}I, [^{18}F]-tetrafluoroborate can also be used as substrates for NIS [57].

Radionuclide based methods are useful in the clinic due to the ability to image signals from deep tissues. However, the logistics of radionuclide techniques are more demanding, which makes them less cost effective for preclinical investigations. Non-radioactive agents, such as fluorocarbon-based probes, have also been used for efficient direct ex *vivo* labeling of cells, and used in conjunction with ^{19}F MRI for in *vivo* detection and imaging [58]. This method, which involves the use of an autologous dendritic cell vaccine to treat colorectal cancer, is currently being evaluated in humans (personal communication). This represents the first clinical trafficking study of a live cell cancer vaccine which has been visualized by MRI in the United States.

On the other hand, optical methods are relatively easy, require simpler imaging equipment and are cost effective, but are not very useful in the clinic due to the lack of effective technology that can detect optical signals from deep tissues. However, optical labels, both direct and indirect, could be very useful for research and development of various strategies aimed at improving immune cell therapy. One cost effective approach is to use optical reporter proteins such as firefly or renilla luciferase to label the cells and monitor them by optical imaging [59, 60]. However, these are currently limited to animal models and their success relies on the successful stable transduction of the reporter gene and the persistence of the reporter gene expression over time. A combination of direct labeling strategy and optical imaging methodology would be ideal, in terms of simplicity and cost effectiveness, for monitoring cell trafficking in preclinical studies. This could be extended to clinical investigations if a suitable imaging component such as ^{124}I or ^{19}F is included in the direct cell labeling strategy.

Studies describing optical imaging of directly labeled immune cells is quite limited. However, using *ex vivo* imaging and other *in vitro* protocols, several DNA-binding, cytoplasmic,

covalent coupling or membrane inserting fluorescent dyes have been investigated for direct labeling of T lymphocytes to track lymphocyte migration and proliferation [61]. Due to interference from autofluorescence and tissue absorbance, most of these dyes are not ideal for *in vivo* optical imaging and their use is limited to *ex vivo* detection. The optical imaging window is primarily limited by absorption, due to either blood at short wavelengths or water at long wavelengths. This could be overcome with the use of near-infrared dyes (NIR) that will allow deep tissue signal localization [62]. The red/NIR tissue optical window between 600 and 1300 nm is the spectral region where light has its maximum depth of penetration in tissues due to minimal absorption and scattering. Among the various options available for direct labeling, the cell membrane dyes retain the signal for relatively longer periods than DNA-binding, cytoplasmic or covalent coupling dyes [63]. Therefore, a combination of NIR based fluorescent cell membrane dyes would offer a direct labeling method for monitoring cell trafficking while exploiting high sensitivity, simple labeling technique, decreased autofluorescence and relatively low costs.

In this project multi-spectral fluorescent imaging was extensively used to investigate the *in vivo* kinetics of labeled T-lymphocytes. In addition, the feasibility of indirect reporter gene imaging, using the (HSV1tk / [^{124}I] FIAU system) was also examined for PET imaging approach.

Chapter Four: Materials and Methods

The following diagram is a summary of the project strategy, details are provided on the following pages.

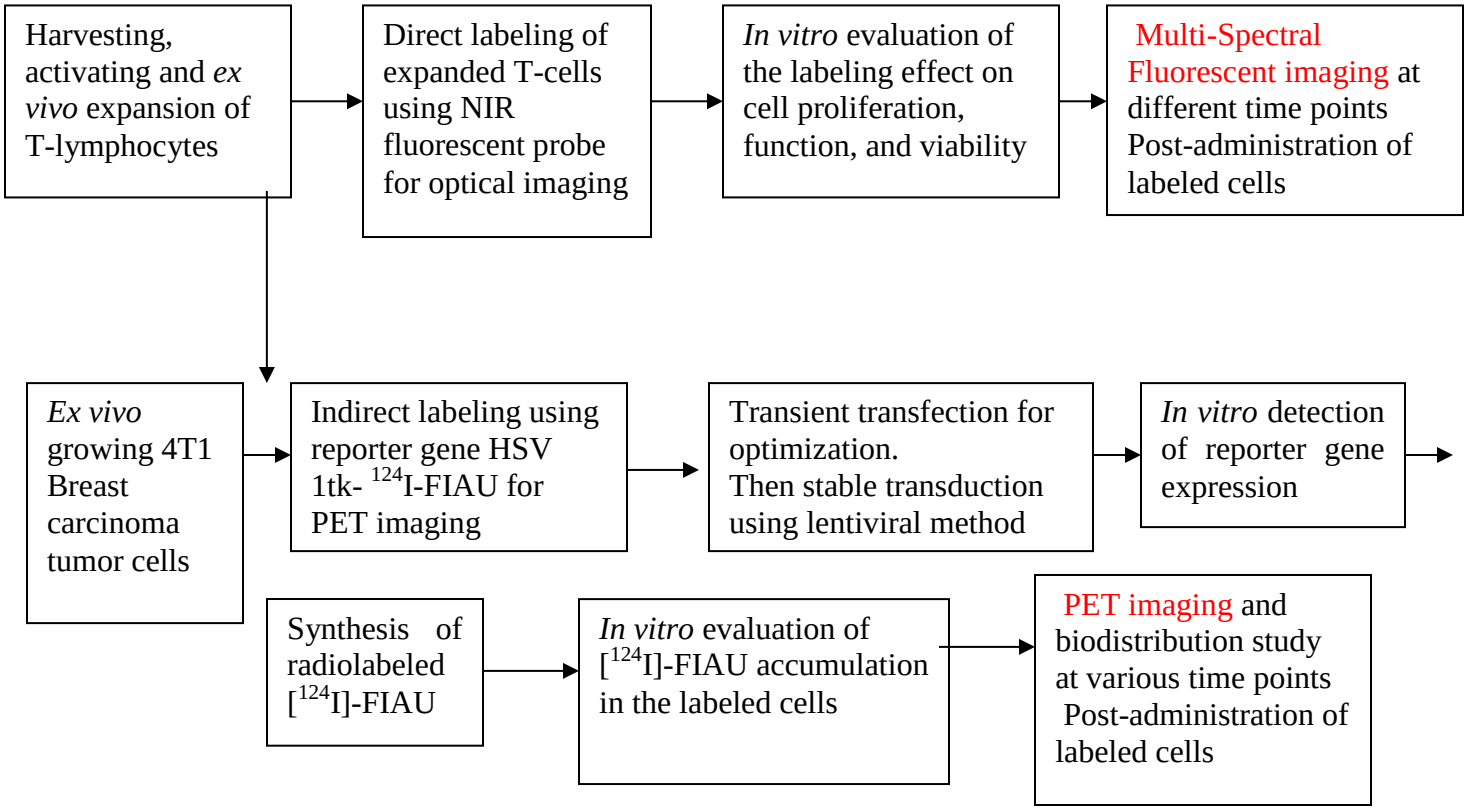

4.1. Animals

Female BALB/c mice, aged between 8-12 weeks, obtained from National Cancer Institute, Bethesda, MD, were caged in groups of five or fewer, and provided with food and water ad libitum. All animal experiments were performed according to the policies and guidelines of the Institutional Animal Care and Use Committee (IACUC) at Virginia Commonwealth University, USA.

4.2. Cell lines

Murine mammary breast carcinoma (4T1) cell line was kindly provided by Dr. Jane Tsai, Michigan Cancer Foundation, Detroit, Michigan. 4T1 cells were maintained in Dulbecco's Modified Eagle Medium (DMEM) with 10% heat-inactivated fetal calf serum (Hyclone, Logan, UT) 1 mM sodium pyruvate, 100 U/ml penicillin, 100 µg/ml streptomycin (Sigma, St. Louis MO) and 10 mM HEPES (Thermo Scientific). Tumor cells were trypsinized with 0.05% trypsin-EDTA (Fisher, Pittsburgh), washed with PBS and used for experiments.

Meth-A sarcoma cells were obtained from American Type Culture Collection (Rockville, MD) and grown in DMEM media, containing 10% heat inactivated fetal bovine serum, 1 mM sodium pyruvate, 100 u/ml pen/strep, 10 mM HEPES, and 2 mM L-glutamine in incubator with 5% CO_2, at 37° C. Cells > 90% confluence were trypsinized and used for experiments.

Jurkat cell line was obtained from ATCC and grown in RPMI media, containg 10% heat inactivated fetal bovine serum, 100 u/ml pen/strep and were grown in the incubator with 5% CO_2, at 37° C. cells were counted every other day and kept at a concentration of one million per ml.

HEK 293 cell line was obtained from ATCC and grown in EMEM media containg 10% heat inactivated fetal bovine serum, 100 u/ml pen/strep and in the incubator with 5% CO_2, at 37° C. Cells > 90% confluence were trypsinized and split to be used for experiments.

4.3. Isolation, activation and *in vitro* expansion of 4T1 tumor specific T lymphocytes

Donor mice were vaccinated in the left hind footpad with viable 1/2 $x10^6$ 4T1 cells. Ten days later, when these mice had a growing tumor in the foot, popliteal draining lymph nodes (DLN) were harvested under sterile conditions and disrupted through mesh screens to yield single cell suspensions. The cells from DLN were filtered and resuspended in complete RPMI media at $1x10^6$ cell/ml concentration. These cells were then activated by incubating them with 5nM Bryostatin 1 (Sigma, St. Louis MO), 1μM Ionomycin (Calbiochem, San Diego, CA) and 80 U/ml IL-2 (Chiron, Emeryville, CA) at 37° C for 18 hours. To expand the lymphocyte population, cells were washed three times with warm, complete RPMI and resuspended at $1x10^6$ cells/ml concentration and divided into 2 groups: group-1 was incubated with 40 U/ml of IL-2 (IL2 cells) and group-2 incubated with IL7+ IL15 (10 ng/ml each) (Chiron, Emeryville, CA) (IL7/15 cells) . The cells were then allowed to proliferate in culture for 6-13 days and were split every other day to maintain $1-2x10^6$ cells/ml concentration. Fresh IL-2 or IL-7 +IL-15 was added at each split. Cell proliferation was calculated by determining the number of viable cells, on every other day of culture, by trypan blue exclusion and comparing it with the number of cells on day 1 of expansion. Luminescence based cell viability assays were also carried out as described below.

4.4. Labeling methods of T- lymphocytes

T lymphocytes were labeled using two approaches: a) direct labeling using NIR fluorescent probe (DiR dye) for optical imaging, b) indirect labeling using the PET reporter gene (PRG) strategy (HSV1 tk RG) for PET imaging. The direct labeling method was used to obtain some information about the *in vivo* trafficking of 4T1 sensitized T lymphocytes and to optimize our experimental model. The indirect labeling method was used to demonstrate its feasibility because it allows cell monitoring for long periods of time and it can be translated to the clinical setting.

4.4.1 Direct labeling with NIR-fluorescent probe

Direct labeling of T- lymphocytes isolated on day-6 after *in vitro* expansion was achieved by incubating the cells with 1,1-dioctadecyltetramethyl indotricarbocyanine Iodide (DiIC18(7) or DiR), a lipophilic Near-Infra red fluorescent dye (Absorption/ Emission: 748/780nm) (PerkinElmer, MA). DiR (scheme 1) allows labeling the cell membrane through the insertion of the long 18-carbon chains into the cell membrane, resulting in specific and stable cell labeling with negligible dye transfer between cells .DiR stock solution was prepared by dissolving 25mg dye in 3ml Ethanol. From this stock, further dilutions were made to the required concentrations in media and incubated with cells for 30 minutes at 37 ^{0}C (cells were shaken every 10- minutes). After incubation, cells were spun down at 1000 rpm at 4° C for 10 minutes, then washed twice with PBS and used for experiments.

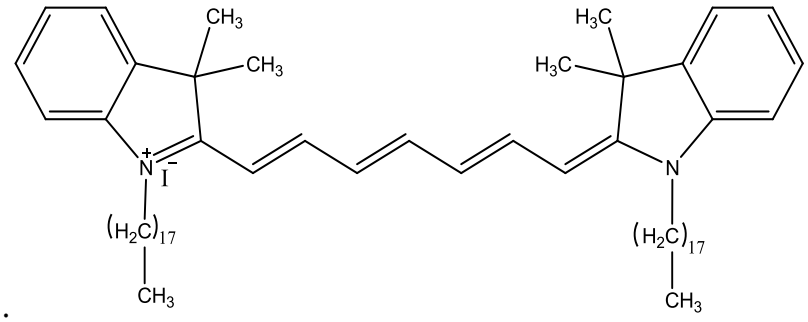

Scheme 1 the chemical structure of the fluorescent probe (DiR)

To examine cell proliferation, viability and function before and after DiR labeling the following assays were performed:

4.4.1.1. Cell proliferation assessment

Cells were counted every other day using 0.4% Trypan blue (Mediatech VA) and the number of viable cells was compared to their number immediately after pulsing with B/I. The result of this comparison is expressed as fold increase. Cell proliferation was assessed based on fold increase in cell number.

4.4.1.2. Cell Viability assays

The highest tolerable concentration of DiR in the staining solution, which can be used to label T-cells, was determined using Cell Titer-Glo Luminescent assay kit (Promega) and flow cytometry. Tumor sensitized lymphocytes, cultured in media for 6 days in IL-2 or IL-7+IL-15 containing media, were labeled with a staining solution containing various concentrations (3.5, 14, 56, 224 and 320 µg/ml) of DiR. Following labeling, 25000 cells/100 µl were plated in triplicates in a 96 well plates, and incubated along with similar number of unlabeled cells in a 37° C CO_2 incubator. After 1, 4 or 7 days of incubation, the Cell Titer Glo reagent was added to the cells and the % Viability was calculated for each labeled group in comparison to unlabeled cells (100% viability). For flow cytometry, DiR labeled and unlabeled T-cells (2 or 7 days post labeling) were double stained with propidium iodide (PI) and AnnexinV-FITC (BD Biosciences Pharmingen, San

Diego, CA) and analyzed using Beckman Coulter Epics XL-MCL flowcytometer and the data were analyzed using EXPO 32 software. Two different sets of experiments were performed to verify the results.

4.4.1.3 Cell function assessment (Interferon- γ release assay)

***In vitro*:** Interferon-γ (IFN-γ) released into supernatants of 4T1 sensitized and expanded T-lymphocytes in response to stimulation with irradiated 4T1 and Meth-A cells (non-specific control) was assayed using BD OptEIA mouse IFN-γ ELISA kit (BD Biosciences, San Jose, CA). T-cells obtained from popliteal DLN, which had been activated and expanded in either IL-2 or IL-7 and IL-15 containing media, were collected on day 6 and incubated with DiR staining solution (320 µg/ml) . The DiR labeled and unlabeled cells were collected 1 day and 7 days post-labeling and incubated with the irradiated 4T1 or Meth-A tumor cells for 24 hrs, and the amount of IFN-γ in the supernatant was analyzed. As a negative control, 4T1 sensitized T cells alone were incubated under similar conditions.

***In vivo*:** Blood was collected from three different groups of animals bearing: i) 10 day old 4T1 tumor, ii) 10 day old 4T1 tumor and injected with 10 million labeled T-cells /mouse, iii) 10 day old Meth-A tumor and injected with similar number of activated and labeled T-cells. One week later, blood was collected and the amount of interferon-γ in serum was determined using the same kit and assay described above.

4.4.1.4. Animal model and T lymphocyte trafficking

For the development of tumor models, mice were inoculated subcutaneously into the right flank with either 4T1 cells or Meth-A tumor cells ($5x10^4$) and the tumor was allowed to grow for 3 days (average tumor volume size 20±5.6 mm^3) or 7 days (average tumor volume size 80±10.3 mm^3) . To follow *in vivo* trafficking of T cells, 4T1 sensitized T-cells were first labeled with DiR

(320µg/ml staining solution). The cells were then filtered through 70-µm nylon mesh strainer and injected intravenously (iv) into the mouse tail vein ($10x10^6$ cells in 0.5 ml PBS per mouse) either a week before or after the tumor cells were injected.

To confirm that the detected signal at the tumor site is associated to the DiR labeled viable T cells, two experiments were performed. First: the DiR at same concentration as used for labeling was diluted in PBS and injected intravenously into 3 animals bearing 4T1 tumor. After fluorescent imaging at 2, 24 and 48 hours, animals were dissected and the *ex vivo* data were collected. Second: DiR labeled T cells were resuspended in PBS and lysed by freezing and thawing protocol for 6 times to ensure full cell lysate. Cell viability was tested using Trypan blue (0.4%). The cell lysate was injected (tail vein i.v. injections) into 6 animals bearing 10 day 4T1 tumors (3 for IL-2 cells and 3 for IL-7/15 cells). Fluorescent imaging was carried out for 2 weeks. One day before injection of DiR labeled T-lymphocytes, mice were pretreated, intraperitoneally (ip), with 100mg/kg Cyclophosphamide (CYP) (Mead Johnson, Princeton, NJ).

4.4.1.5. Multi-spectral fluorescence imaging

Fluorescent images were taken from day 1 to day 21 to monitor the homing and localization of labeled T lymphocytes at the tumor site. Multi-spectral fluorescence imaging system (Maestro-2 by PerkinElmer, USA) was used to monitor DiR labeled T-lymphocyte trafficking and localization in host mice with and without tumors. A NIR/Orange double filter setup (640nm to 820nm) and spectral unmixing was used for image acquisition and processing. Image processing and data analysis were performed using Maestro-2 software version 2.10. Images were obtained at different time points (2 hours, 24 hours, 48 hours, 72 hours, 6-days , 8-days, 10-days, 13-days, 15-days, 17-days, 20-days, and 21-days) post-injection of labeled T-lymphocytes. Six mice per

time point were used; and four imaging positions, Dorsal, Ventral, Left and Right sides, were used at each time point.

4.4.1.6. Immunohistochemistry analysis

After imaging, mice were euthanized, organs and tumors were collected, embedded with Optimal Cutting Temperature compound (O.C.T, Tissue-Tek, USA) and stored at -80° C. Using a cryostat system (LEICA CM1850 UV), five-micron thick serial sections of the samples were collected onto glass slides. The sections were fixed for 15 min in 3% freshly prepared paraformaldehyde in PBS (pH 7.4) at room temperature, and then washed three times with 0.3M glycine in PBS. Antigen retrieval was done using heat and citric acid buffer method. Following this, sections were washed three times in PBS for 5 min each, then incubated with blocking buffer (5% normal goat serum + 0.1% Triton X-100 in PBS, pH 7.4) for 1 hour at room temperature. Tissue sections were incubated overnight, at 4°C with Anti-F4/80 and Anti-CD69 primary antibodies (Abcam, USA). This was followed by incubation, for 1hr at room temperature, with Alexa Fluor 488 goat anti-rat IgG and Alexa Fluor 568 Goat anti-hamster IgG (Abcam, USA), which were used to detect macrophages and activated T cells respectively. The sections were cover-slipped with Vectashield Mounting Medium (Vector Laboratories, Burlingame, CA), and were then imaged and analyzed using Zeiss LSM 700 confocal laser scanning microscope.

4.4.2. Indirect labeling method using PET Reporter Gene (PRG)

The second method was the indirect labeling of T- lymphocytes through transduction of reporter gene (cell cytoplasm labeling Herpes Simplex Virus type 1- thymidine kinase (HSV-1 tk). The product of this reporter gene is an enzyme that phosphorylates a radio labeled substrate 2-fluoro-2-deoxy-1 β- D- arabinofuranosyl-5- ^{124}I iodouracil [^{124}I] FIAU for PET imaging. Before we established this method, we performed transient transfection using transfection reagents to

transfect Jurkat cells (these cells are T cells derived from a subject who had lymphoma; they are similar in their features to T cells and produce IL-2). The transient transfection method, as described below, was done to optimize our detection method (western blot) of the HSV1 tk expression.

4.4.2.1. Transient transfection

4.4.2.1.1. HSV1tk vector isolation:

An expression vector containing the HSV-1 tk fusion gene (pORF9-HSV-1tk: Sh ble) (Invitrogen) was transformed to E.coli bacteria strain GT116. The E coli bacteria was grown by streaking of 50µl of the E coli stock on LB agar plates and incubated for 24 hours at 37 ^{0}C. One single colony was picked up and grown in 10 ml of the LB media overnight at 37 ^{0}C. Then the 10 ml Ecoli grown media was added to 150 ml of the LB media to grow overnight at 37 ^{0}C. The 150 ml volume of the Ecoli grown media was enough to isolate good concentration of the plasmid vector. The plasmid vector was isolated by Gen Elute HP- plasmid maxiprep kit (Sigma-Alridsh) following the kit protocol. The HSV1tk plasmid (DNA) concentration and purity was measured as following:

The HSV1-tk plasmid concentration was calculated using the following formula:

Concentration (µg/ml) = (A_{260} reading – A_{320} reading) × dilution factor × 50µg/ml

A_{260} and A_{320} are the DNA and RNA absorbance respectively, measured by spectrophotometer, dilution factor = 100, the formula multiplied by 50µg/ml because as role of thumb OD of 1 = 50µg/ml.

Total yield is obtained by multiplying the DNA concentration by the final total purified sample volume.

DNA yield (µg) = DNA concentration × total sample volume (ml)

DNA purity was calculated using the following formula:

DNA purity (A_{260}/A_{280}) = (A_{260} reading – A_{320} reading) ÷ (A_{280} reading – A_{320} reading)

A_{280} = other contaminants absorbance.

Good-quality DNA will have an A_{260}/A_{280} ratio of 1.7–2.0. In our experiments we frequently have obtained DNA concentration between 500 to 700 µg/ml and DNA ratio of 1.7 -1.8.

4.4.2.1.2. Confirmation of the presence of HSV1-tk gene in the isolated vector

Using restriction enzymes (NcoI-HF and NheI-HF) (Invitrogen) to perform single and double cut of the HSV1-tk plasmid and perform gel electrophoresis to determine the plasmid size and confirm the presence of HSV1tk gene. The DNA resulted from maxiprep was heated at 75^0 C for 10 minutes to inactivate DNase. Then 5 samples were prepared: sample 1 and sample 5 is 2ul 1Kb DNA ladder + 2ul gel loading dye to help as guide to calculated DNA size. Sample 2 is 2.5ul intact plasmid DNA + 2ul gel loading dye, sample 3 is single cut of DNA by Nco-I digestion enzyme (7ul + 2ul loading dye), sample 4 is double cut of DNA by Nco-I and Nhe-I digestion enzymes (10ul + 2ul loading dye).

Sample 3 (single cut of DNA) preparations was done as following:

11.5ul dH2O+ 2ul 10X NE buffer+ 0.5ul Nco-I enzyme+ 6ul DNA.

Sample 4 (double cut of DNA) preparations was done as following:

10ul dH2O+ 2ul 10X NE buffer + 1ul BSA + 0.5ul Nco-I + 0.5ul Nhe-I + 6ul DNA.

Preparation of 1% Agarose gel was done as following:

o.6gm of Agarose powder + 60ml of 1X TAE buffer heated in the microwave then left to be cooled, 3ul Ethidium bromide was added then poured in the gel casting tray.

After all samples were loaded the gel electrophoresis was ran at 90V for one hour then imaged using UV Versa Doc imaging system.

4.4.2.1.3. Transfection of Jurkat cells using polymer-based transfection reagent

Fugene-HD a polymer-based transfection reagent (Promega), was used to transfect Jurkat cells. Fugene-HD is a mixture of lipids and other components in 80% Ethanol. It does not require any ingredients of human or animal origin and also does not require removal of serum but using of antibiotics (AB) in the transfection medium is not recommended. DNA concentration has to be between 200µg/ml and 1mg/ml, its purity (A_{260} / A_{280}) has to be 1.7-1.9. The transfection procedure was done as following:

Cells were plated in 96 well plate 20,000/100µl media+ serum but no AB. DNA (at concentration of 489 µg/ml and purity of 1.9) was diluted in 100µl free serum media then Fugene transfection reagent was added to the diluted DNA at ratio of 6:1 (Fugene :DNA). (e.g. 2µg of DNA and 6µl of Fugene). The mixture was incubated at room temperature (RT) for 10 minutes. Cells transfection was done by adding 5 µl of this mixture to each well of the 96 well plate and mixing gently by pipetting up and down 4 to 5 times. The plate was incubated at 37 ^{0}C for 24, 48, 72 and 96 hours, and cells were collected and cell lysate was prepared for total protein calculations and Western blot to detect HSV1-tk expression.

4.4.2.1.4. Cell lysate preparation

Cells were counted and rinsed with cold PBS twice. (Washing and centrifuging). The final cell pellet was prepared without any remaining phosphate buffer saline (PBS) (Thermo Scientific). Lysis buffer was prepared by using RIPA lysate buffer (Thermo Scientific) 100 µl for each one million cells containing 1µl Halt complete protease inhibitor and µl EDTA (Thermo Scientific). Lysis buffer solution was added to the cell pellet, mixed by pipetting up and down many times then incubated in ice at RT for 30 minutes. Then the mixture was spun at 3000 rpm for 10

minutes at 4^0 C. The supernatant was aliquated and stored at -80 ^{0}C for the following experiments.

4.4.2.1.5. Protein concentration determination in cell lysate

Protein assay kit (Pierce BCA) (Thermo Scientific) was used to determine the total protein concentration in the cell lysate. Serial dilution of the bovine serum albumin (BSA) stock (2 µg/ml) in the RIPA lysis buffer (Thermo Scientific) was prepared as in table-1.

Table 4 Serial dilution of BSA in RIPA lysis buffer

	BCA stock µl	Diluent µl (RIPA buffer)	Concentration(µg/ml)
A	**200**	**-**	**2000**
B	**90 from A**	**30**	**1500**
C	**60 from A**	**60**	**1000**
D	**60 from B**	**60**	**750**
E	**60 from C**	**60**	**500**
F	**60 from E**	**60**	**250**
G	**60 from F**	**60**	**125**
H	**56 from G**	**14**	**25**
I	**-**	**100**	**Blank**

In eppendorf tubes all of the standard samples from A to I as on the table were prepared first. Then in 96 well plate 10µl from A to I and 10 µl from our samples were put in duplicate. 200µl of working reagent (mixing of BCA reagent A and reagent B at ratio 50:1) was added to each well. The plate was put in the incubator, shaken for 30 sec then incubated without shaking for 30 min at 37^0 C. The samples were allowed to cool at RT for 5 min then were read at 595nm in the plate reader and spectrophotometer to compare both measurements. The average OD of A to H was used to make the standard curve and calculate total protein concentration in each sample.

4.4.2.1.6. Determination of the HSV1tk expression by Western blot

All samples were put at 100^0 C for 5 min in the water path., for protein denaturation to expose more epitopes (polypeptide fragment of the protein) to the primary antibody.

A mixture of Laemmle's sample buffer (Gen DEPOT) and plus one Mercaptoethanol (GE Health Care - Biosciences) at ratio of 100:1 was prepared then added to samples at ratio of 4:1. Samples were loaded in 10% poly acrylamide gel , then the gel was run for 90 minutes at 120V in the running buffer (25mM Tris base (Trizma) 4.53gm, 192 mM glycine 21.6gm, 7.5ml of % 20 SDS solution and distilled water was add to total volume of 1.5 L) . Two molecular weight markers were used: a) 2 µl of Xpert 2 Prestained protein marker (Gen Depot) was used as rainbow marker to confirm the transfer process, b) 2µl of Odyssey molecular weight marker (Li-Cor) was used for quantification. The gel was transferred to PVDF membrane (Immobilon transfer membranes-Millipore) at 4 ^{0}C for 1 hour at 100 V in the transferring buffer (25mM Tris base (Trizma) 4.53gm, 192 mM glycine 21.6gm, methanol 300ml and distilled water was added to total volume of 1.5 L). Transfer buffer was Stored at 4^{0} C for 30 to 60 minutes. Before the transfer process the PVDF membrane was wet in methanol for 1-2 minutes then in cold transfer buffer for 5 minutes. The gel was equilibrated for 3-5 minutes in the cold transfer buffer before transferring.

The membrane was blocked using 10 ml of block buffer (Odyssey buffer Li-Cor) in the shaker at low speed at RT for 1 hour. Thymidine Kinase HSV-1 TK primary antibody (Santa Cruz Biotechnology) and Beta Actin mouse mAB primary antibody (cell signaling) were diluted with 10 ml of Odyssey buffer and 20 µl of Tween 20 (Promega) at concentration of 1:10000. The membrane was incubated with the diluted primary antibodies overnight on the shaker at low speed at 4 ^{0}C. On the second day the membrane was washed four times with washing buffer (50 ml PBS + 50µl of Tween20) each time10 ml of the washing solution was added to the membrane and put on the shaker at medium speed for 10 minutes. Secondary antibodies against HSV-1TK (Donkey anti-Goat IRDye 680) (Li-Cor USA), and against beta-Actin (Donkey anti-Mouse IRDye 800 CW (Li-Cor) were diluted at concentration of 1:10000. The membrane was incubated

in the diluted secondary antibodies at RT on the shaker at low speed for 1 hour. The membrane was washed exactly as previous step after primary antibody incubation. Then the membrane was ready for imaging using Odyssey LX imaging system (Li-Cor).

4.4.2.2. Stable transduction of Jurkat, HEK 293, 4T1 and T cells using HSV1tk lentiviral vector

To be able to image T cells for long periods of time, stable transduction using Vira Power Lentiviral expression system (Invitrogen) was performed as follows:

An expression vector containing HSV-1 tk fusion gene pMOD-HSV1tk (Invitrogen) was transformed to an E.coli bacteria strain GT100. The E coli bacteria was grown and the HSV1tk plasmid extraction, concentration and purification was performed using same methods described with the expression vector containing the HSV-1 tk fusion gene (pORF9-HSV-1tk: Sh ble).

To confirm the presence of HSV1tk gene, the pMOD-HSV1tk plasimed vector was cut (single and double cut) using restriction enzymes (NcoI-HF and NheI-HF) then Gel electrophoresis experiment was performed as described for the pORF9-HSV-1tk: Sh ble plasmid.

To ensure that the pMOD-HSV1tk Ecoli is expressing HSV1TK protein, the Ecoli was grown and the optical density (OD) of 1.5 ml extraction of the E coli culture was measured using spectrophotometer (Beckman Coulter DU 730) at wavelength of 600 nm. The reading was 2.2 (it should be between 1.5 and 3.5). The bacterial cells were spun at 5000 rpm at 4 ^{0}C for 10 minutes. Then cells were resuspended in 300 µl of the lysis buffer (25 mM TrisHCLpH=8, 0.1 M NaCl, 10% glycerol, 0.1 % Triton X-100 and 1mM PMSF) and vigorous overtaxing until the suspension is homogenous. The bacterial lysate was spun at 13000 rpm at 4 ^{0}C for 5 minutes to separate soluble proteins from insoluble proteins in the pellet. The supernatant was collected and stored at

– 80 ^{0}C for Protein assay and western blot assay. Both of these assays were performed as explained previously.

4.4.2.2.1. Purification of HSV1TK protein

Once the expression of HSV1tk was confirmed in the Western blot result, the HSV1TK protein was purified from pMOD-HSV1tk Ecoli to be used as positive control for the following western blots. The HSV 1-TK Protein purification was done as follows:

BL21/de3 E. coli were transformed with the pet21dTK plasmid and a stock of the transformant was made and stored at –80 C. The bacteria were grown in LB medium at 37 C until the A600 = 0.5, then transferred to 18C, and when cooled 100 mg/l IPTG was added. The growth was continued at 18 C for 18 hours, and then the bacteria harvested by centrifugation. Bacteria were disrupted by a single pass through an Avestin emulsiflex operating at a pressure of 25000 psi, and the lysate was clarified by centrifugation at 25000 rpm in and SW28 rotor for 30 min. The histidine tagged TK was purified by chromatography on a nickel –NTA agarose column as follows. The lysate was added to the column, and then the column was washed extensively with 25 mM tris, 300 mM NaCl, 10 mM imidazole until no 280 nm absorbing material eluted. The bound protein was then eluted with 100 mM imidazole in the same buffer. Fractions containing A280 absorbing material were checked by SDS gel electrophoresis. The protein containing fractions were pooled, concentrated to 4 ml by ultrafiltration. The material was then chromatographed on a sephacryl S200 column. The fractions were monitored by SDS gel electrophoresis and TK containing peak fractions were pooled. Molecular weight = 40856.39 about 41 KD, Residues = 374, Average Residue Weight = 109.242 Charged = 1, Isoelectric point = 8.00, Extinction coefficient = 38240 Therefore 1 mg/ml = A280 = 0.93

4.4.2.2.2. HSV1tk Lentivirus construction

The pMOD-HSV1tk vector was cloned to pLenti6/UbC/V5/DEST (Lentiviral vector containing) following the Vira Power system protocol. After the generation of the expression vector containing HSV1-tk (pLenti6-UBC-V5-DEST/pDONR221/HSV1tk). This vector was cotransfected to the 293FT cell line along with the packaging mix vectors (pLP1, pLP2, and pLP/ VSVG required to produce the lentivirus). The cotransfection was done using Lipofectamine 2000 transfection reagent based on cationic lipid-based formulation suitable for the transfection of this cell line with high efficiency. The 293 FT cell line is a very suitable host for lentivirus production. Then the viral supernatant was collected and titrated to be used for stable transduction. Virus tittering was done following the Lenti-X GoStix kit (Invitroge). The final virus concentration is 9.2×10^5 IU/µl. The production and tittering of HSV1tk lentivirus, was made at the VCU Macromolecule Core Facility, supported, in part, with the funding from NIH-NCI Cancer Center Core Grant 5P30CA016059-29

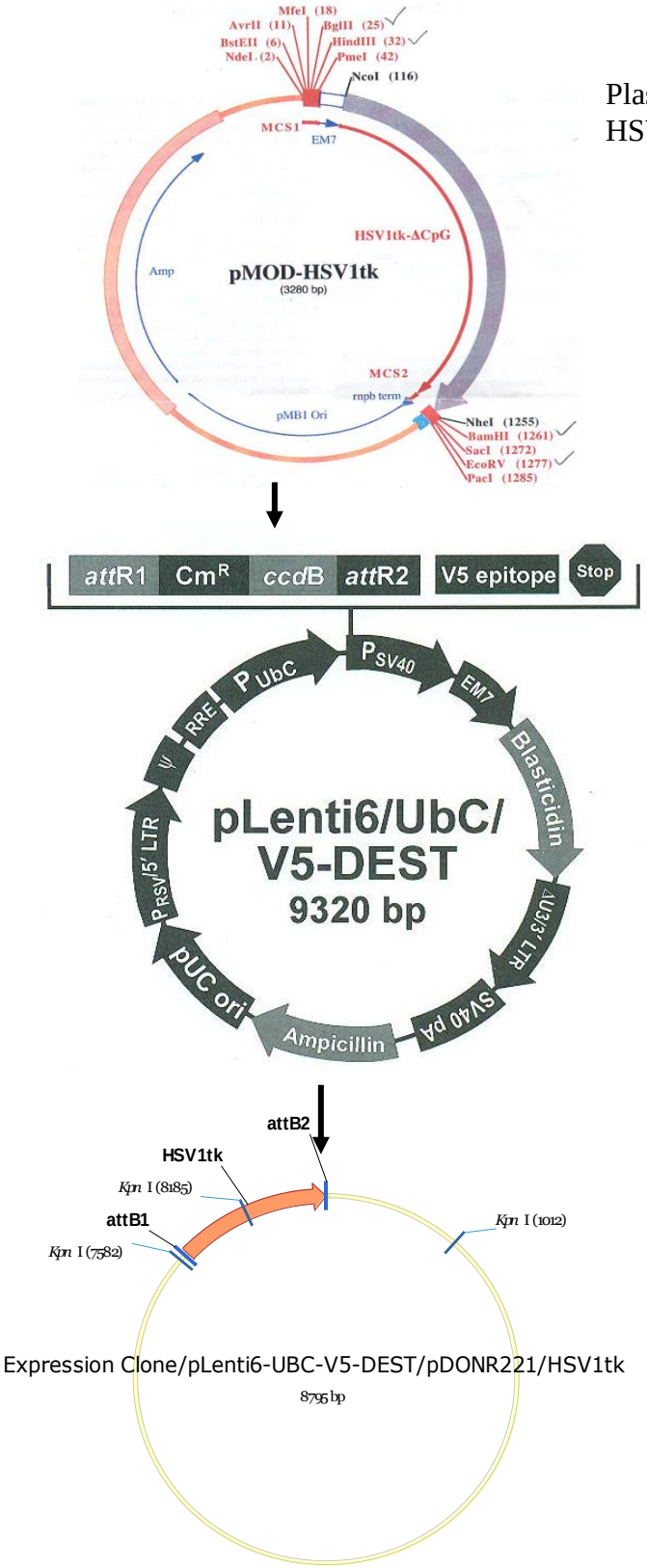

Plasmid map of pMOD-HSV1tk

Lentiviral plasmid map in which the HSV1tk was cloned to.

The final vector after cloning which was used for Lentivirus construction

Figure 8 the pMOD-HSV1tk was cloned to pLenti6/UbC/V5/DEST and the result is pLenti6-UBC-V5-DEST/pDONR221/HSV1tk (HSV1tk-Lentiviral vector).

4.4.2.2.3. Creating stable transduced cell line

HSV1tk-Lentiviral vector contains Blasticidin resistant gene instead of GFP as a selection marker. Therefore a stable transduced cell line was created before T lymphocytes were transduced. Three cell lines were used: Jurkat, HEK 293, and 4T1 breast carcinoma tumor cell line.

4.4.2.2.4. Transduction procedure

Cells were plated at concentration of 9.2 $x10^5$ in 2.5 ml of their complete media in 6 well plate in duplicate. The virus stock was diluted in Opti-EMM reduced serum medium (Invitrogen) (10 µl of the virus stock to 500µl of the media). The multiplicity of infection (MOI) defined as the ratio of virus particles to the cell number was equal to 10. Polybrene (Millipore) at concentration of 8µg/ml was added just before the virus stock was added to cells. The diluted virus was added as 500 µl/ well gently drop by drop and cells were incubated at 37 ^{0}C for 24 hours. Then cells were washed 3 times with their media was then incubated at 37 ^{0}C for 5 days to allow the HSV1tk gene expression. The cells were split every other day and kept at concentration of 1 $x10^6$ /ml.

4.4.2.2.5. Selection of stable transduced cells using Blasticidin

As the pLenti6-UBC-V5-DEST/pDONR221/HSV1tk vector has a Blasticidin resistance gene, all transduced cells should be resistant to Blasticidin. Based on this, Blasticidin (Invitrogen) was used to select only stable transduced cells. To know the optimum concentration of Blasticidin that will kill all cells, different concentrations of Blasticidin (1, 2, 4, 6 and 8µg/ml) were added to cells (25 % confluent) in 6 well plate. Viability assay was performed every 3 days and fresh media with Blasticidin at the same concentration was added. Cells were incubated with Blasticidin for 14 days. The optimum concentration for each cell line was determined. Then it was added on day 5 post transduction to all cell lines and cells were incubated for 14 days. This experiment was

repeated 2 to 3 times to make sure all transduced cells were selected. The transduced cells were cultured for several weeks and some were frozen for following experiments

4.4.2.2.6. Confirmation of the presence of HSV1tk in the stable transduced cells by RT-PCR

To confirm the presence of the HSV1tk gene in the stably transduced cells, Real-Time quantitative polymerase chain reaction (RT-PCR) was performed. Total RNA was extracted from Jurkat, 4T1, and HEK cells (8 to 10 million of each) using Trizol reagent (Invitrogen). The extraction procedure followed the reagent protocol. Then the RNA was purified using RNeasy mini kit (Qiagen) following the kit protocol. The RNA concentration and purity was measured using spectrophotometer. The purity in most of our experiments was 1.8. The RT-PCR experiments were performed using the ViiA 7 system (Life Technologies) and TaqMan One Step PCR Master Mix Reagents Kit (Applied Biosystems). All the samples were tested in triplicate under the conditions recommended by the fabricant. The cycling conditions were: 48 ^{0}C/30min; 95 ^{0}C/10min; and 40 cycles of 95 ^{0}C/15sec and 60 ^{0}C/1min. HSV1 tk primers: forward: CTCATGGCATGGGCAAGAC**,** reverse: CTCCTAGCACTCTCCAGTAGGTCAT,

probe: ACCACTCAACTGCTGGTGGCACTGG. Mouse beta actin was used as a housekeeping gene for normalization. Beta actin primers: forward: ACG GCC AGG TCA TCA CTA TTG, reverse: TCA CAC TTC ATG ATG GAA TTG AAT G. TaqMan probe: FAM- CCA GCC TTC CTT CTT GGG TAT GGA ATC CT – TAMRA

Reactions were performed in the VCU Nucleic Acid Research Facilities.

4.4.2.2.7. Detection of the HSV1tk expression in the stably transduced cell lines by Western blot

Transduced and untransduced cells (Jurkat, HEK and 4T1 (10 x 10^6 of each)) were lysed after 2 rounds of selection period using Blasticidin post-transduction and the total protein concentration was calculated using a protein assay kit; then western blot was done using 300 µg of the total protein as explained previously.

4.4.2.2.8. Radiosynthesis of [^{124}I]-FIAU (synthesis, mechanism of trapping by cells and characterizations)

[^{124}I]-FIAU was synthesized as described previously [64] with some modifications as shown in Scheme 2. Briefly, ^{124}I was produced on the IBA Molecular cyclotron using the ^{124}Te(p,n)^{124}I nuclear reaction on an enriched $^{124}TeO_2/Al_2O_3$ solid target. The 2'-fluoro-2'-deoxy-1-β-D-arabinofuranosyl-5-(tri-*n*-butyltin)-uracil (FTBSnAU) precursor (0.5 to 1 mg) was dissolved in 50 µL methanol and added 1 to 15 mCi (100 µL 0.1 M NaOH), followed by the addition of a 100-µL mixture of 30% hydrogen peroxide/ acetic acid (1:3, v/v). Reaction mixture was sonicated for 20 min at room temperature. After confirmation by radio- Thin Layer Chromatography (radio-TLC) (BIOSCINCE AR-2000) and radio-High Performance Liquid Chromatography (radio-HPLC) (Waters 1525), aqueous saturated sodium metabisulfate (100 mL) was added to quench the reaction. Then the reaction mixture was loaded onto a preconditioned (10mL water-ethanol-water) tC_{18}-1gm Sep-Pak cartridge system (Waters, Milford, MA). The tC_{18} cartridge system was eluted with water (5 mL), followed by methanol (3–4 mL) to isolate the ^{124}I-FIAU. The methanol was evaporated and the ^{124}I-FIAU was formulated in PBS for *in-vitro* and *in-vivo* study. Final product was analyzed by Rado-TLC and Radio-HPLC by co-elution with FLT standard. The

radiolabeled product was isolated in 95% radiochemical yield, with radiochemical purities of 97%.

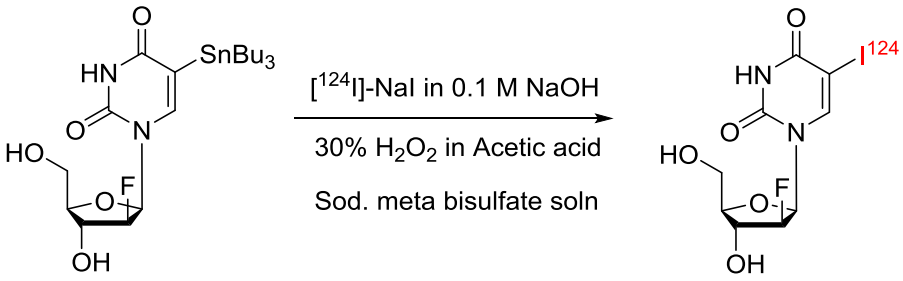

Scheme 2: Radiosynthesis of [^{124}I] FIAU

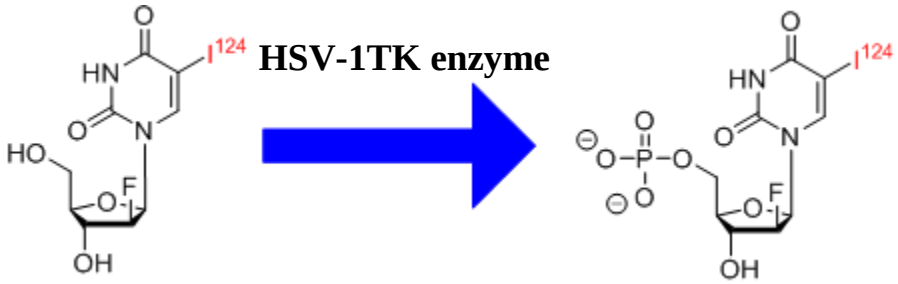

[^{124}I] FIAU free **[^{124}I] FIAU trapped in the cell**

Scheme 3 Mechanism of [^{124}I] FIAU trapping by cell**.** Viral Thymidine kinase enzyme (HSV-1TK) transfers a γ phosphate group from ATP to the 5' hydroxyl group of pyrimidine deoxynucleosides. The lipophilic tracer diffuses into the cell and is phosphorylated by HSV1-TK enzyme activity, and trapped within the cell.

Radio-TLC was performed using radio–thin-layer chromatography (silica gel plates [Sigma-Aldrich, St. Louis, MO]; eluent, ethyl acetate/acetone/H_2O, 14:8:1) as shown in Figure 9.

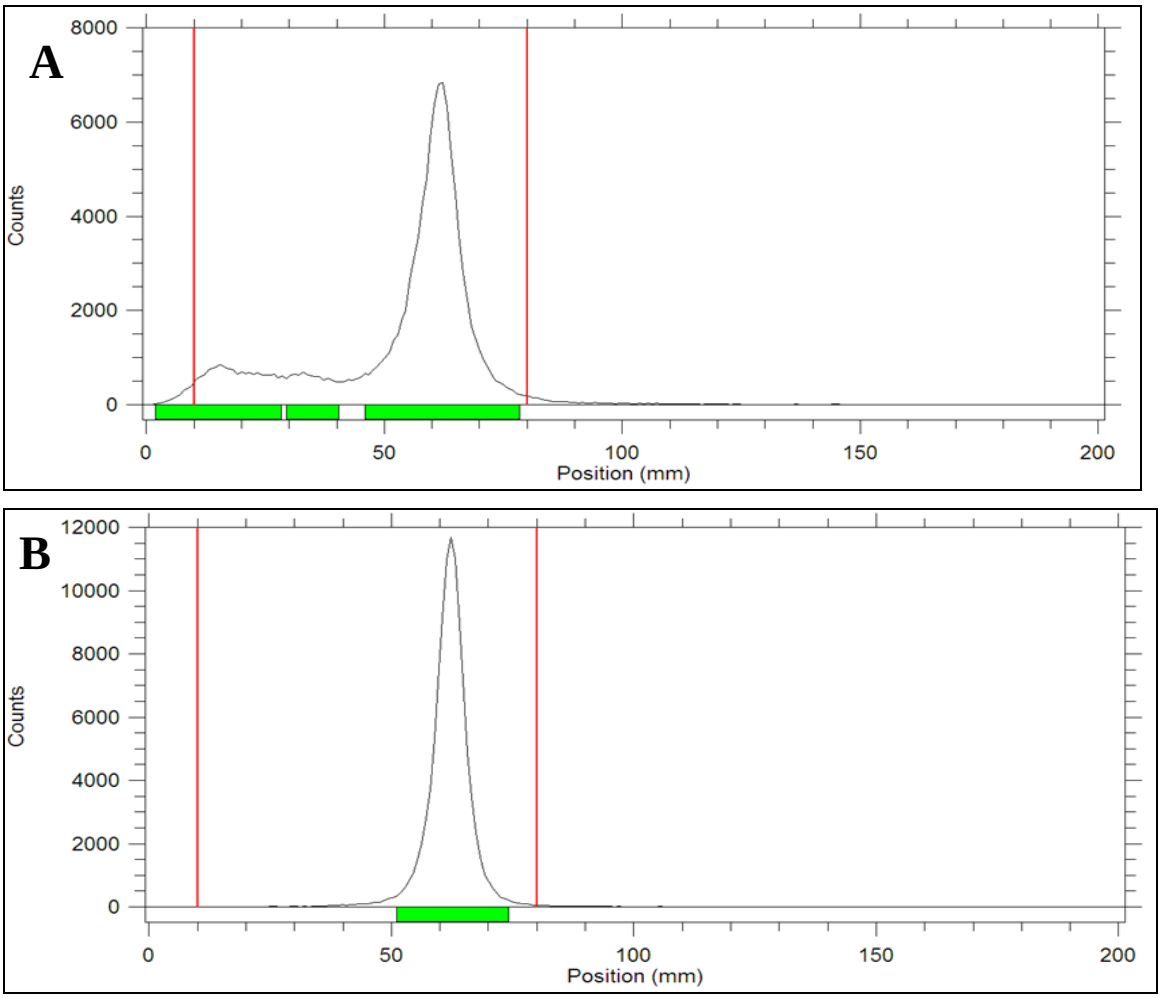

Figure 9, Radio-TLC of [^{124}I]-FIAU before purification (panel A) and Radio-TLC of [^{124}I]-FIAU after purification (panel B).

Radio-HPLC analysis: The [^{124}I]-FIAU was analyzed by radio-HPLC using the following conditions: using column C-18 luna Phenomenex 5µ C18 150 x 4.6 mm, mobile phase 10% Ethanol in 0.05 Molar NaH_2PO_4 at flow rate 1 mL/min, UV 2254 nm. The radiochemical identity was confirmed by co-injections with non-radioactive standard FIAU compound (Figure 10), and gave the same retention time as [^{124}I]-FIAU, = 8.6 min.

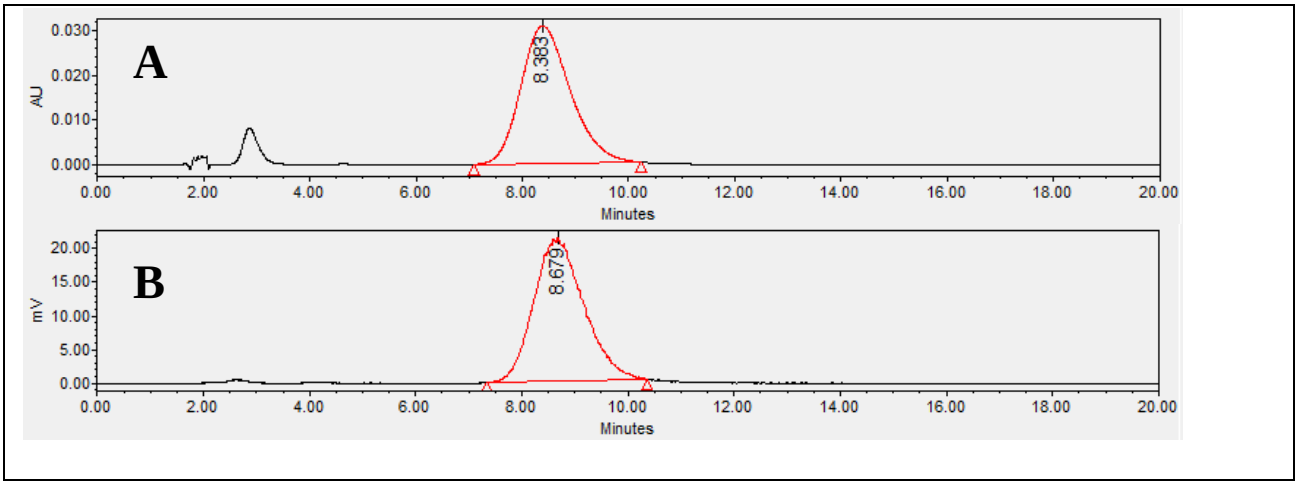

Figure 10, HPLC profile of [^{124}F]-FIAU (panel A) spiked with standard cold FIAU (panel B).

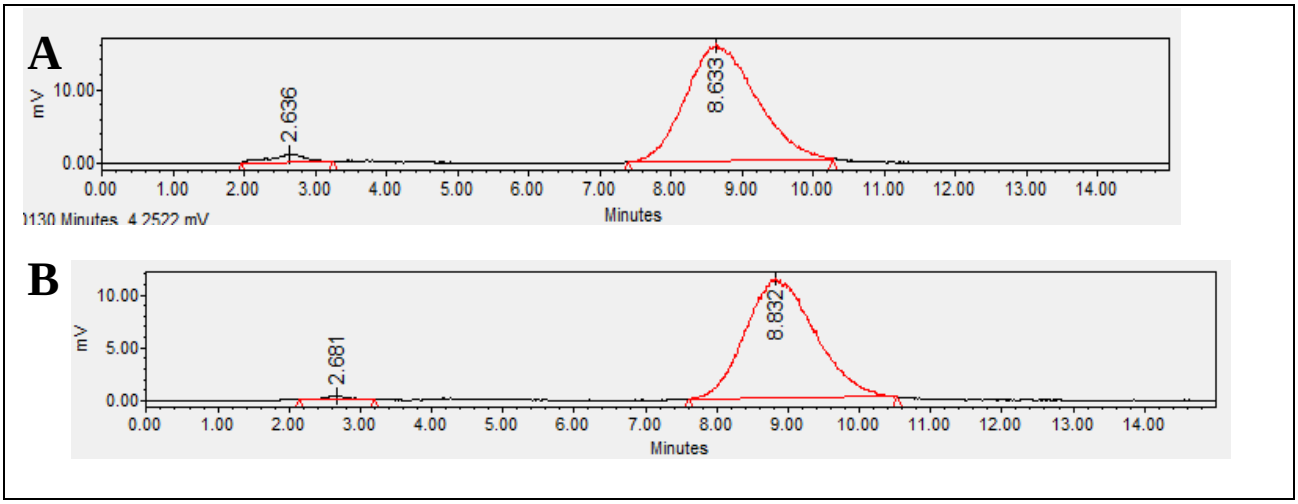

Figure 11, HPLC profile of [^{124}F]-FIAU (A) before Sep-Pak purification, and after Sep-Pak purification (B).

4.4.2.2.9. ^{124}I- [FIAU] uptake by Jurkat, 4T1 and HEK cells

Transduced and untransduced Jurkat cells were put in gamma counting tubes at a concentration of $5x10^6$ / 3 ml of media in triplicate. Transduced and untransduced HEK 293 and 4T1 cells were plated in 12 well plate at of 300 $x10^5$ cells / 2 ml of media in triplicate. ^{124}I- [FIAU] was added at concentration of 1µci/ml. Cells were incubated at 37 ^{0}C for different time points (1, 2, 4 and 18 hours). After each time point cells were spun at 1500 rpm at 4 ^{0}C for 8 minutes and cell

supernatant was collected for counting. Cells were washed 3 times with PBS and all wash was collected for counting. 50µl of cold PBS was added to the cell pellets and 50 µl of the supernatant and the wash was taken for counting. The % of cell uptake was calculated as following:

% uptake = (CPM of cell pellets)/ (CPM of sum of cell pellet, cell supernatant, cell wash) multiplied by 100

4.4.2.2.10 T lymphocytes transduction

T lymphocytes were isolated, activated and expanded as described previously. After the 18 hours incubation with Bryostatin/Ionomycin (B/I) cells were washed three times with warm, complete RPMI and resuspended at 1–2 x 10^6 cells/ml with 40 U/ml of IL-2 or with IL-7 and IL-15 (10 ng/ml each) for 48 hours . On day 3 post expansion, cells were transduced with HSV1tk Lentivirus at different MOIs (10, 5, 2, 1, 0.2 and 0.03) to determine the best MOI for our in vivo studies. Cells were then plated at 1x10^6 cells /ml in 24 well plates. Polyberene (as transfection reagent used to increase the transduction efficiency) was added at 8µg/ml just before cells were plated. Cells were incubated 37 ^{0}C for 4 hours. Then cells were washed with media 3 times and incubated at 37 ^{0}C for 6-7 days. Cells were resuspended and fresh media with fresh cytokines was added every other day and cells kept grown at concentration 1-2 x10^6/ml.

4.4.2.2.11. Detection of HSV1tk expression in transduced T lymphocytes

To check if the T lymphocytes were successfully transduced or not, real time PCR and western blot were performed as follow:

In order to determine the changes in the expression level of HSV1tk with time, on days 1,3,5,and 7 post transduction, transduced and untransduced IL-2 and IL-7/15 at were collected and counted and about 20 x 10^6 of each were used for real time -PCR. The procedure was done as described previously.

The HSV1TK protein was detected using Western blot assay. Transduced and untransduced IL2 and IL7/15 T cells (25 x 10^6) were lysed and the total protein concentration was calculated using protein assay kit; then western blot was done using 300 µg of the total protein as explained previously.

4.4.2.2.12. Transduced T lymphocytes proliferation and viability

Cell proliferation was assessed based on cell number and fold increase calculation every other day. Fold increase was calculated as the ratio of cell number each other day compared to the cell number immediately after pulsing with B/I.

The cell viability at different MOIs was assessed using Cell Titer Glo Luminescent assay kit at different time points post transduction. Transduced and untransduced cells were plated in triplicate 96 well plates at 25000cells/100µl of media. The kit reagents were mixed and added to cells according to the kit protocol then was read by the plate reader (DTX 880 Multimode detector Beckman Coulter) at 580 nm. The % viability was calculated for each group in comparison to unlabeled cells and expressed as % of viability.

4.4.2.2.13. Transduced T lymphocytes phenotyping

To investigate whether there is any effect of the transduction on the T lymphocyte phenotype; T lymphocytes were stained and tested using flow cytometry. Four groups of T cells (IL2 untransduced and transduced cells, and IL7/15 transduced and untransduced cells) were double stained with CD8 or CD4 /CD62L or CD8 or CD4/CD69 antibiotics. One million of cells for each group was used in duplicate and stained with PECY5 anti mouse CD4 antibody, FITC anti mouse CD8 antibody, PE anti mouse CD69 antibody and PE anti mouse CD62L antibody (Bio Legend). The antibody concentration was 1µg/million of cells and FC (CD16/ CD32) block was used at the same concentration to remove any non-specific staining. Cells were resuspended in 2% FBS in

1X PBS and incubated with the antibodies for 30 minutes in a dark room, then spun and washed twice in 1X PBS with 2% FBS. Cells were tested using flow Cytometry to compare the percentages of CD8/CD69 and CD8/CD62L between transduced and untransduced cells.

4.4.2.2.14 Interferon- γ production pre and post transduction

To examine the interferon-γ production from T lymphocytes before and after transduction, the ELISA assay was performed. 4T1 tumor cells were irradiated using Gamma cell 40 Exactor system (10,000 rad for 30 to 60 minutes) to stop their proliferation. The irradiated cells were counted and brought to 1 x 10^6 /ml. On day 6 post transduction, the transduced and untransduced T lymphocytes (grown in IL2 or IL7/15) were plated in 24 well plates at 2 x 10^6 / 2 ml concentration. The irradiated 4T1 cells (200µl) were added to each well (1:10 dilution) and incubated overnight at 37 ^{0}C. The interferon-γ (INF-γ) protein released into supernatants was collected and assayed using BD OptEIA mouse INF- γ ELISA kit (BD Biosciences, San Jose, CA). All samples were tested in duplicate and 8 groups were analyzed: 1) transduced IL2 T lymphocytes + 4T1 cells, 2) untransduced IL2 T lymphocytes + 4T1 cells, 3) Nil transduced IL2 T lymphocytes, 4) Nil untransduced T lymphocytes, and similar 4 groups for IL7/15 T lymphocytes. (Nil stands for T cells incubated alone without irradiated 4T1 cells).

4.4.2.2.15. ^{124}I- [FIAU] uptake by T lymphocytes

Transduced T cells (IL-2 and IL-7/15cells) and transduced Jurkat cells were put in gamma counting tubes at concentration of 5x10^6 /3ml of their media in triplicate. ^{124}I- [FIAU] was added at concentration of 1µCi/ml. Cells were incubated at 37 ^{0}C for different time points (1, 4 and 18 hours). After each time point, cells were spun at 1500 rpm at 4 ^{0}C for 8 minutes and cells supernatant was collected for counting. Cells were washed 3 times with PBS and all wash was collected for counting. 50µl of cold Lysate buffer (RIPA lysate buffer) was added to the cells

pellets and 50 µl of the supernatant and the wash was taken for counting. The % of cell uptake was calculated as following:

% of uptake = CPM of cell pellet/ CPM of sum of cell pellet, cell supernatant, cell wash multiplied by 100.

4.4.2.2.16. Multi-labeled T lymphocytes trafficking and imaging (Optical & PET)

Transduced and untransduced IL2 and IL7/15 T cells were labeled with DiR at 320µg/ml concentration as described previously. For development of tumor models, animals were inoculated subcutaneously into the right flank with 4T1 breast carcinoma tumor (5×10^4) and allowed the tumor to grow for 10 days. One day before injection of labeled T cells, animals were pretreated (ip) with 100mg/kg Cyclophosphamide to reduce the number of T regulatory cells by increasing the number of effective CD8 and CD4 cells. The transduced and untransduced T cells were prepared (10×10^6 in 0.5 ml PBS per animal) and injected i.v. via tail vein into four groups of animals (IL2 transduced-6 animals, IL2 untransduced-3 animals, IL7/15 transduced-6 animals and IL7/15 untransduced-3 animals) were injected (tail vein injections) with ^{124}I [FIAU] (activity between 300 to 500 µCi). Because the imaging time was carried out for two weeks and the half-life of ^{124}I is 3.8 days, the activity of ^{124}I [FIAU] was injected in the first and second week of imaging. The multi-spectral fluorescence imaging was established as described previously.

4.4.2.2.17. Biodistribution study

In order to track and localize the transduced T cells post ^{124}I [FIAU] injections into the four groups of animals, biodistribution study was carried out at different time points (day 3 and day 10 post radionuclide injections). Animals were dissected on day 3 post first radionuclide injections (3 animals from each transduced cells group) and the other 3 animals with the untransduced cells groups were dissected on day 10 of imaging and it was day 3 post the second injection. Most of

the animal tissues were collected and their activities in CPM were measured using Gamma counting system (1282 COMPUGAMMA CS universal Gamma counter). The % ID/g of each tissue was calculated using the following formula:

% ID = 100 x tissue activity (µCi) / injected activity (µCi) x tissue mass (g)

Tissue activity in µCi was calculated from tissue activity in CPM converted to dpm using efficiency factor as following:

dpm = CPM / efficiency factor , 1 µCi = 2.22 x 10^6 dpm.

Efficiency factor was calculated by measuring 4 different activities of [^{124}I] FIAU (2.1399±0.7912, 2.7959±0.6867, 4.1044±0.5687 and 3.1908±0.6438) in µCi using Gamma Spectrophotometer system (ORTEC-50 AMETEK) and same activities were measured in CPM by gamma counter. Then DPM was calculated by multiplying activities measured in µCi by 2220000. The efficiency factor is CPM/DPM, which is 0.31 for ^{124}I in our measurements and was used for our Biodistribution study calculations.

4.4.2.2.18. Detection of HSV1TK at some organs in vivo

Some of the organs (liver, lungs, spleen, tumor and lymph nodes) were collected after animal dissection and immediately were snap frozen in liquid nitrogen. Protein assay and Western blots were performed as described previously to verify the localization of transduced T cell at these organs.

4.5. Studying the trafficking pattern of T lymphocytes to 4T1 metastasis

The final objective in this project was, to study the trafficking pattern of IL2 and IL7/15 T cells to 4T1 tumor metastasis. 4T1 cells were successfully transduced with HSV1tk gene as verified by RT-PCR and western blot. Transduced 4T1 cells were implanted in the abdominal fat mammary pad of some of animals (orthotopic tumor) and others were implanted in the right flank of the

animal and untransduced 4T1 tumor was implanted in the left flank. PET imaging was performed on the third and fourth week post tumor implantation. Firefly-luciferase expressing T cells were provided kindly from Dr Bear's lab and injected i.v. on the third week post 4T1 implantation into the abdominal fat mammary pad animals and bioluminescence imaging were performed for one week. Then animals were dissected and Western blot of some organs was performed.

4.6. Statistical analysis

The significant differences in the *ex vivo* and *in vivo* studies were determined using the equal variance analysis (ANOVA) (JMP software), or Student's t-test. P value of < 0.05 was considered as statistically significant difference. The data shown in graphs are mean ± SEM.

Chapter Five: Results

5.1. Direct labeling of T lymphocytes using DiR probe

5.1.1. DiR signal detection and labeling efficiency

To test how long the DiR signal is maintained after staining of cells, DiR labeled T lymphocytes were cultured and imaged at different time points. DiR labeled cells (0.5 or 1.0 x 10^6 per well) were washed and plated in 6 well plates at each and time point then imaged up to 9 days. The result showed good signal maintenance and detection for more than one week (Figure 12, panel A). The efficiency of DiR labeling of T cells was tested using flow Cytometry (Figure 12 panel B). The result showed that nearly 100% of cells were labeled.

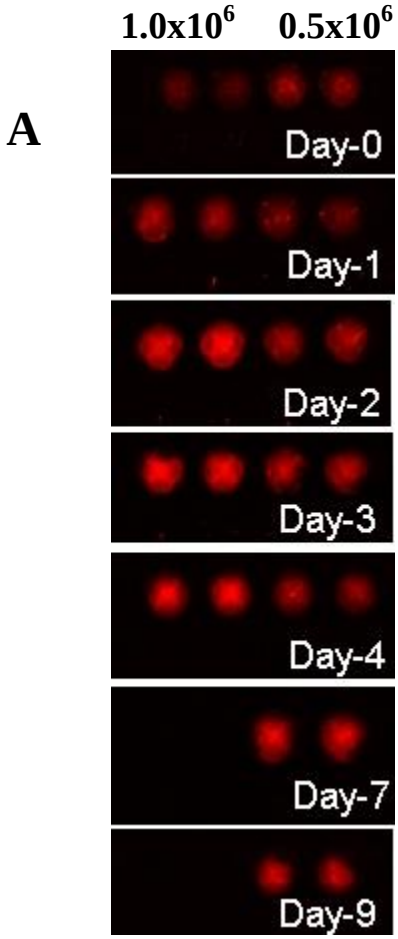

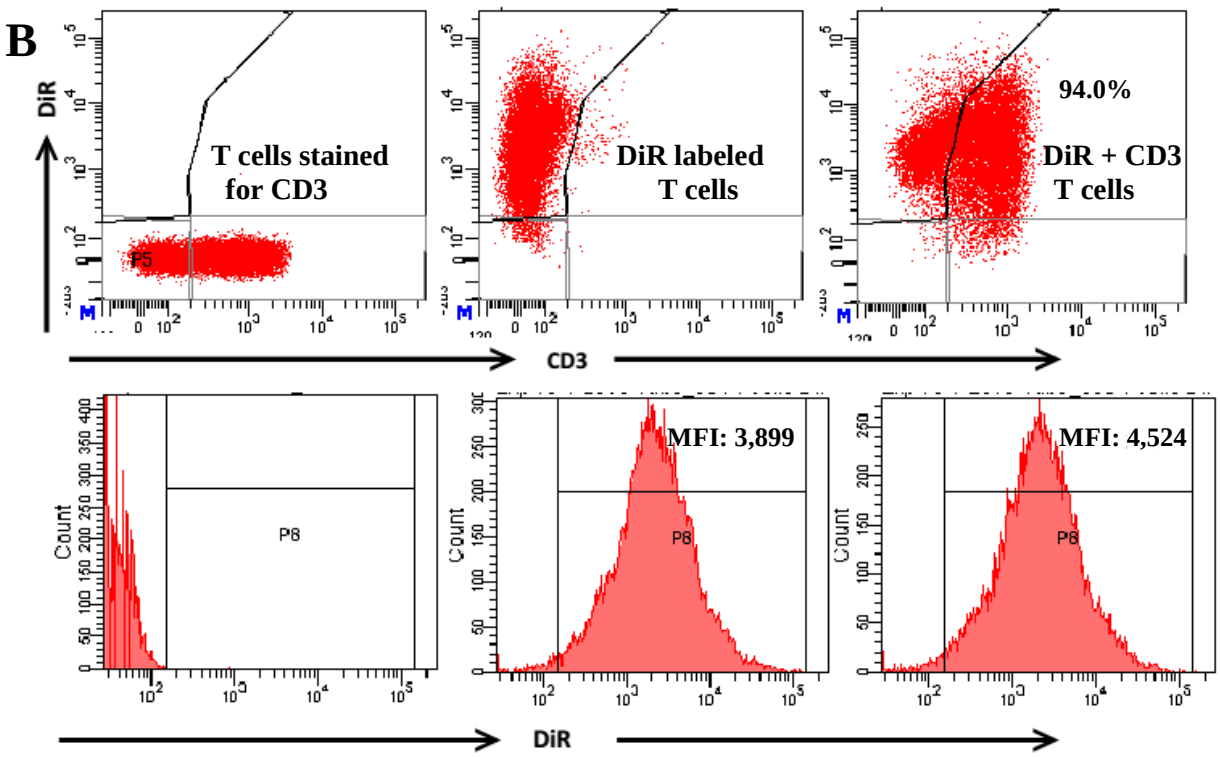

Figure 12 DiR labeled T cells were imaged at different time points up to day 9 (Panel A). DiR labeled T cells showed detectable signal for more than one week. On days 7 and 9 only few cells were left, that's why only half million of cells were plated. Even on day 9 the DiR signal looks stronger than previous days, because of the fluorescence quenching phenomenon. This means decrease of the fluorescence signal given from too much intense fluorescence material. In our case, as cells divided the DiR is diluted with each division and the DiR become more and more diluted (less intense) leading to prevent fluorescence quenching and increase DiR fluorescent signal. Panel B is flow cytometry data showed that the mean fluorescent intensity (MFI) is increasing with DiR labeled CD3 T cells and the labeling efficiency with DiR is 94 %.

5.1.2. DiR labels T cells with negligible transfer to tumor cells

DiR has two long 18- carbon chains that insert into the cell membrane, which showed specific and stable cell labeling with negligible transfer between cells. To test this property of DiR, T lymphocytes were labeled with DiR and incubated with 4T1 tumor cells for 24 hours in 6 well plates. Then DiR labeled T cells were washed out from 4T1 cells wells (T cells are flouting cells and 4T1 are adherent cells). Multi-spectral fluorescent imaging system was used to image the plates (Figure 13). The DiR signal was clearly detected in the DiR T cell well, but not in the DiR

T cells + 4T1 tumor cells well, indicating that, DiR specifically labeled T cells and did not transfer to 4T1 tumor cells.

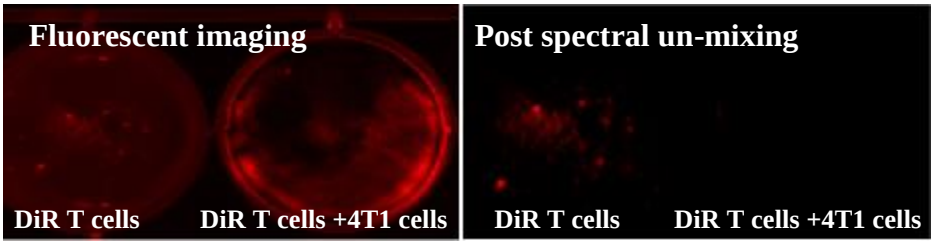

Figure 13 DiR labeled T cells incubated with 4T1 tumor cells for 24 hrs, showed negligible to no transfer between both cells. (Post Spectral un-mixing refers to auto fluorescence signal subtraction and show only DiR signal)

5.1.3. Cell proliferation pre and post labeling were comparable

The proliferation of 4T1 sensitized T lymphocytes isolated from tumor DLN activated with B/I and expanded in IL-2 or IL-7 + IL-15 containing media was observed for 10 days. Since the number of T lymphocytes from day 6 was high (figure 14), these cells were labeled with DiR to be adoptively transferred into 4T1 tumor bearing mice, and the effect of labeling cells with DiR on proliferation was determined. The results confirmed that, cells labeled with DiR showed similar proliferation as the unlabeled T cells (Figure 14). Both unlabeled and labeled cells continue to proliferate at the same rate until day 4 post-labeling (day 10 of expansion). These results showed that labeling of cells with DiR does not affect the proliferation of the T lymphocytes grown in the presence of IL-2 or IL-7 + IL-15 even for 10 days of expansion.

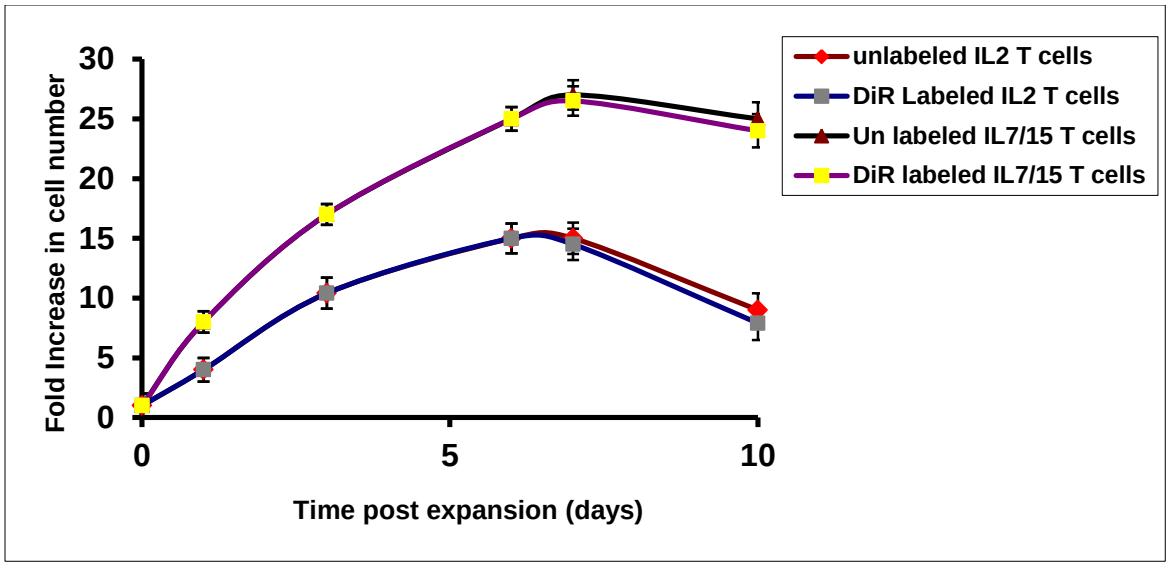

Figure 14 T cell proliferation based on viable cell counts on each day compared to the number of cells on day 1 of ex vivo expansion. Cell number was highest on day 6. Therefore, this was the chosen time for labeling. Furthermore, no significant differences between labeled and unlabeled cell proliferation post-labeling. (Fold increase in cell number is the number of cells at each day pre or post labeling compared to the cell number on day 1 directly after the activation in B/I)

5.1.4. DiR labeled cells showed 80-90 % viability when labeled using 320µg/ml of labeling solution

The viability of lymphocytes labeled with various concentrations of DiR was assessed to determine the optimum non-toxic concentration with which cells could be labeled. Since T cells which have been B/I activated and expanded in IL-2 or IL-7+IL-15 containing media for six days were used for *in vivo* studies, the viability of cells from day 6 onwards was monitored, when labeled with DiR and compared with unlabeled T cells. The results show that there were no significant differences in % viability among the various concentrations of DiR tested compared to unlabeled cells on days 1 and 4 post-labeling. However there is a significant difference ($p < 0.05$) in the viability of cells recovered on day 7 compared to viability tested at unlabeled cells and to days 1 and 4. Since on days 1 and 4 the cells were 80-90% viable even at the highest

concentration of DiR used (320 µg/ml), this concentration was used for further *in vitro* and *in vivo* studies (Figure 15 Panel A, Panel B)) as the higher amount of DiR on cell membranes is likely to allow signal retention and *in vivo* detection for relatively longer durations.

Tumor sensitized lymphocytes were labeled with 320µg/ml of DiR and on day 2 and 7 post-labeling, were incubated with Annexin V/PI to determine the cause of cell death. The flow cytometry results showed that, the cell viability of unlabeled and labeled cells was comparable (figure 16). As explained previously, cells grown in IL7/15 higher viability than cells grown in IL2 regarding of labeling.

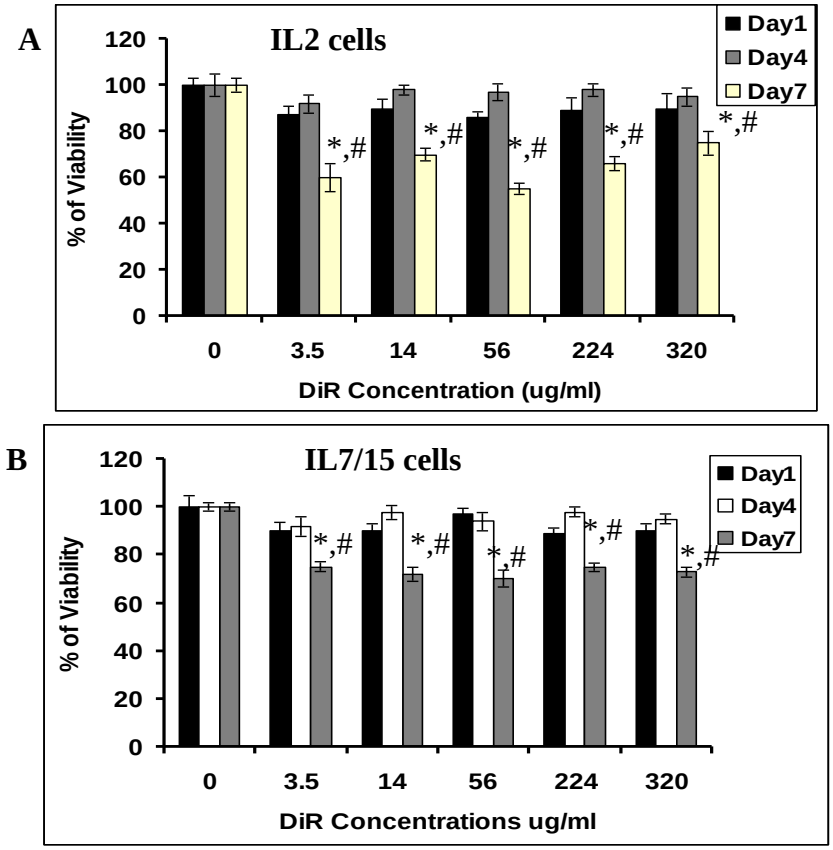

Figure 15 Percent viability of T cells labeled with various concentrations of DiR measured using Cell TiterGlo assay. Bryostatin/Ionomycin (B/I) activated 4T1-cells grown in IL-2 were labeled on day 6 of their *ex vivo* expansion. Viability of T-cells 1, 4 and 7 days post-labeling was compared with unlabeled cells and expressed as percent viability. * and # means there is a significant difference in the cell viability between day 1 to day 7 and day 4 to day 7 respectively. These differences were more observable with IL2 cells than IL7/15 cells. Cells showed 80 to

90 % viability on days 1 and 4 post-labeling and no significant differences compared to unlabeled cells. On day 7 post-labeling which is day-13 post-labeling, cell viability was 60% or below and showed significant differences compared to unlabeled cells because these are primary cells and their viability decreases beyond day 10 of *ex vivo* expansion. Average ±S.D from three different experiments are shown in the graph.

Day 2 post DiR labeling

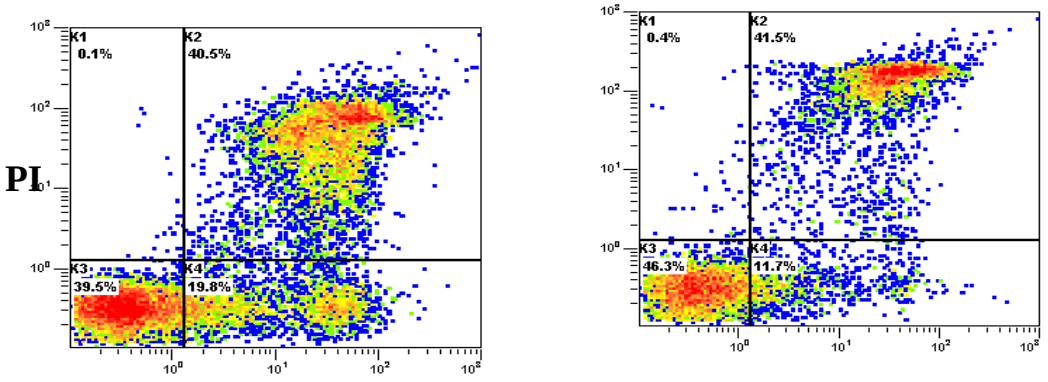

UN-labeled IL2 cells (% of viability = 39.5%) Labeled IL2 cells (% of viability = 46.3%)

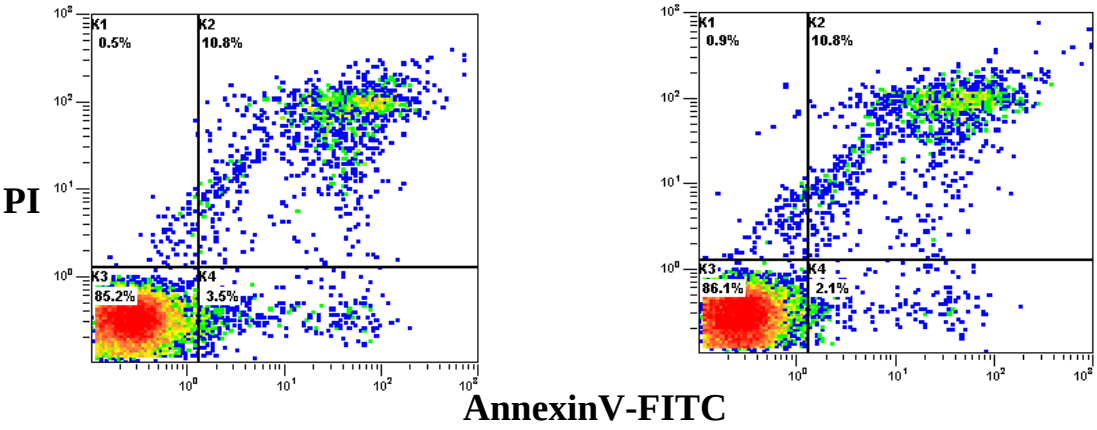

UN-labeled IL7/15 cells (% of viability = 85.2%) Labeled IL7/15 cells (% of viability = 86.1%)

Day 7 post labeling

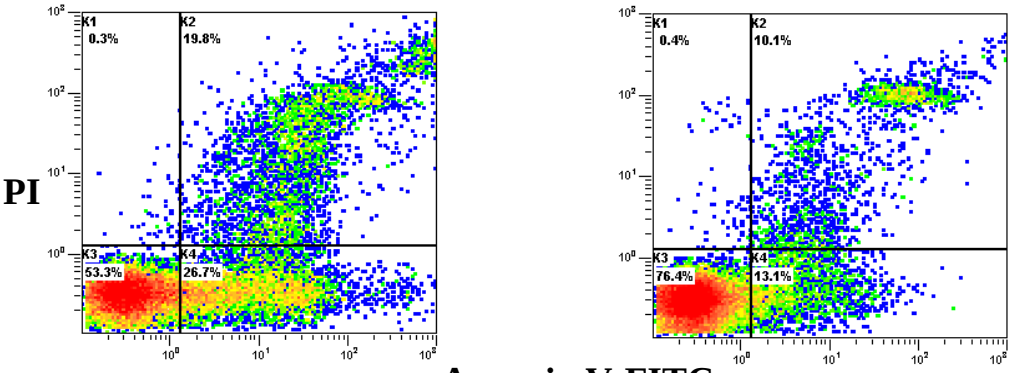

UN-labeled IL2 cells (% of viability = 63.3%) Labeled IL2 cells (% of viability = 76.4%)

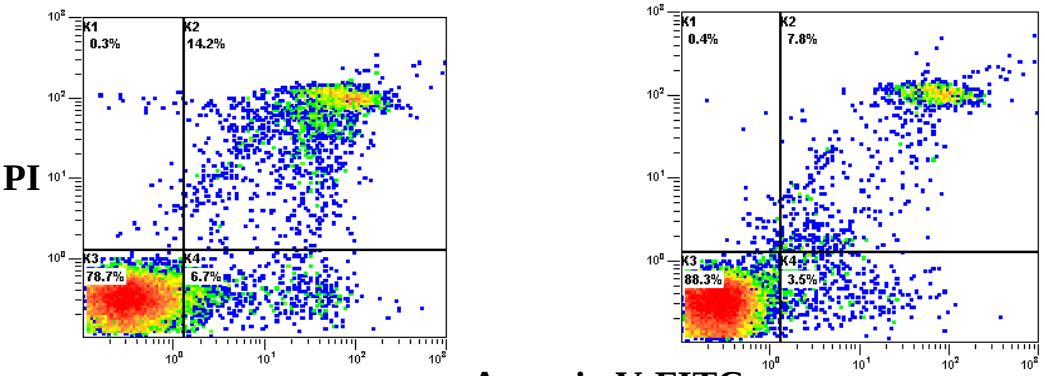

UN-labeled IL7/15 cells (% of viability = 78.7%) Labeled IL7/15 cells (% of viability = 88.3%)

Figure 16 T cells % of viability tested by flow cytometry (apoptosis kit). DiR labeled cells were tested on days 2 and 7 post labeling. All results showed that, the viability of DiR labeled cells is somehow higher than unlabeled cells, indicating that, DiR probe does not affect cell viability.

5.1.5. Interferon-γ production in *vitro* and *in vivo*

In vitro activated 4T1 sensitized T cells were expanded for 6 days, and incubated (either unlabeled or DiR-labeled) with irradiated 4T1 tumor cells or MethA tumor cells for 24 hours in IL-2 or IL7/15 containing media. The levels of IFN-γ in the supernatant were determined. The results showed that, with time there is accumulation of IFN-γ in the media but there is no significant difference in the IFN-γ levels in the supernatant of T cells, incubated alone compared to T cells incubated with non-specific Meth A tumor (Figure 17 panels A & B) on respective days. However, T cells incubated with 4T1 tumor cells showed significantly higher release of

IFN-γ into the media ($p<0.05$) than cells incubated alone (Nil cells) or with Meth A tumor. Since no significant differences in cytokine levels released were observed between unlabeled and labeled T cells, the data also demonstrate that labeling the cells with DiR does not affect their interaction with tumor cells. Figure 17 panel C shows that, the amount of IFN-γ in the mice bearing 4T1 tumor which have been injected with labeled T cells, is higher in their blood serum compared with mice bearing 4T1 tumor only (no T cells infused) and mice bearing Meth A and which have been injected with labeled T cells.

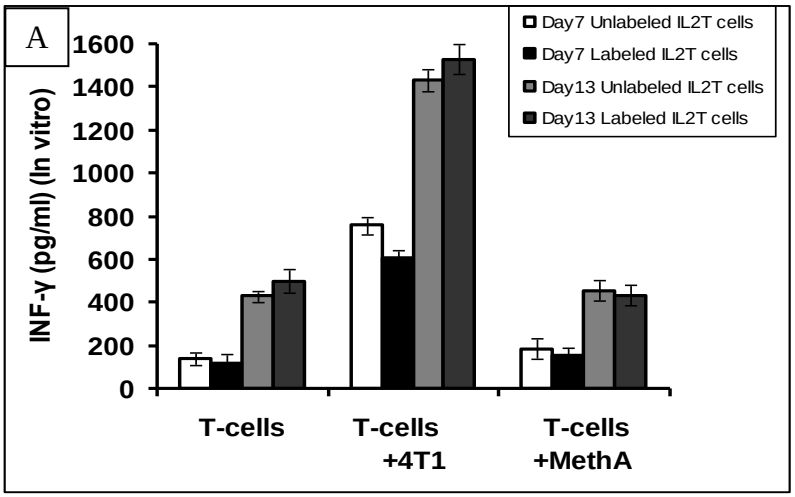

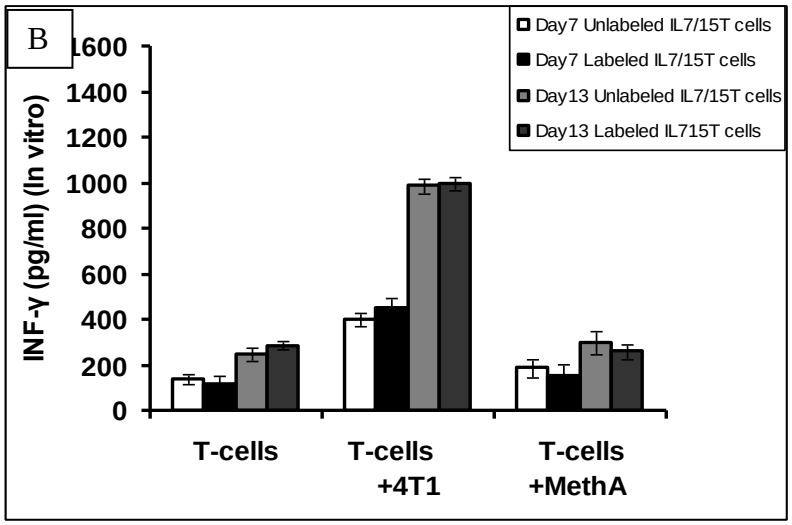

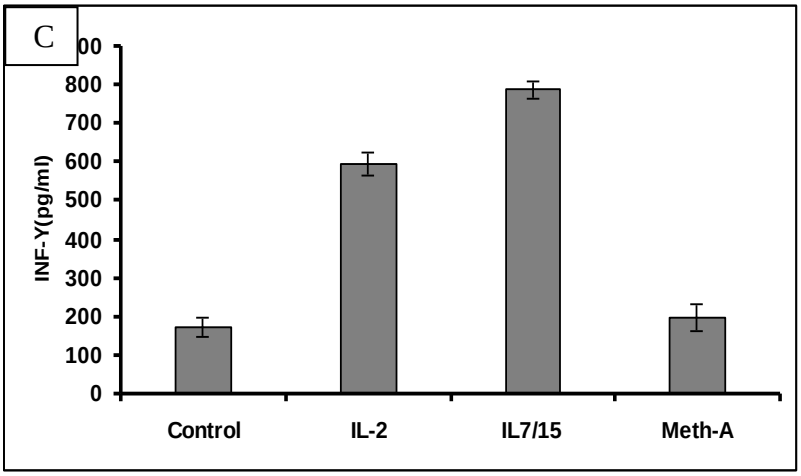

Figure 17 The amount of interferon-γ released in the cells supernatant and *in vivo* mice serum showed higher amount of this cytokine in both cases, when the 4T1 specific T cells or in the mice injected with 4T1 specific T-cells compared to other groups as shown in panel A, B and C.

5.1.6. Multi-spectral fluorescent imaging of T cell trafficking

Adoptive transfer of DiR labeled 4T1 sensitized T lymphocytes which had been expanded in vitro for 6 days, were administrated intravenously 4 day or one week after tumor implantation. Imaging of the mice using Maestro-2, revealed homing of 4T1 sensitized lymphocytes to the site of 4T1 tumor. The signals from DiR labeled cells persisted in tumor bearing mice for up to 21 days (Figure 18A). The tumor/Background ratio (Tumor/BKG Ratio) shows that the peak signal intensity is obtained on day 6 after adoptive transfer, following which the signal intensity started to gradually diminish (Figure 18C). In contrast, when the 4T1 sensitized lymphocytes were injected into a Meth A tumor bearing mice, there was no migration of DiR labeled cells to the tumor site. This is indicated by lack of fluorescence signal obtained from the tumor site (Figure 18, panel B). This suggests that these IL-2 grown T cells are antigen specific. For T cells grown in IL7/15, their signal was lower than IL2 cells signal and peaked on day 8 (figure 20). This may due to the IL7/15 *in vivo* proliferation at the tumor site. They proliferate more than IL2 cells, which may lead to the dilution of the labeling probe and reduced signal.

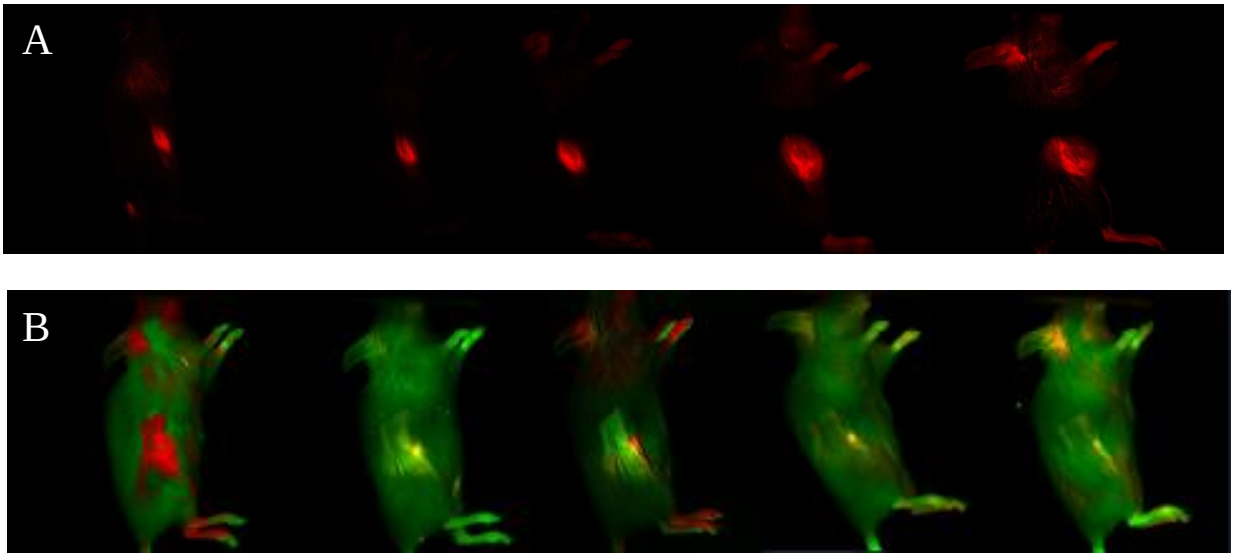

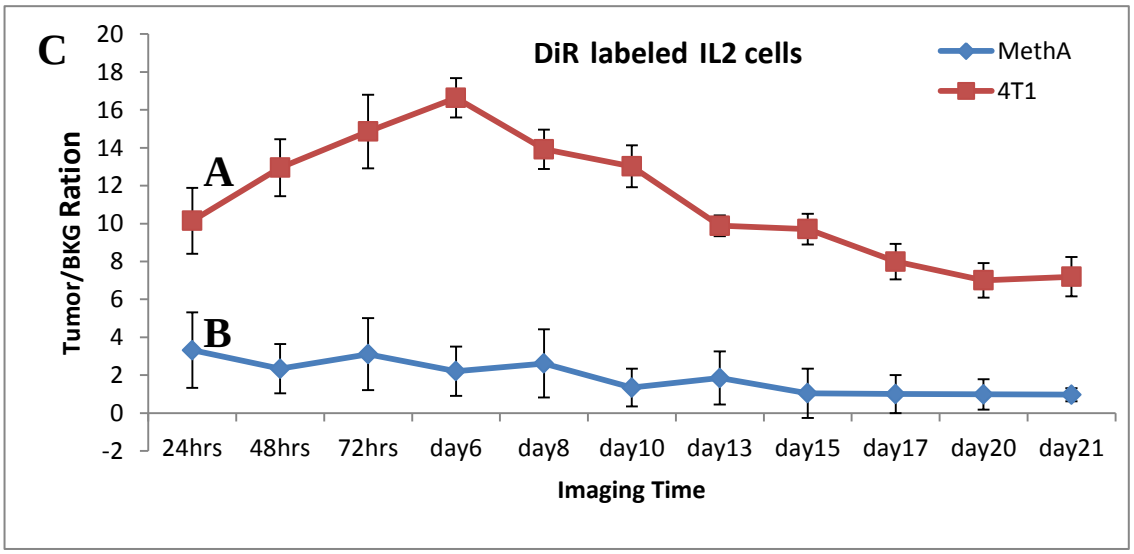

Figure 18**.** Fluorescence imaging of T cell trafficking. Homing of 4T1 sensitized DiR labeled T cells to (Panel A) 4T1 tumor site (green color codes for Autofluorescence signal , and red color codes for DiR signal), (Panel **B)** Meth-A carcinoma tumor site (used as negative control tumor) 4 days after the tumors have been implanted. Red color indicates the signal from the NIR DiR Dye used to label the T cells. (**C)** Tumor/ Background ratios graph showed that, cells localized at the tumor site on day 1 peaked on day 6 and persisted up to 21 days in the animal. While in case of Meth A tumor, there was no localization of 4T1 specific T cells at the tumor site.

To determine whether signals from DiR labeled 4T1 sensitized T cells can persist *in vivo* for a prolonged period of time, 4T1 tumor cells were introduced one week after the mice had already

received infusion of activated/expanded T cells. Interestingly, the T cells migrated to the site of tumor as early as 2 hours post injection of tumor cells and the signals from DiR tagged T cells were detectable for more than 2 weeks (Figure 19A). Further examination of the tumor/background (BKG) ratio revealed that the signal intensity had increased modestly on day 3 and then began to gradually decline (Figure 19 B).

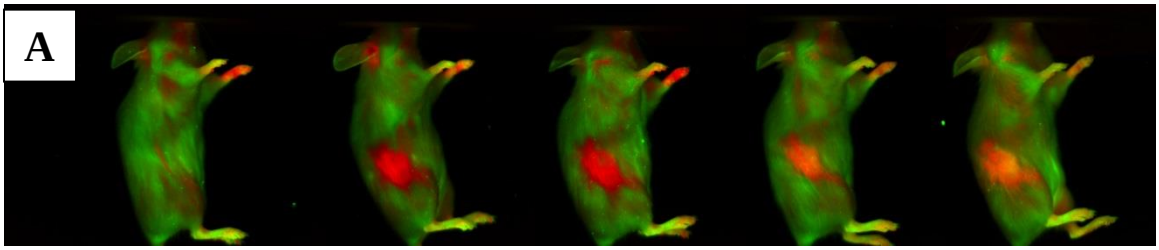

Pre- 4T1 inoculation {2 hrs 24 hrs 1 week 2 weeks}

{Post 4T1 inoculation}

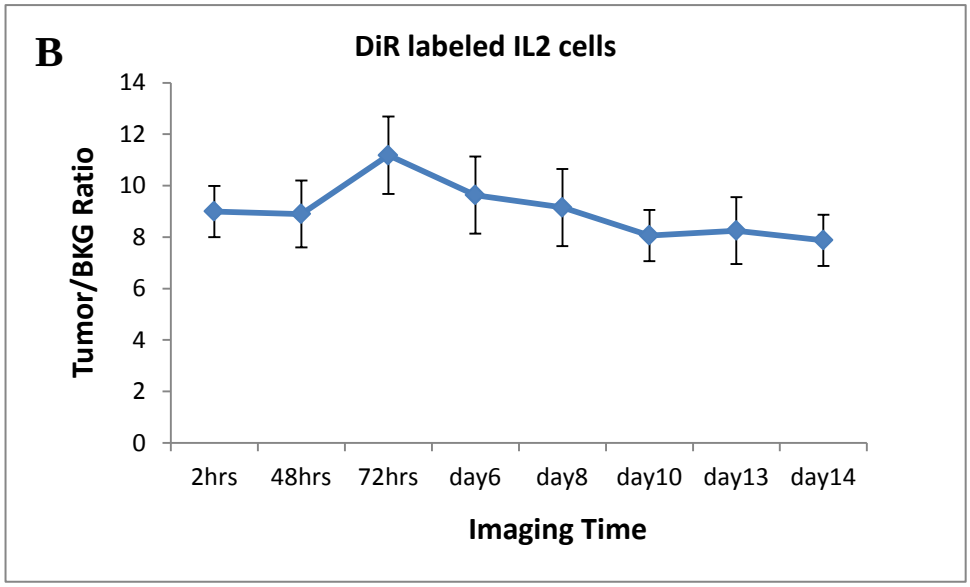

Figure 19**.** Fluorescence imaging of T cell trafficking **(A)** Adoptive of 4T1 sensitized T cells expanded in IL-2 media, injected one week prior to 4T1 challenge. The labeled 4T1 specific T cells were able to leave the lymphoid compartment and localized at the tumor site in 2 hours. Green color denotes Autofluorescence and the Red color denotes the signal from DiR labeled lymphocytes. **(B)** Tumor/ Background ratios obtained from mice injected with T cells and

inoculated with 4T1 cells a week later. The graph showed the signal appeared on day 1 (on the 2 hours image) peaked on day 3 and persisted 21 days in the mice.

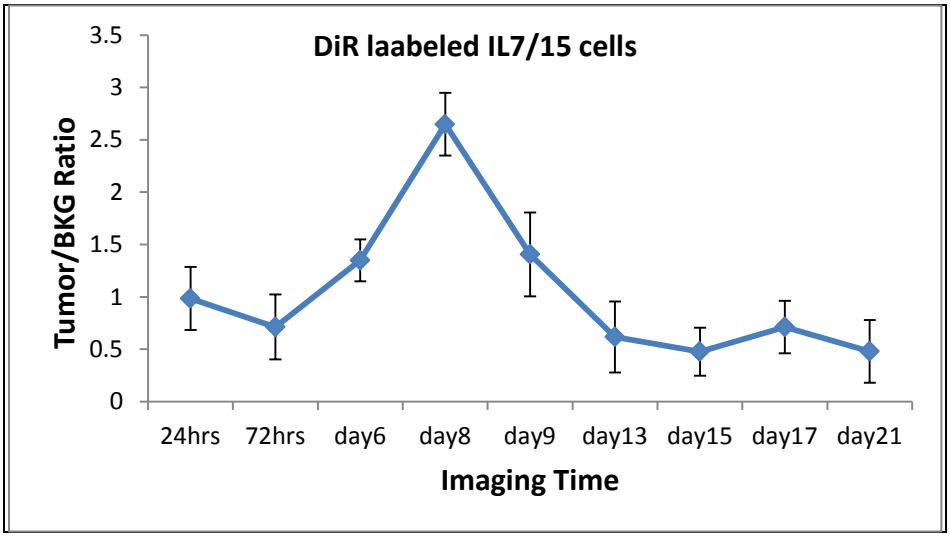

Figure 20 Tumor/ Background ratios graph of animals bearing 3 days 4T1 tumor and injected with IL7/15 cells. The graph showed that, cells localized at the tumor site on day 1, peaked on day 8 then decreased sharply with time up to 21 days in the animal.

To confirm that the signal that was detected at the tumor site was linked to viable DiR labeled T cells, a cell lysate was injected in number of animals and imaged at different time points starting from day 1 to day 14. No signal was detected at the tumor site or lymph nodes in the cell lysate group. However, there was signal detected in lung, spleen and liver because of the route of administration (i.v. injections of cell lysate). In contrast, after infusion of viable DiR labeled cells, tumor and lymph nodes showed detectable signal which increased with time, indicating that more T cells are migrated or proliferated at these sites.

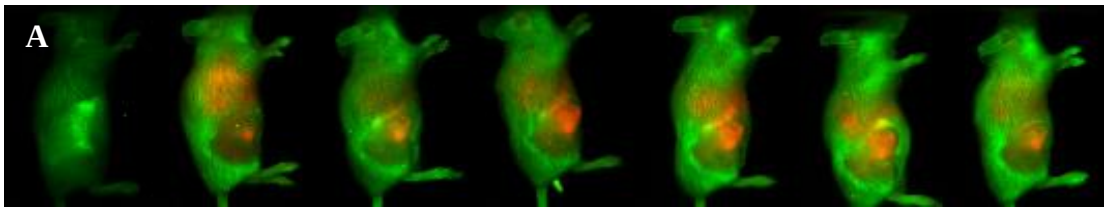

Pre IL2 T cells injection **2hrs** **24hrs** **48hrs** **72hrs** **day 6** **day14**

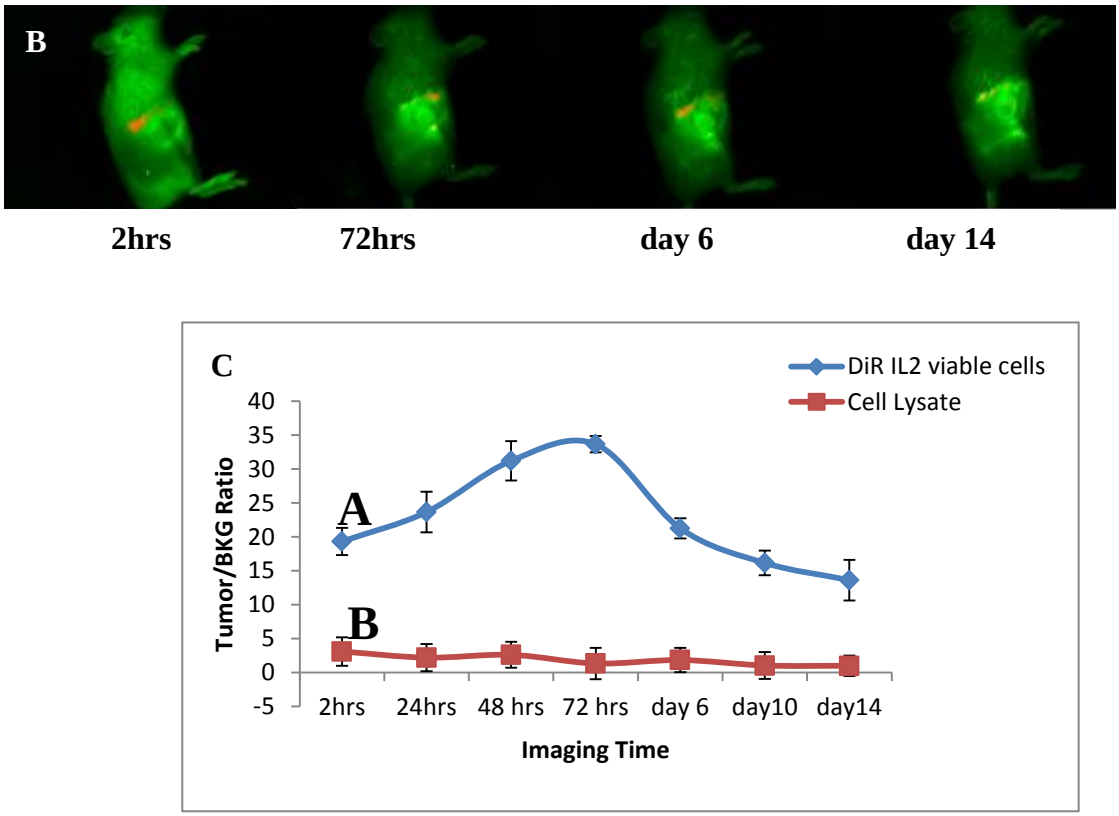

Figure 21 Fluorescence imaging of IL2 cell trafficking. Homing of 4T1 sensitized DiR labeled cells to 4T1 tumor site 7 days after the tumors have been implanted (panel A), Panel B fluorescent imaging of animals injected with the IL2 cell lysate supernatant. Red color indicates the signal from the NIR DiR Dye used to label the T cells. (**C)** Tumor/ Background ratios graph showed that, cells localized at the tumor site on day 1(on 2hrs) peaked on day 3 and persisted up to 14 days in the animal. While in case of IL2 lysate, there was no localization of 4T1 specific T cells at the tumor site.

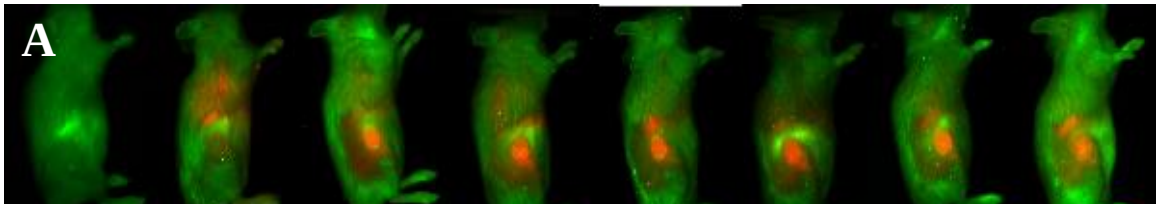

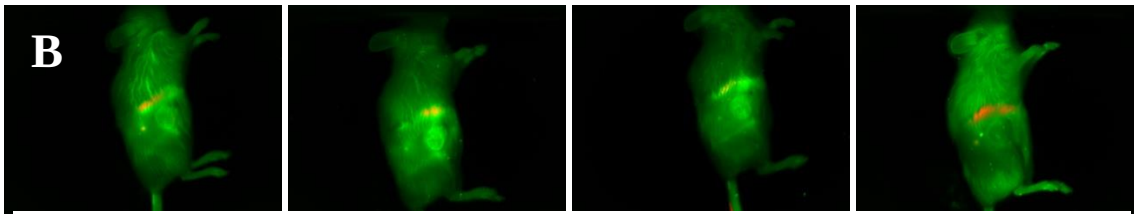

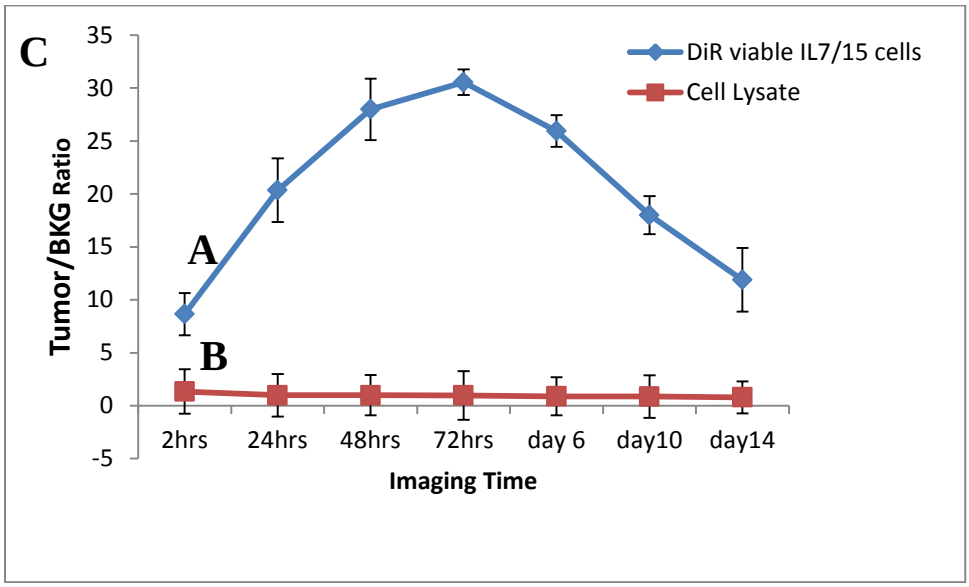

Figure 22 Fluorescence imaging of IL7/15 cell trafficking. Homing of 4T1 sensitized DiR labeled cells to 4T1 tumor site 7 days after the tumors have been implanted (panel A), Panel B fluorescent imaging of animals injected with the IL7/15 cell lysate. Red color indicates the signal from the NIR DiR Dye used to label the T cells. (**C)** Tumor/ Background ratios graph showed that, cells localized at the tumor site on day peaked on day 3 and persisted up to 14 days in the animal. While in case of IL7/15 lysate , there was no localization of 4T1 specific T cells at the tumor site.

5.1.7. Localization of labeled T-lymphocytes at tumor and non-tumor tissues

To investigate the migration pattern of 4T1 sensitized T cells following inoculation to sites besides the tumor site, tumor bearing mice were dissected at various time points following inoculation with DiR labeled T cells and different organs were removed and imaged *ex vivo*. Besides tumor, labeled T lymphocytes were also seen to have localized to liver, spleen, lungs, lymph nodes and bone marrow, as shown in Figure 23 panels A, B,C and D. Figure 23 panels E and F show signal to background ratio of labeled T-lymphocytes in these organs on days 3 and 10 post-injection of labeled T cells. The signal increased modestly with time, which would indicate that additional labeled cells were migrating to these sites.

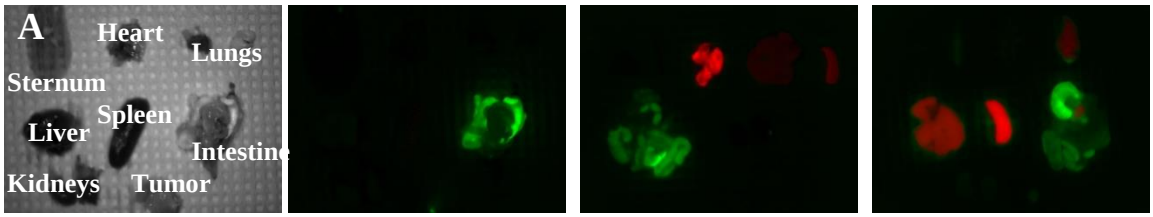

Bright field image Of all organs

organs of control animal

organs of animal injected with IL2 cells lysate

organs of animal injected with IL7/15 cells lysate

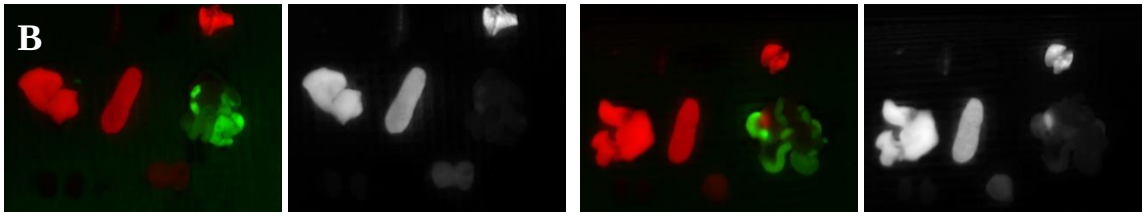

Organs of animal injected withViable DiR IL2 cells

Organs of animal injected with Viable DiR IL7/15 cells

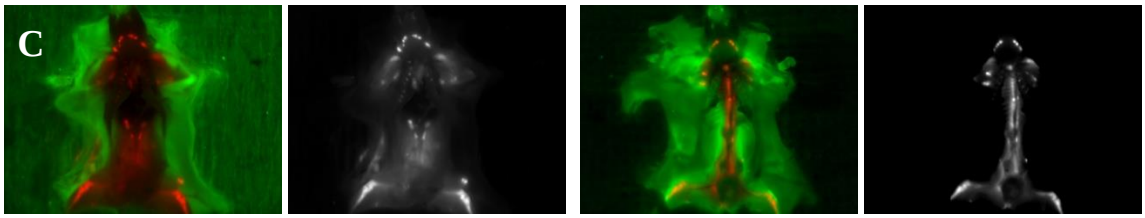

Animal skeleton without organs injected withViable DiR IL2 cells

Animal skeleton without organs injected with Viable DiR IL7/15 cells

Showed strong signal in lymph nodes and bone marrow

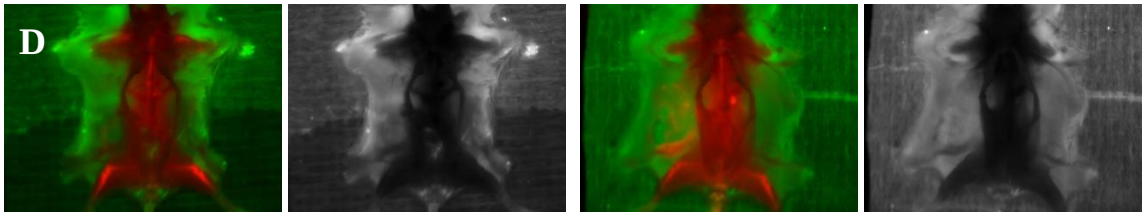

Animal skeleton without organs injected with DiR IL2 cells lysate

Animal skeleton without organs injected with DiR IL7/15 cells lysate

Showed no signal in lymph nodes or bone marrow

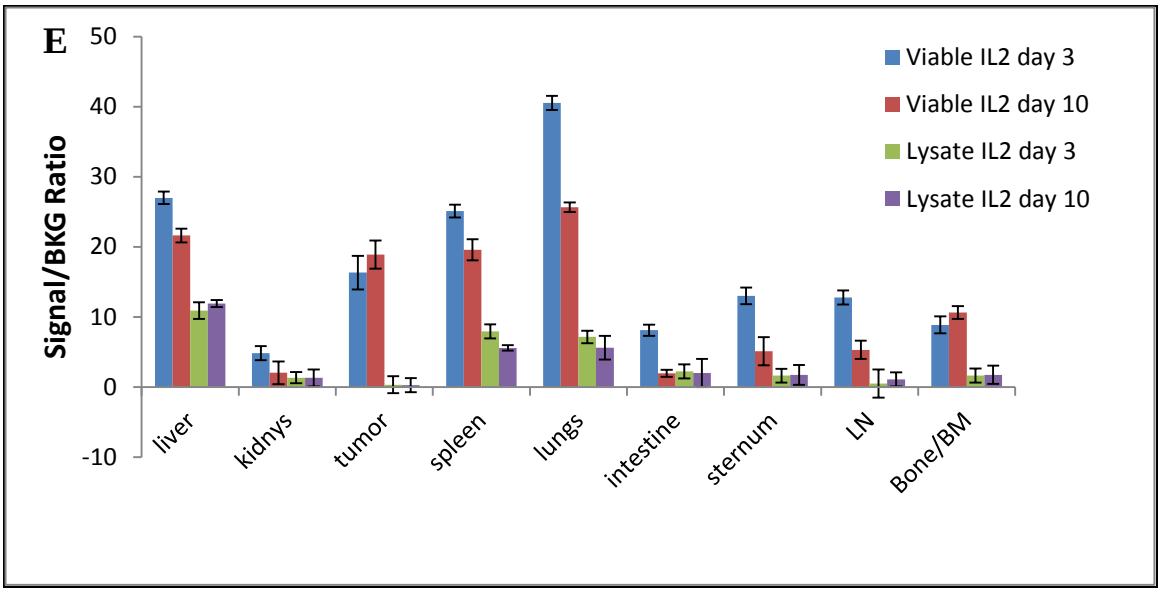

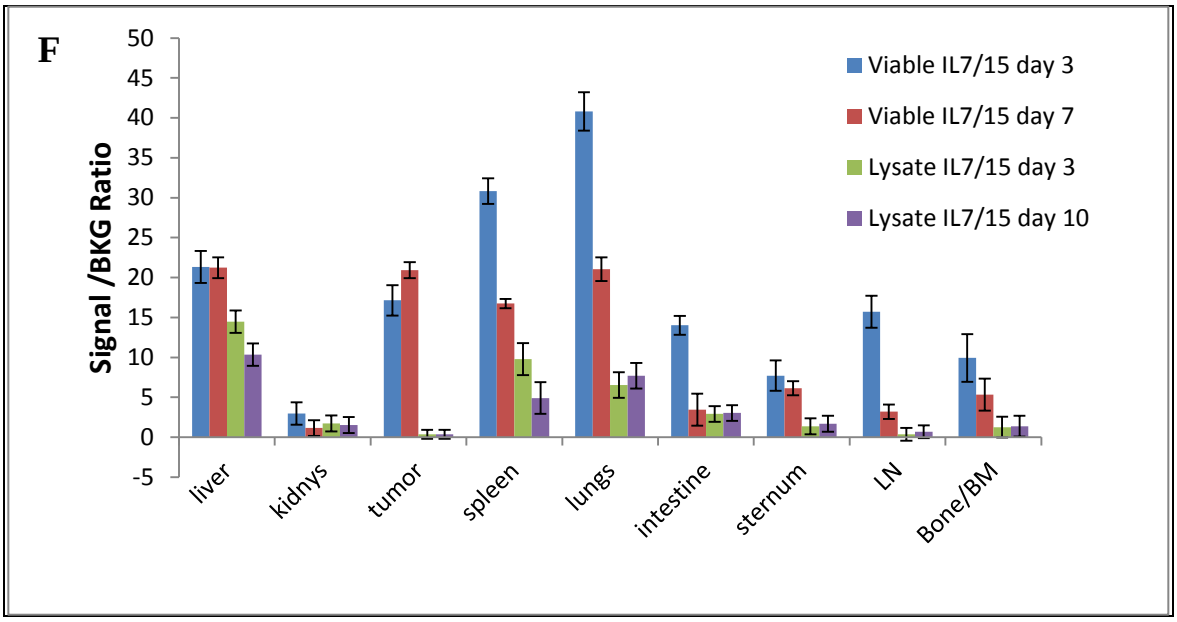

Figure 23 panels A,B,C and D Fluorescence imaging of tumor, liver, lungs, spleen, and bone marrow *ex vivo*. (E,F**)** Quantitation of the signal from labeled T-lymphocytes at the tumor site and other organs on days 3 and 10 post T-cells administration.

5.1.8. T cells specificity and their AIT function with or without DiR labeling *in vivo*

To test the specificity of T cells as antigen specific cells for 4T1 tumor with and without labeling with DiR and their immune function in vivo, number of animals were classified into 8 groups (6 animals in each), group 1 animals with 4T1only (control 4T1) group 2 same as group 1 for Meth A tumor (control meth A), group 3 animals with 4T1 injected with cychlophosphamide (CYP) only (CYP 4T1), group 4 same as 3 but for Meth A (CYP Meth A), group 5 animals injected with T cells and CYP (CYP 4T1 AIT), group 6 same as group 5 but for Meth A (CYP Meth A AIT), group 7 and 8 same as groups 5 and 6 but T cells were labeled with DiR (CYP AIT 4T1 DiR) and (CYP AIT Meth A DiR). The tumors were implanted intradermally in the left flank, CYP was given on Day 3, and AIT (ex vivo activated T cells with and without labeling with DiR) on Day 4 after tumor implantation. Tumor volume was measured for about one month post treatment. Figure 24 showed the results of this experiment; two important observations are noticed; first T cells are antigen specific against 4T1 tumor and no activity was observed against Math A tumor. This result is consistent with our previous data shown in figure 18. Second, DiR does not show any effect on the T cells function *in vivo* after adoptive transfer.

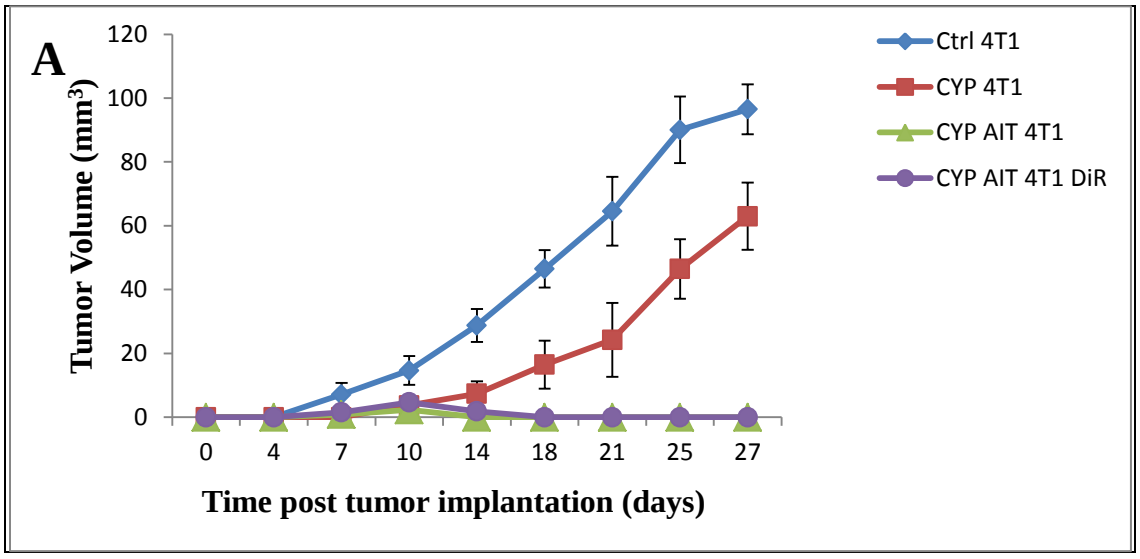

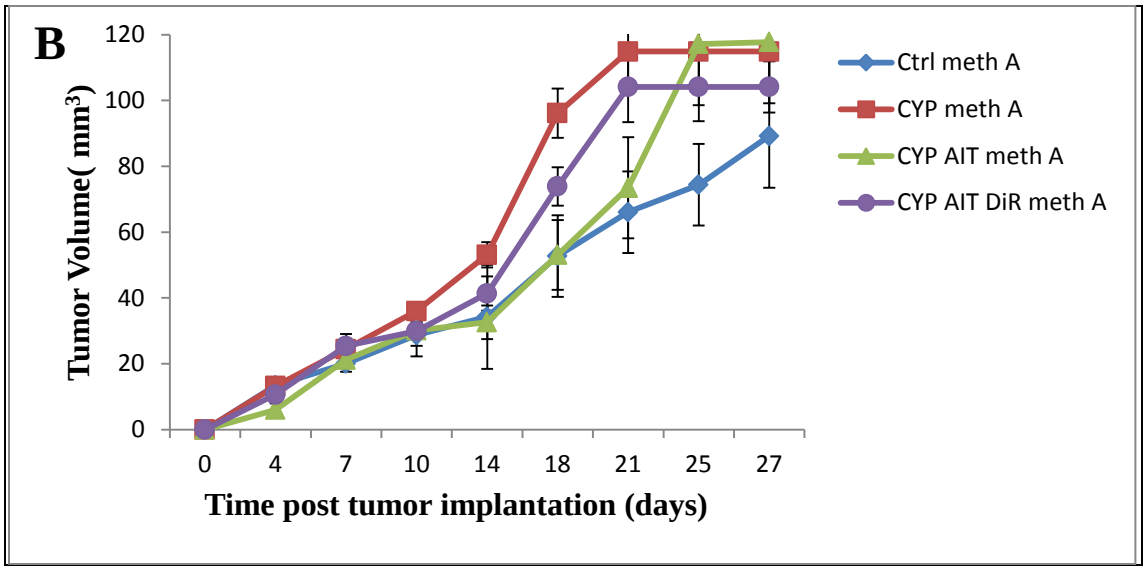

Figure 24 T cells with and without DiR labeling function in vivo against 4T1 and Meth A tumors. Panel A T cells activity against 4T1 tumor, tumor volume was zero starting from day 6 after AIT (T cells with or without DiR labeling) administrations. Control and CYP groups showed an increase in the tumor volume as time increases. Panel B T cells activity against Meth A tumor, no decrease or regression in the tumor volume with time and no differences compared to other groups (control and CYP), indicating that T cells are antigen specific against 4T1 tumor.

5.1.9. Immunohistochemistry confirms localization of activated T cells at the tumor site

To confirm the localization of the activated T-lymphocytes to the tumor site, 5 micron thick tumor sections from mice inoculated with DiR labeled T cells were stained for CD69 and F4/80 to detect activated T-lymphocytes and macrophages respectively. Both activated T lymphocytes and macrophages were visualized at the tumor site as shown in Figure 25. A, B, C and D are different sections of the tumor from outside to deep inside the tumor. The activated T lymphocytes were mostly localized at the superficial layer of the tumor; macrophages were localized deeper inside the tumor tissues. To ensure that the localization of macrophages at the tumor site was not to attack and engulf labeled activated T-lymphocytes, we implanted 4T1 breast carcinoma tumor in a number of mice and dissected them after 10 days when they have the same tumor size as in our previous experiments. These mice were not injected with activated T lymphocytes. Tumors were sectioned, double stained for CD69 and F4/80 and then imaged. Figure-25 E, F, G and H illustrate the images of these sections, and we did not see any activated T cells at these tumors and this was expected. Spleen sections were used as positive control for T-lymphocytes. Whereas, liver was used as positive control for macrophages, both spleen and liver images are demonstrated in Figure-25 E and F.

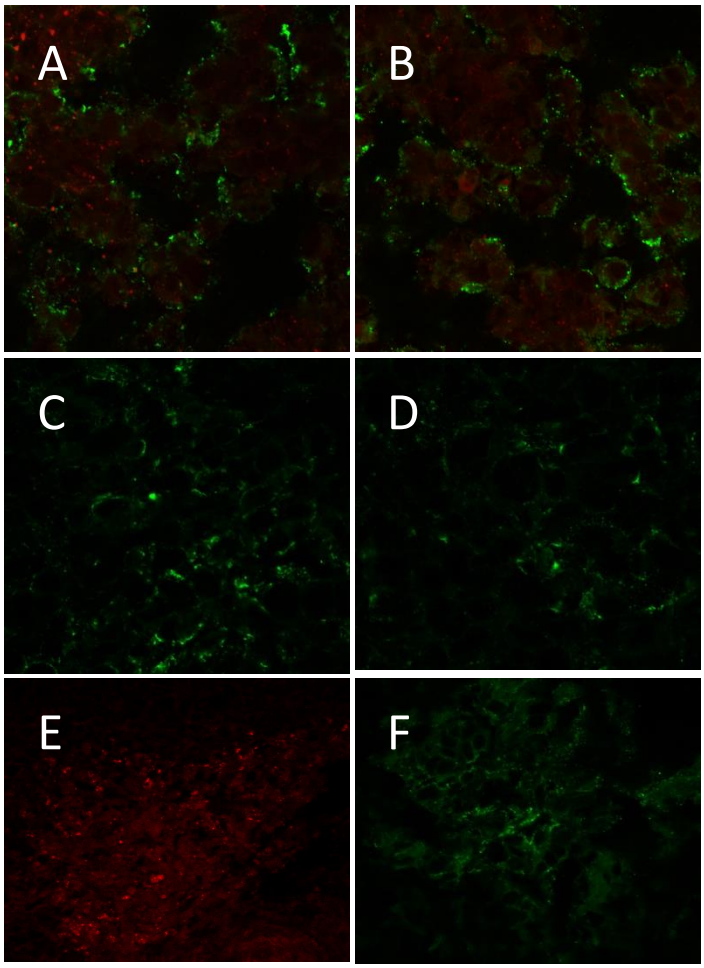

Figure 25 (A-B) Mouse bearing 4T1 tumor was injected with activated T-cells and the tumor sections were stained for CD69 activated T-cells (red color) marker and F4/80 macrophage (green color) marker. (C-D) Images of 4T1 tumor sections obtained from mouse bearing 4T1 tumor but not injected with activated T cells, stained for CD69 and F4/80 markers. (E) Spleen section stained for CD69 (used as positive control for activated T-cells) and (F) Liver section stained F4/80 (used as positive control of macrophages).

5.1.10. Confirmation of immunehistochemistry results by flow cytometry

To validate that adoptively transferred labeled T cells (AIT) are not engulfed by macrophages or the DiR is transferring to other immune cells, tissues (liver, spleen, bone marrow (BM) and tumor) that showed high accumulation of T cells were collected and digested on day 7

post AIT injections. Following tissues were also stained for macrophages (F4/80) and immune cell marker (CD45) for flow cytometry analysis. CD45 is expressed on almost all hematopoietic cells except for mature erythrocytes. We are testing if DiR is associated with any other cells than T cells, particularly macrophages and other hematopoietic cells. The result (figure 26) shows that no DiR was associated with F4/80 or CD45 indicating that, DiR is linked to T cells and did not transfer to other cells.

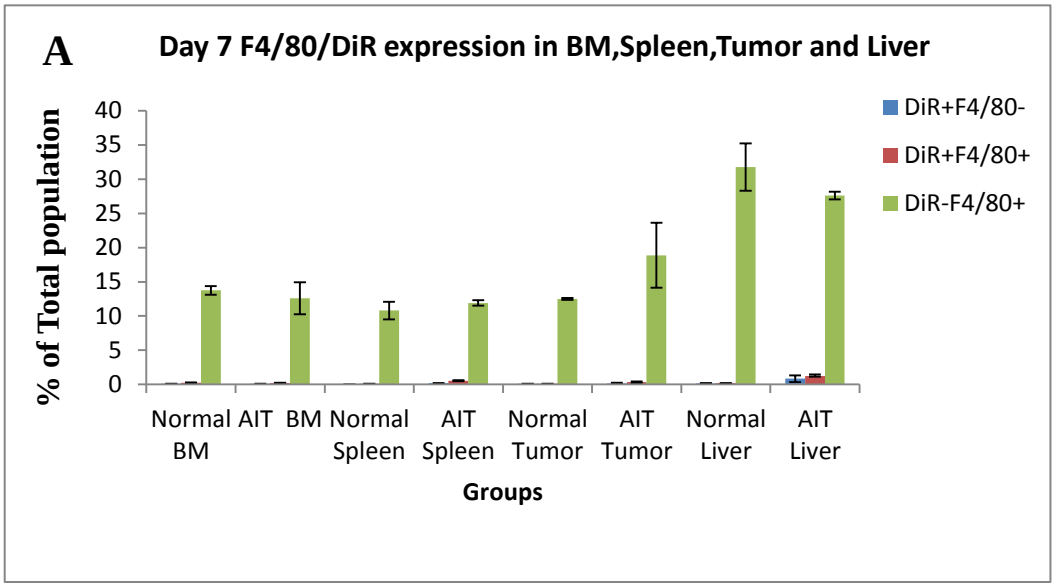

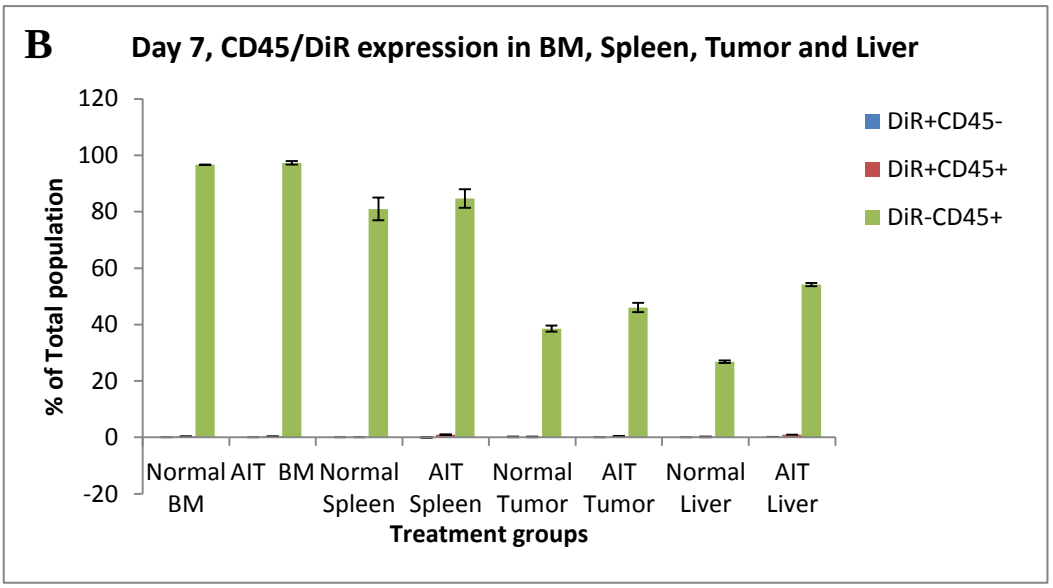

Figure 26 assessment of immunohistochemistry result by flow cytometry. Panel A tissues were stained for macrophages (F4/80), panel B tissues were stained for immune cell marker CD45. Both confirm that DiR is linked to T cells and no transfer of DiR to other cells.

5.1.11. Verification of DiR labeled cells localization at tumor site

To validate whether the DiR signal at the tumor site is connected to the DiR labeled cells, DiR stock was diluted and prepared in PBS as described previously and injected to number of animals bearing 4T1 tumor. Fluorescent imaging was done at 3 time points (2, 24 and 48 hours post i.v. injection). The animals were dissected after 48 hours and organs were removed and sectioned. Figure 27 showed the fluorescent images of liver, heart and tumor sections. No signal was detected at the tumor section indicating that, the DiR signal at the tumor site connected to DiR labeled T cells.

Liver **Heart** **4T1 tumor**

Figure 27 fluorescent images of liver, heart and 4T1 tumor sections of animal injected with DiR only. From the ex vivo imaging higher signal was detected in the liver and no signal was in the heart, that is why liver was used as positive and heart negative controls. 4T1 tumor section showed no signal of DiR indicating that, the signal detected at the tumor site is correlated to DiR labeled cells.

5.2. Indirect labeling of T lymphocytes by PRG (HSV1tk)

5.2.1. Transient transfection by transfection reagent

To optimize the HSV1tk gene expression detection, transient transfection was performed with Jurkat cells. pROF9-HSV1 tk-sh plasmid was isolated from GT116 Ecoli and was then cut to

single and double cuts using restriction enzymes to perform gel electrophoresis assay. The result shown (figure 28) confirmed the presence of HSV1tk gene in the Ecoli plasmid. According to the band size calculations in relation to the DNA ladder, bands 3 and 4 showed HSV1tk size exactly as shown in the plasmid map.

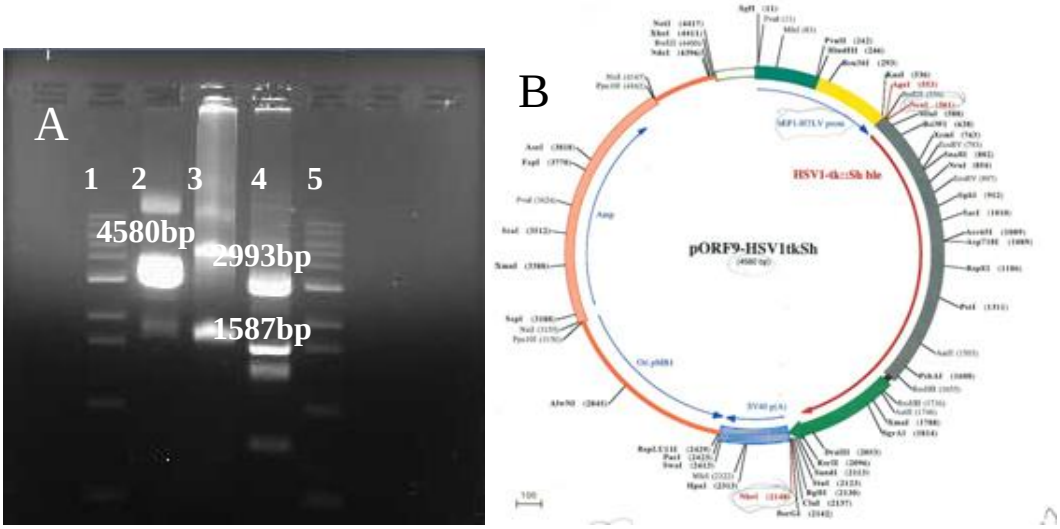

Figure 28 Gel electrophoresis result (panel A) confirmed the presence of HSV1tk gene.1 and 5 DNA ladder, 2= plasmid intact DNA move as coils can't calculate its size, 3= single cut Using NcoI restriction enzyme (linearized plasmid) (first band= 4580bp), 4= double cut using 2 restriction enzymes NcoI, and NheI (first band = 4580bp- (2148bp-561bp) = 2993bp)(Second band = 2148bp-561bp = 1587bp). Panel B showed pROF9-HSV1tk-sh plasmid map.

The HSV1tk vector was used for transient transfection of Jurkat cells. Figure 29 shows the western blot result post transfection using polymer based transfection reagent (Fugene). Ecoli lysate was used as positive control for HSV1TK protein. Cells showed expression of the gene up to 4 days (the end of cell lysate collection). This experiment was done to optimize western blot protocol and make sure the primary antibody is specific for HSV1 TK enzyme.

Figure 29 western blot result of transfected jurkat cell exhibit HSV1 tk expression in jurkat cells at different time points post transfection.

5.2.2. Stable transduction by HSV1tk lentivirus

5.2.2.1. Confirmation of the presence of HSV1tk gene in pMOD-HSV1tk plasmid

HSV1tk gene was transformed to pMOD-HSV1tk plasmid (GT100 Ecoli,) and then was extracted to be cloned to the lentiviral vector to construct HSV1tk lentivirus as described previously**.** Figure 30 shows HSVtk plasmid map (panel B) and according to the calculations of the band sizes in the gel electrophoresis result (panel A), the HSV1tk gene is present in the pMOD-HSV1tk vector.

To make sure the HSV1tk gene expresses HSV1TK enzyme, the Ecoli was lysed and western blot assay was performed as shown in figure 31. HSV1TK enzyme bands are clearly observed at 7, 10, 13 µg of the total protein of the Ecoli lysate. Based on this result this plasmid vector was chosen to construct the HSV1tk lentivirus.

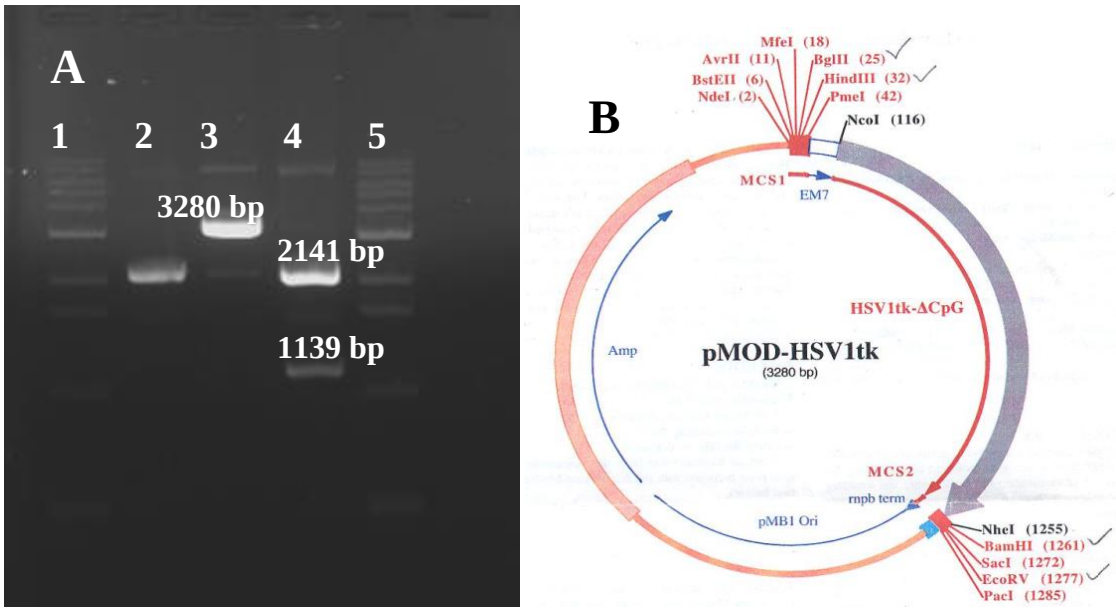

Figure 30 panel A gel electrophoresis result, panel B pMOD-HSV1tk map. According to the standard size of DNA ladder and the pMOD-HSV1tk plasmid map, HSV1tk gene showed the exact size as shown in the map .The size of linearized plasmid DNA is 3280bp, size of DNA fragments from digested DNA with Nco-I and Nhe-I are 1255-116=1139 (single cut), 3280-1139=2141 (double cut).

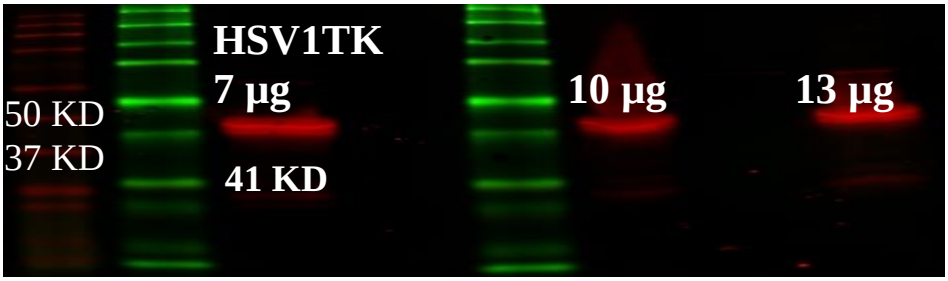

Figure 31 western blot result of pMOD-HSV1tk Ecoli lysate showed HSV1TK enzyme of different masses from total protein of Ecoli lysate.

HSV1 TK protein was purified from pMOD-HSV1tk Ecoli to be used as a positive control for western blot assays. Different concentrations of the primary antibody and different amounts of the protein were tested by western blot to choose the right mass of protein that can be loaded for western blot assays (figure 32).

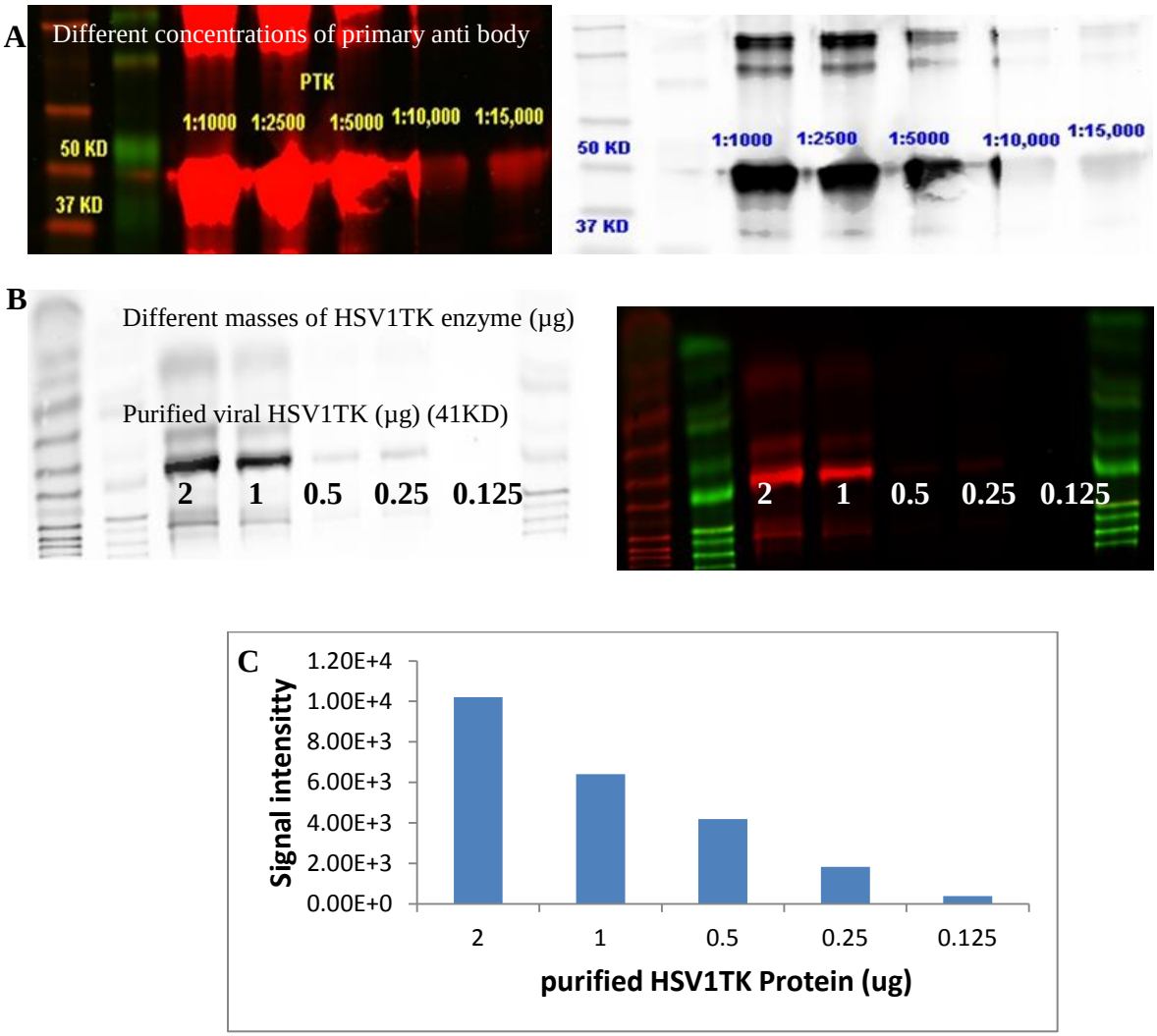

Figure 32 western blot result of purified HSV1TK enzyme, panel A 2µg of HSV1TK enzyme was tested against different concentrations of primary antibody. To obtain single band without nonspecific binding 1:10,000 concentration was selected for the following western blot assays (panel A). Panel B different masses of HSV1TK enzyme were tested against the chosen primary antibody concentration. Panel C showed HSV1TK signal quantification at different masses. Based on these findings 0.5 µg was selected for following western blot assays.

5.2.2.2. Selection of stable transduced Jurkat, HEK 293 and 4T1 cells

Before T lymphocytes were transduced with HSV1tk lentiviral vector, stable transduction was performed with HEK 293, Jurkat and 4T1 cell lines. These cells can be cultured for long periods of time; therefore they are suitable to be selected using Blasticidin selection marker, which requires 14 days of incubation. T lymphocytes on the other hand are a primary cell line and they

can be cultured only for 10 to 13 days. The reason to create stable cell lines was to compare the uptake of T lymphocytes to stable transduced Jurkat cells and estimate the transduction efficiency of T lymphocytes based on that.

To create stable cell lines, cells were first incubated with different concentrations of Blasticidin for 14 days as described previously. This experiment was done to select the optimum concentration that will end up with zero viability of non-transduced cells. This optimum concentration was chosen to select stable transduced cells post transduction.

Figures 33, 34 and 35 presented the % of viability of Jurkat, HEK and 4T1 cells respectively. Jurkat cells showed 0% of viability at 2µg/ml of Blasticidin concentration at day 14 of incubation, while HEK cells were more resistant, they were at 0% of viability at 10µg/ml at day 14. 4T1 cells showed 0% of viability at 8µg/ml concentration at day 14.

These concentrations were chosen for stable transduction selection and were added to cells on day 5 post transduction. Cells were incubated at the selected concentration of Blasticidin for more than one month. RT-PCR and western blot assays were performed on the transduced cells post Blasticidin selection.

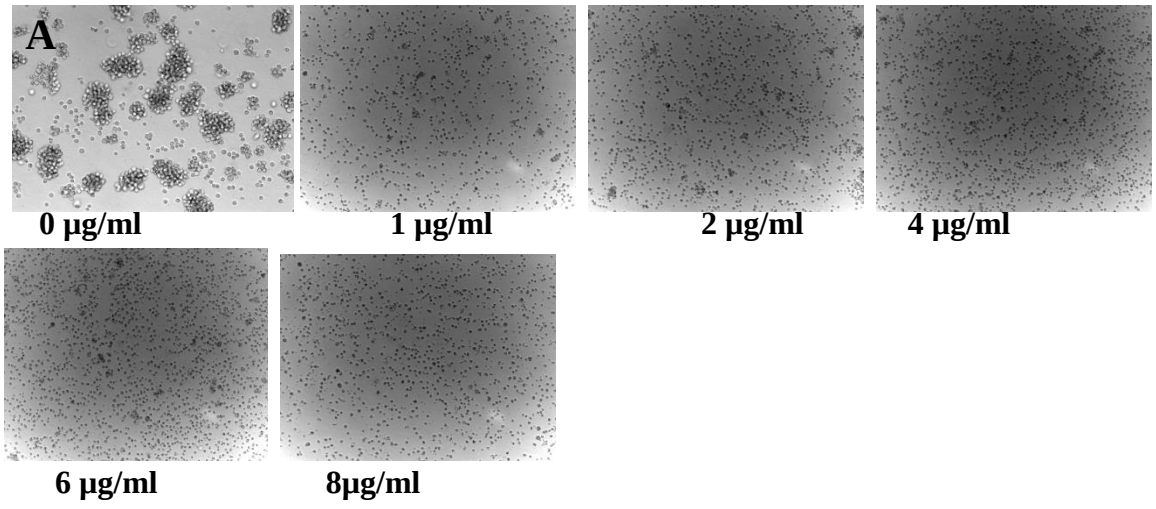

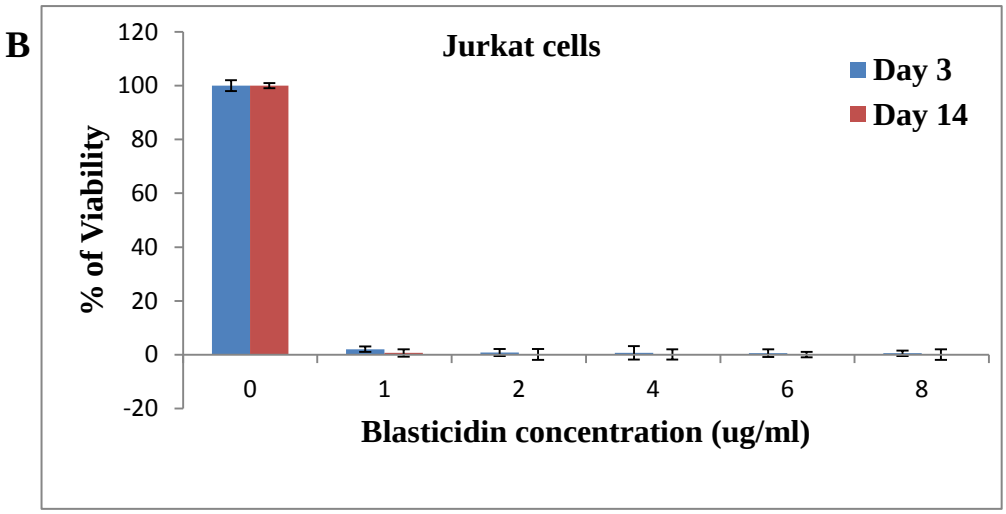

Figure 33 Panel A bright field images taken by fluorescent microscope of Jurkat cells at different concentrations of Blasticidin, cells are not able to proliferate and produce colonies in Blasticidin compared to 0 concentration. Panel B the % of viability of jurkat cells at different concentrations of Blasticidin on days 3 and 14 of incubation. At 2µg/ml on day 14 of incubation cells were at 0% of viability.

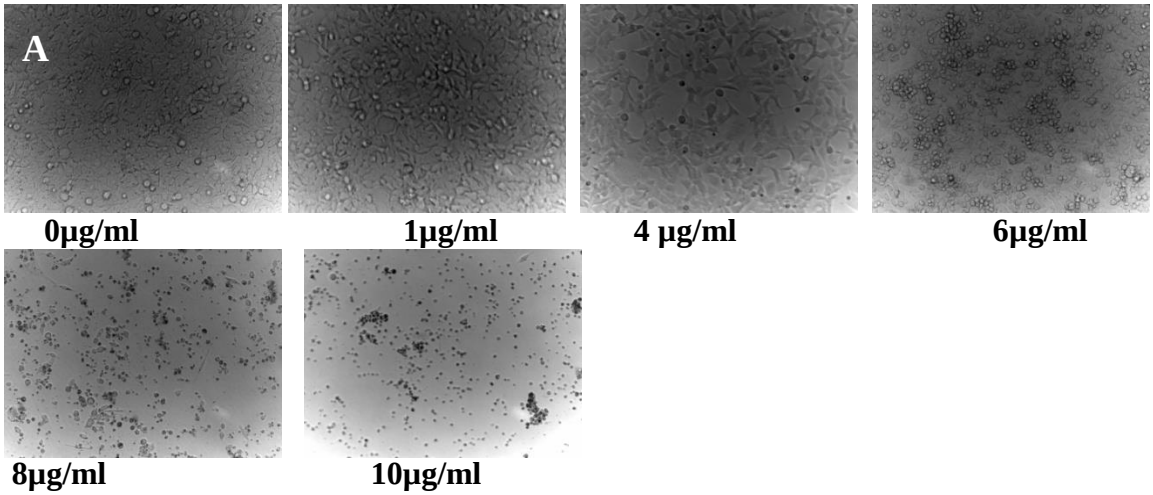

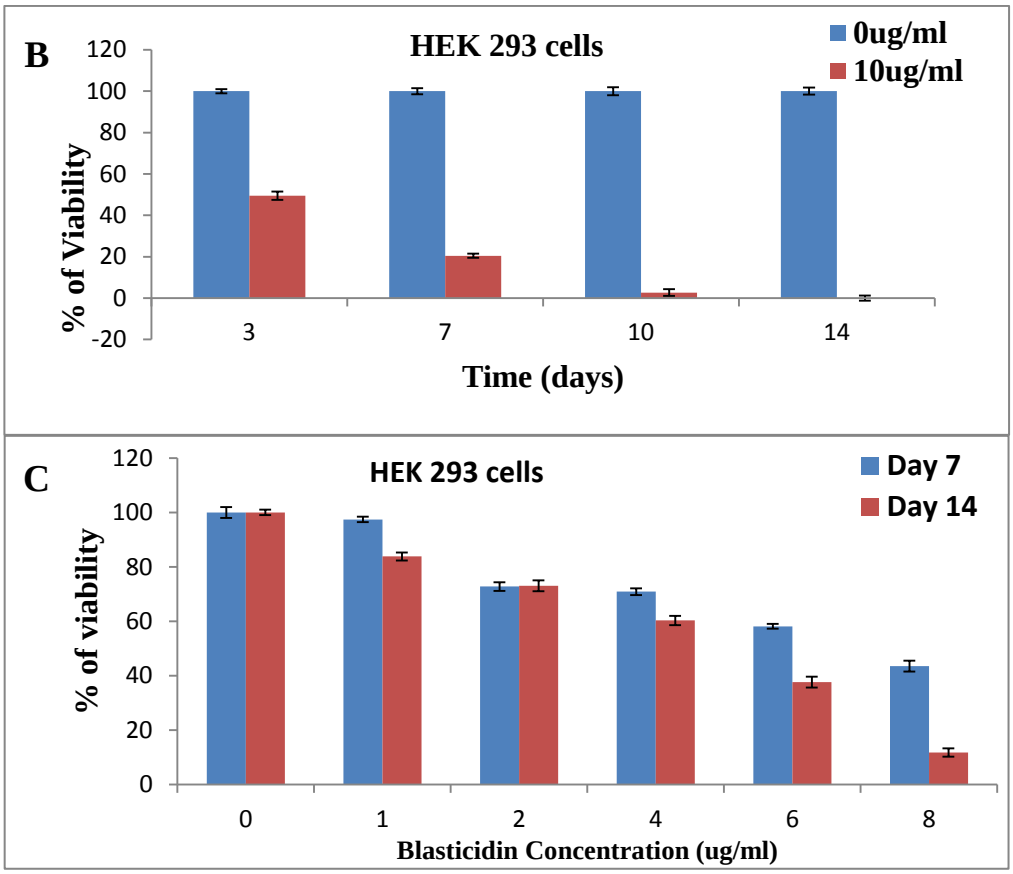

Figure 34 panel A bright field images of HEK 293 cells. The % of viability of HEK 293 cells at different concentrations of Blasticidin on days 7 and 14 of incubation (panel B), even at 8µg/ml of Blasticidin concentration on day 14 of incubation, cells showed about 11% viable cells. Panel C, cells were incubated with 0 and 10 µg/ml of Blasticidin and the viability was tested on days 3,7,10 and 14 post incubation. The 0% of viability for HEK cells was at 10µg/ml on day 14 of incubation.

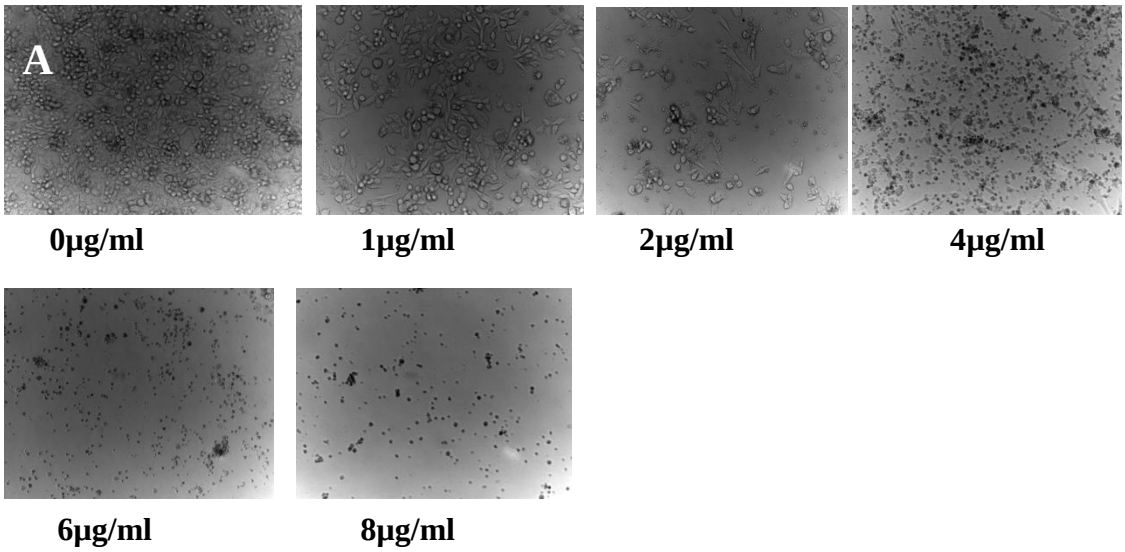

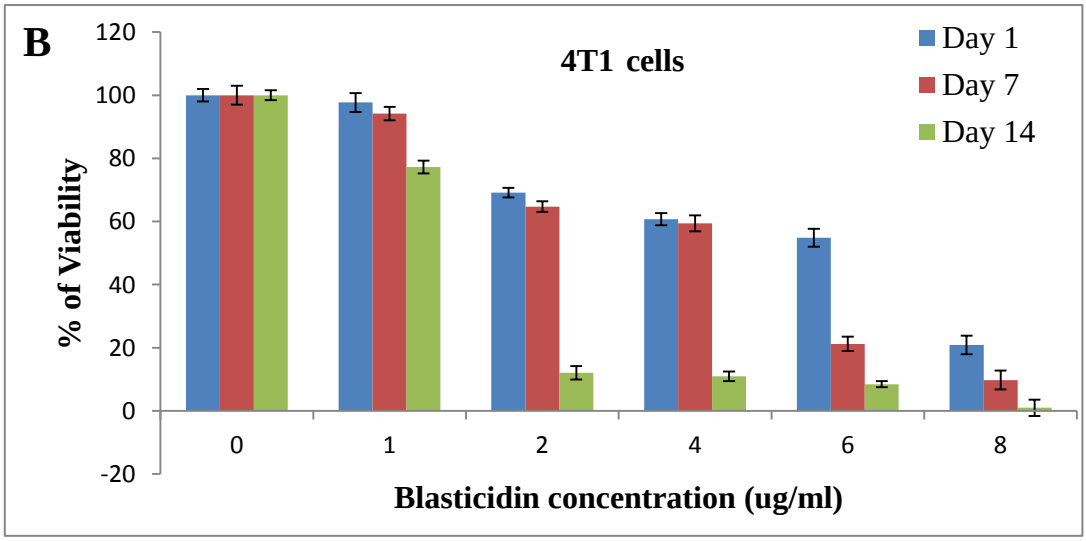

Figure 35 panel A bright field images of 4T1 cells at different concentrations of Blasticidin. Panel B the % of viability of 4T1 cells at different concentrations of Blasticidin on days 1, 7 and 14 of incubation. At 8µg/ml on day 14 of incubation
cells were at 0% of viability.

5.2.2.3. Verfication of HSV1tk gene expression by RT-PCR and westren blot

To verify that Jurkat , HEK 293 and 4T1 cells are transduced with HSV1tk, RT-PCR and westren blot assays were performed as described previuosly. Figure 36 shwed RT-PCR result of the three cell lines.

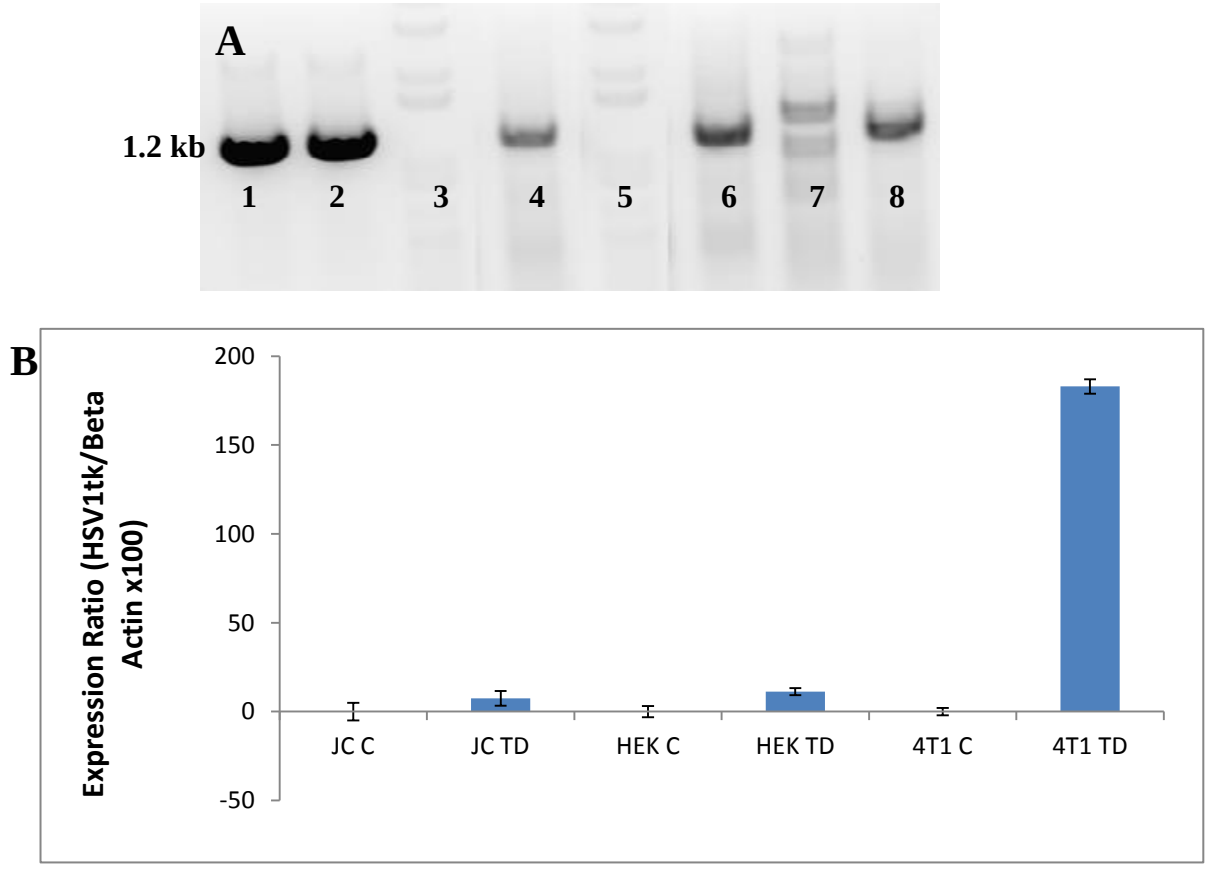

Figure 36 Panel A RT-PCR result showed HSV1tk gene in the transduced cells. Lane 1 and 2 used as positive controls. Lane 1 is the pMOD-HSV1tk DNA (bacterial vector), lane 2 is pLenti6-UBC-V5-HSV1tk (viral vector). Acording to the DNA ladder both lanes are between 1.6 and 1 kb and the expected size is 1.2 kb. Lane 3 Jurkat cell cDNA control, Lane 4 Jurkat cell cDNA transduced with HSV1tk lentivirus. Lane 5 HEK cell cDNA control. Lane 6 HEK cell cDNA transduced with HSV1tk lentivirus. Lane 7 4T1 cell cDNA control. Lane 8 4T1 cellcDNA transduced with HSV1tk lentivirus. Panel B the expression ratio of HSV1tk/Beta Actin, JC= Jurkat cells, C= control, TD=transduced. 4T1 cells exhibit the higher ratio compared to jurkat and HEK cells. There is significant differenc between transduced 4T1 and both Jurkat and HEK ($p < 0.05$) but no significant difference between Jurkat and HEK cells.

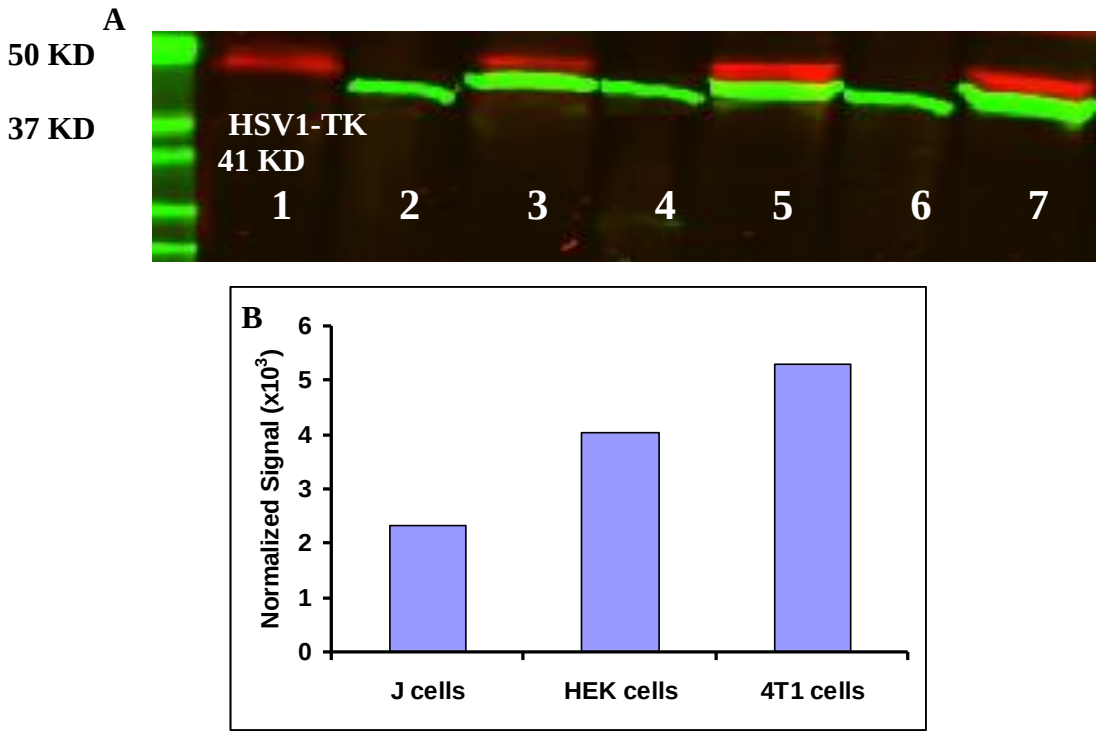

Figure 37 western blot result showed HSV1-TK enzyme expressed in the transduced cells.
1 = the purified HSV1TK protein, 2 = untransduced jurkat cells, 3 = transduced jurkat cells, 4 = untransduced HEK cells, 5 = transduced HEK cells, 6 = untransduced 4T1 cells, and 7 = thransduced 4T1 cells (300µg of total protein of cell lysate was loaded) (panel A).
Panel B showed the normalized signal of HSV1TK to beta-actin.

5.2.2.4. ^{124}I [FIAU] uptake by transduced Jurkat, HEK 293 and 4T1 cells

The uptake of ^{124}I-[FIAU] by transduced Jurkat, HEK 293 and 4T1 cells was investigated by incubating these cells with ^{124}I-[FIAU] for 1, 2, 4 and 18 hours as described previously. Figure 38 panels A, B and C demonstrated the uptake results of these cells. Transduced Jurkat cells showed gradual increase in the uptake which was most pronounced at 18 hours (panel A). For HEK cells there was no significant differences in its uptake at 1, 2 and 4 hours, but was more obvious at 18 hours (panel B). 4T1 cells showed higher uptake at all time points, they showed the maximum uptake among the three cell lines (panel C).

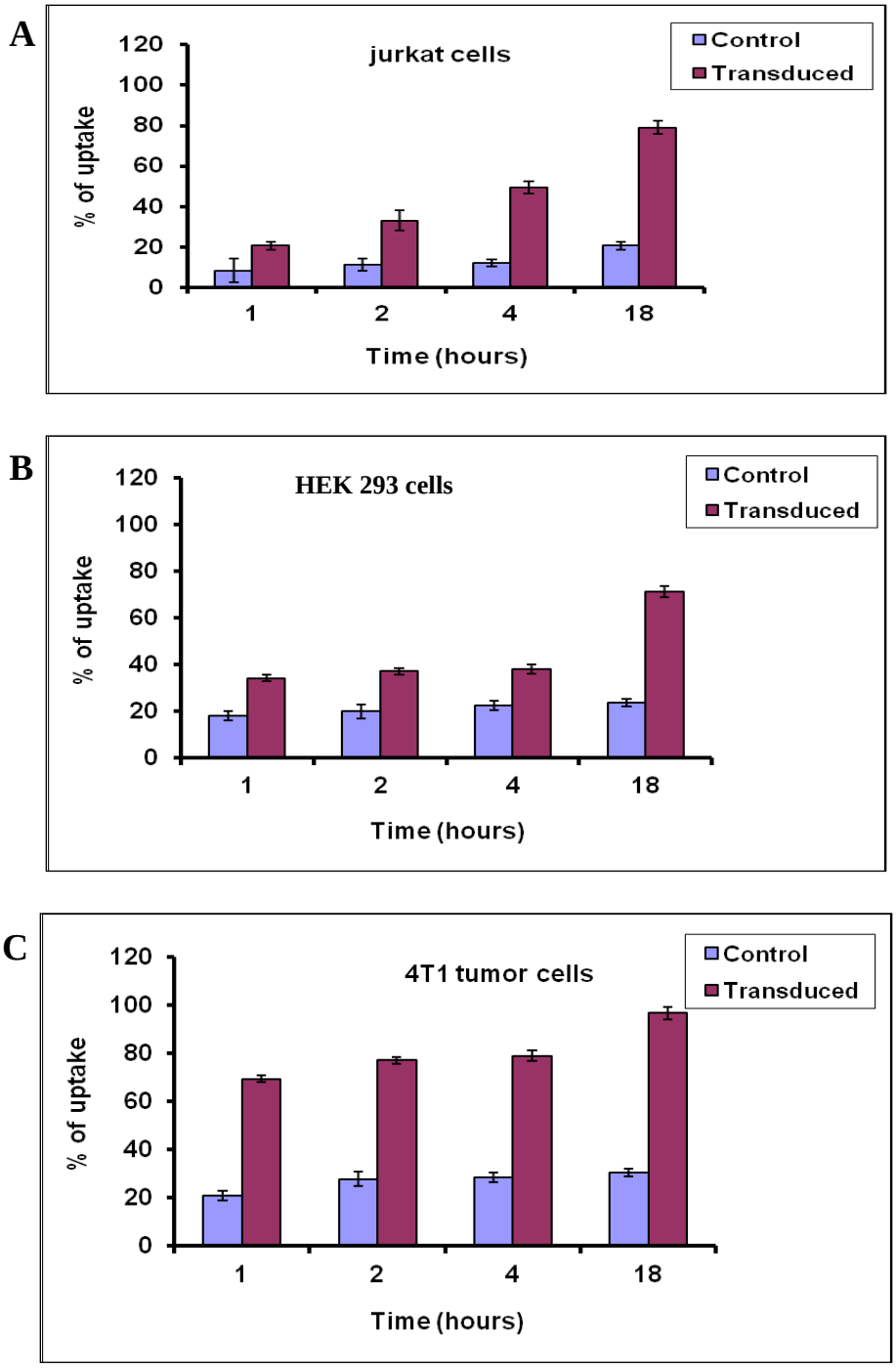

Figure 38 [^{124} I] FIAU uptake in transduced Jurkat cells (panel A), HEK cells (panel B) and 4T1 cells (panel C). 4T1 cells showed the maximum uptake among the three cell lines at the different time points.

5.2.2.5. PET imaging of 4T1 tumor

Transduced 4T1 tumor was implanted in a number of animals and imaged at different time points as shown in figure 39.

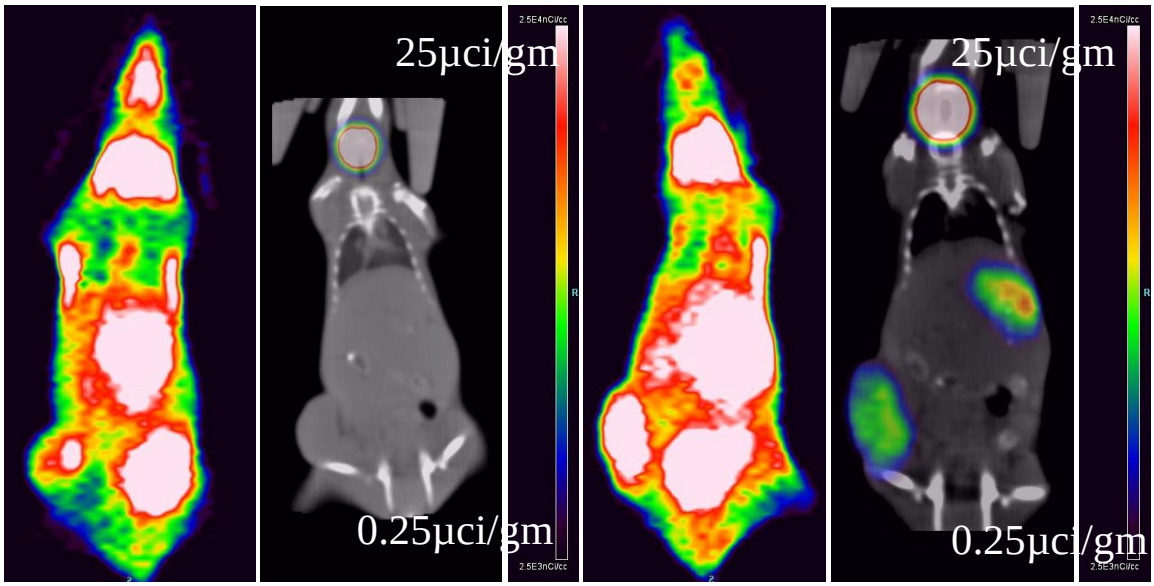

Figure 39 4T1 wild type tumor (A, B) on the left flank of a mouse imaged 1 hour (A) and 24 hours (B) post injection of ^{124}I-FIAU, shows the radiotracer completely clearing from the tumor (2.87 %ID/g to 0 %ID/g). Whereas, the HSV1-tk stably transduced 4T1 tumor (C, D) in the left flank of another mouse shows the tumor activity to retain the radiotracer from 2.54 %ID/g at 1 hour (C) to 1.05 %ID/g after 24 hours (D). Also seen are the stomach (3.83 %ID/g) and the thyroid (21.2 %ID/g).

5.2.2.6. T-lymphocytes transduction

5.2.2.6.1. T lymphocytes proliferation and viability before and after transduction

IL2 or IL7/15 T lymphocytes were transduced on day 3 post ex vivo activation and expansion with different MOIs (10, 5, 2, 1, 0.2 and 0.03) as described previously.

At MOI of 10, the viability of T cells was very low (almost 90% of cells died). At MOI of 5 and 2, the % of viability was less than 40% (figure 40 panel A). However at MOI 1, 0.2 and 0.03, the % of viability was in average of 80% (figure 40 panel B). Cell proliferation was assessed by calculating the fold increase in cell number (comparing cell number every other day post

transduction to the cell number immediately post activation by B/I). Figure 40 demonstrates cell proliferation of IL2 or IL7/15 cells at MOI of 1. There are no significant differences ($p > 0.05$) between transduced and untransduced cells post transduction. Based on this result, MOI of 1 was chosen for the following experiments.

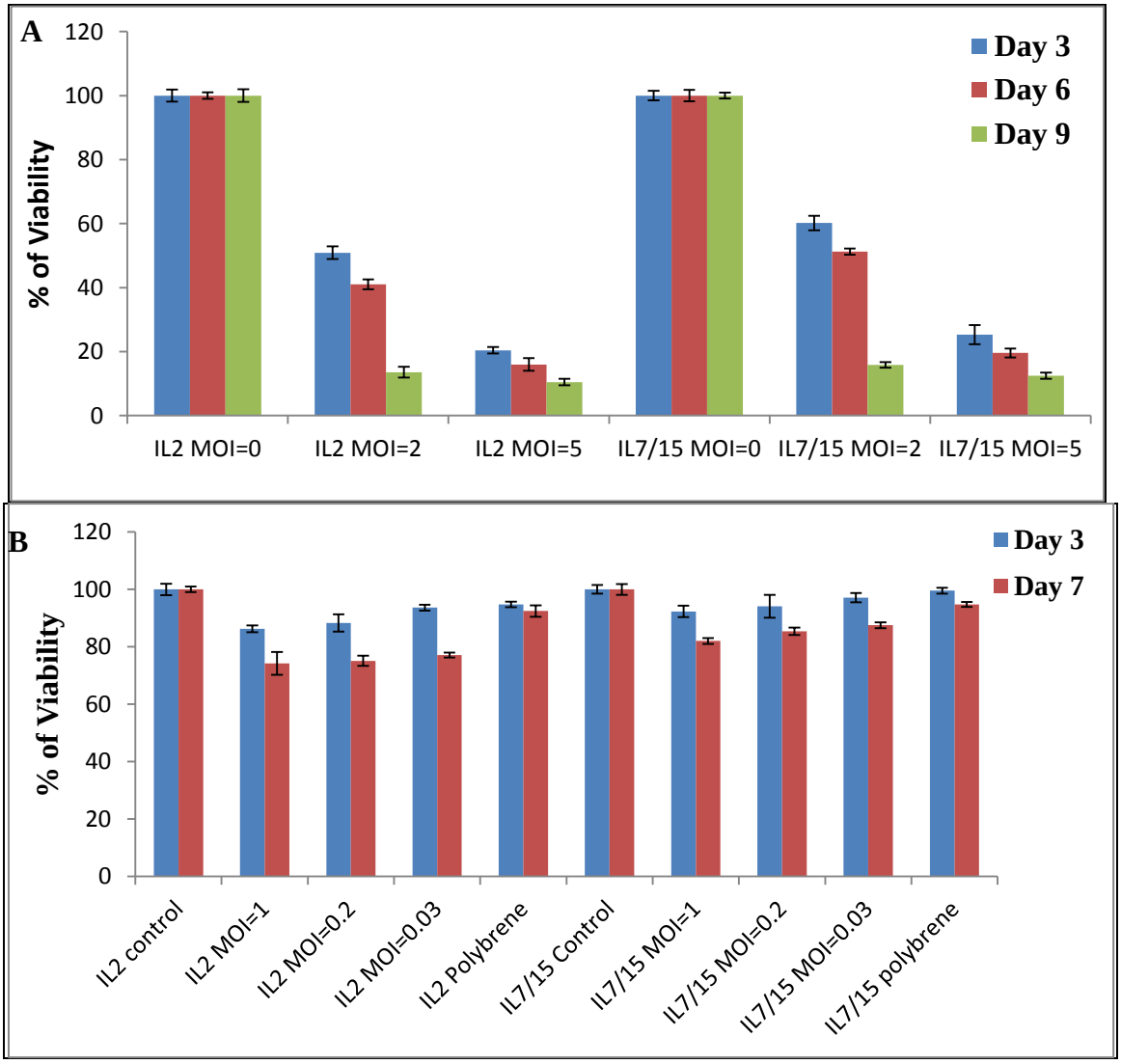

Figure 40 the % of viability of IL2 or IL7/15 at MOI of 2 and 5 (panel A), cell viability at MOI of 2 decreases to less than 60% on day 3, 6 and become about 20% on day 9 post transduction. While at MOI of 5 at days 3, 6 and 9 decreases to be less that 30%. At MOI of 1, 0.2 and 0.03 the average viability about 80% (panel B).

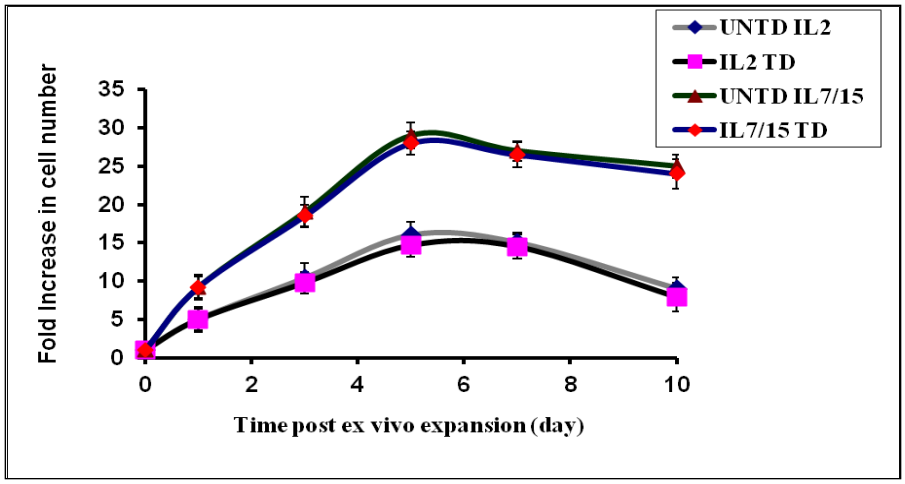

Figure 41 fold increase in cell number for transduced (TD) and untransduced (UNTD) IL2 or IL7/15 cells at MOI of 1(transduction was done on day 3 post ex vivo expansion). No significant differences between TD and UNTD cells.

5.2.2.6.2. Confirmation of HSV1tk gene expression in transduced T cells

Based on the viability results, transduced cells at MOI of 1, 0.2 and 0.03 were analyzed using quantitative real time-PCR and western blot on day 5 post transduction to verify that HSV1tk gene has been integrated to cells genome via the lentiviral vector. Figure 42 shows the expression ratio of HSV1tk to Beta Actin; at MOI of 1, IL2 cells showed the highest expression ratio and it is significantly different ($p<0.05$) from IL2 cells at MOI of 0.2, 0.03 and IL7/15 cells at all three MOIs. With IL7/15 cells at the three MOIs showed no significant differences in the expression ratio.

To test the HSV1tk expression, T cells lysate was prepared from IL2 or IL7/15 cells. Total protein in the cell lysate was determined using protein assay kit, and then 300µg was used for western blot assay (figure 43).

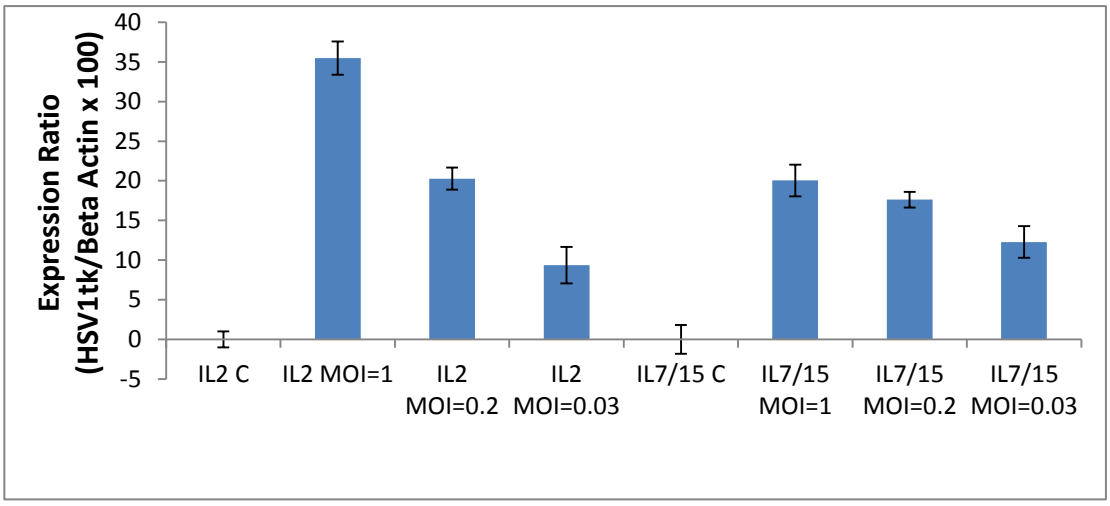

Figure 42 the expression ration of HSV1TK to Beta actin in IL2 or IL7/15 cells at different MOIs. At MOI of 1 IL2 cells shwed the higher expresion ratio. While IL7/15 cells showed almost same ratio for all MOIs.

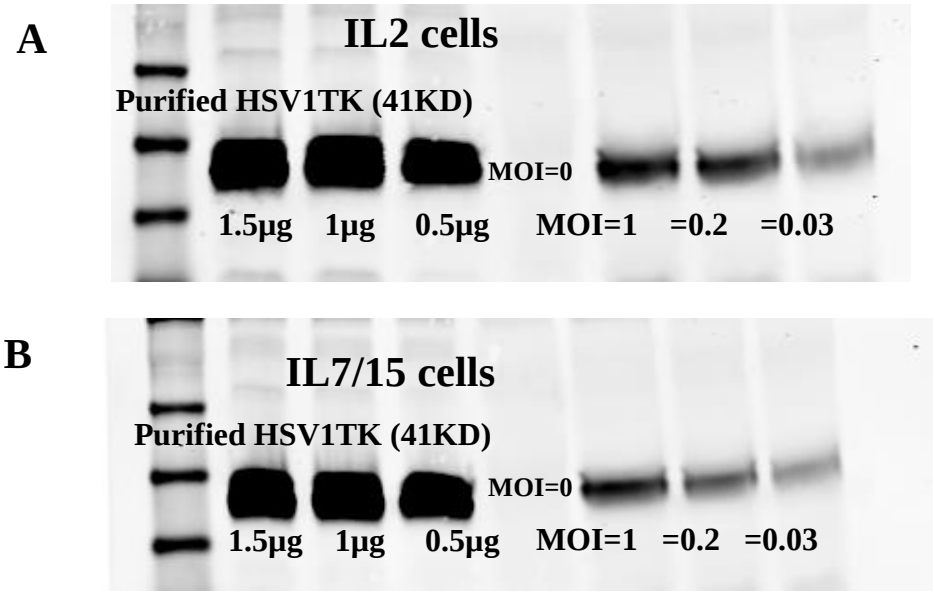

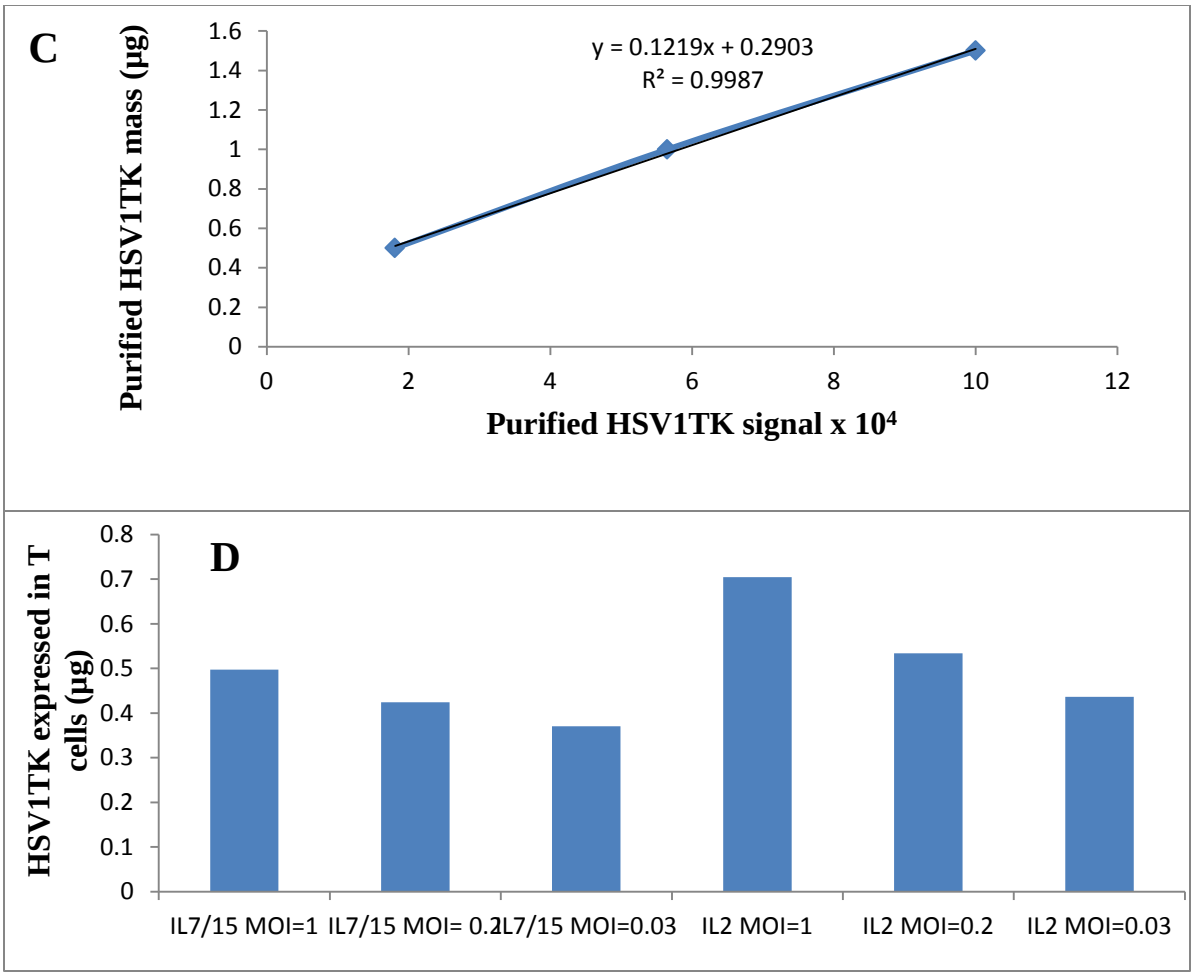

Figure 43 western blot results of transduced IL2 or IL7/15 cells at MOI of 1, 0.2 and 0.03. Based on the linear relationship of the purified HSV1TK (panel C) the HSV1TK mass was calculated as illustrated in panel D. IL2 cells at MOI of 1 showed the highest expression of HSV1TK and this result is consistent with RT-PCR result.

To know the changes in the HSV1tk expression over time, RT-PCR was performed on day 1, 3, 5 and 7 post transduction at MOI of 1 as described previously. The result showed that the highest expression for both IL2 and IL7/15 cells was at days 1 to day 3; after that the expression decreased with time (figure 44). IL2 cells showed higher expression than IL7/15 cells on days 1 and 3 while on days 5 and 7, both cells were similar in their gene expression.

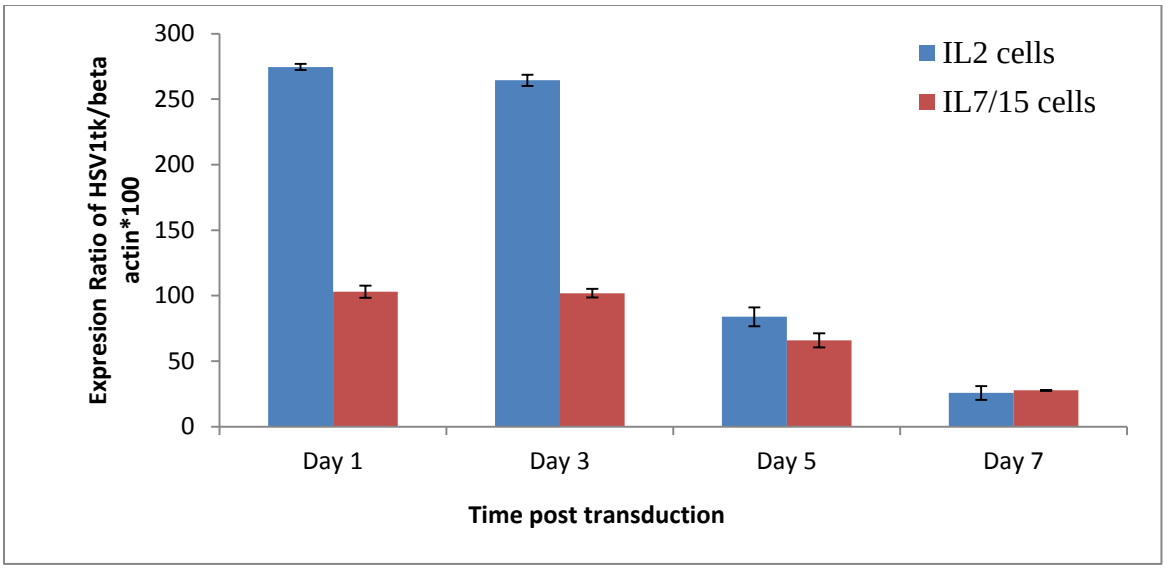

Figure 44 the expression ratio of HSV1tk to Beta Actin at days 1, 3, 5 and 7 post transduction. IL2 cells showed higher expression than IL7/15 cells. Moreover day 1 and day 3 showed the higher expression for both cells. Based on this result transduced cells were used for the in vivo and ex vivo studies on day 3 post transduction.

5.2.2.6.3. Interferon- γ protein release before and after T cell transduction

To test if there are any differences in the ability of IL2 or IL7/15 cells to produce interferon- γ before and after transduction, interferon-γ release assay was performed on day 3 post transduction at MOI of 1 as described previously. Figure 45 represents the result; IL2 cells produce more interferon-γ protein than IL7/15 cells. This result is consistent with our previous result when we tested the effect of DiR labeled cells on cell protein production. Moreover, there are no significant differences ($p > 0.05$) in the amount of the interferon-γ released from cells before or after transduction. However there are significant differences between nil cells and control (C) or transduced (TD) cells (Nil cells are T cells incubated alone, control cells are untransduced or transduced cells incubated with irradiated 4T1 tumor cells).

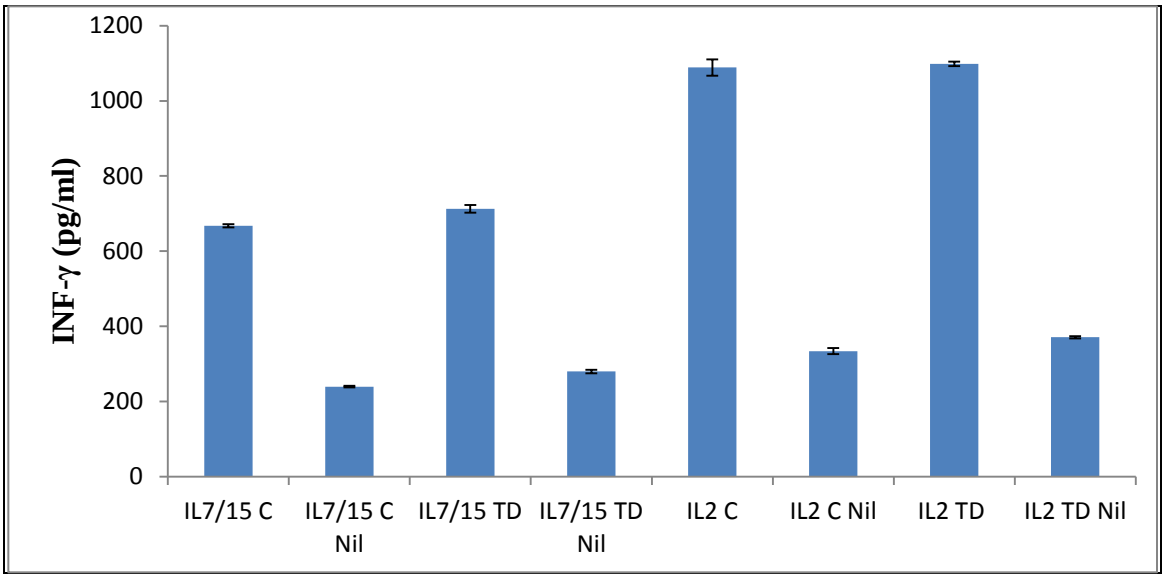

Figure 45 the production of interferon γ protein from transduced and untransduced cells.
Nil is stated for cells that were incubated alone. Other cells were incubated with 4T1 tumor cells to stimulate cell to release interferon γ in their supernatant. No significant differences ($p<0.05$) were observed before and after transduction for both cell groups.

5.2.2.6.4. Cell phenotype before and after T cells transduction

Cell phenotype was tested by flow cytometry before and after transduction to investigate if there is any effect of the transduction on cell phenotype. On day 3 post transduction (MOI=1), cells were double stained for either CD8/CD69 or CD8/CD62L. CD8 is the marker for cytotoxic T cells, CD69 is the marker for activated T cells and CD62L is also called L-selectin acts as a "homing receptor" for T lymphocytes to enter secondary lymphoid tissues via high endothelial venules. IL7/15 cells showed higher population of activated cytotoxic T cells than IL2 cells. No significant differences ($p<0.05$) between transduced and untransduced cells in the % of CD8/CD69 or CD8/CD62L populations was observed (figure 46).

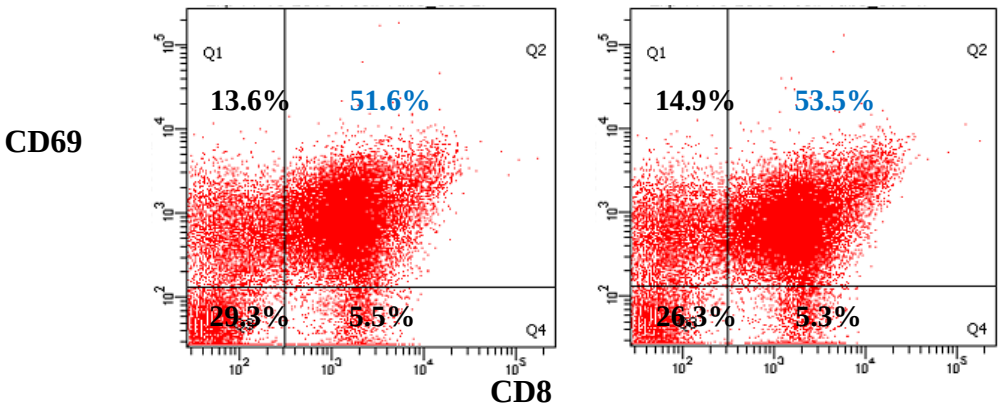

Un transduced IL7/15 cells **Transduced IL7/15 cells**
stained for CD8/CD69

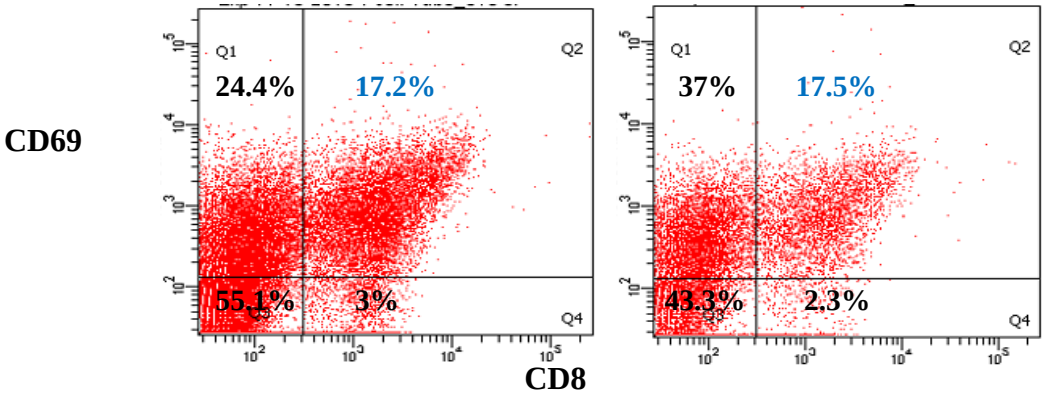

Un transduced IL2 cells **Transduced IL2 cells**
Stained for CD8/CD69

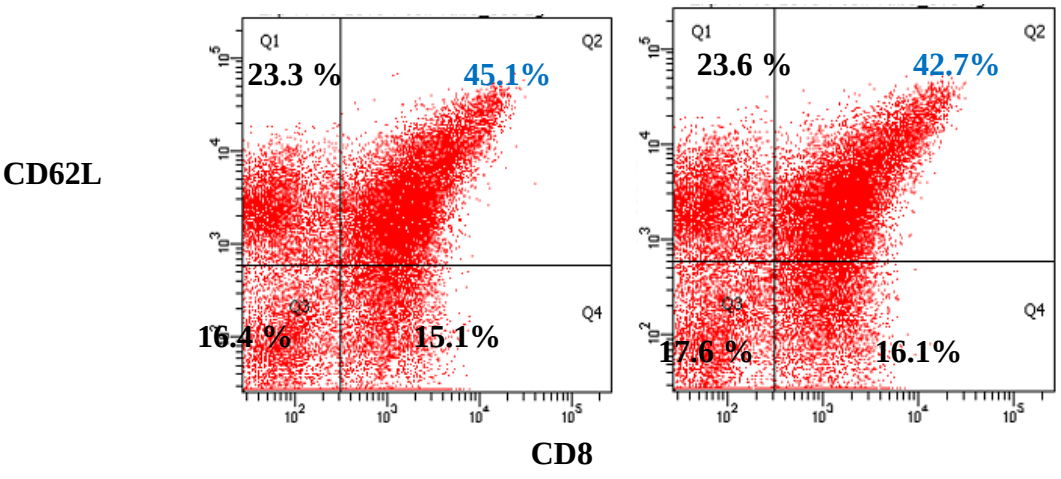

Un transduced IL7/15 cells **Transduced IL7/15 cells**
stained for CD8/CD62L

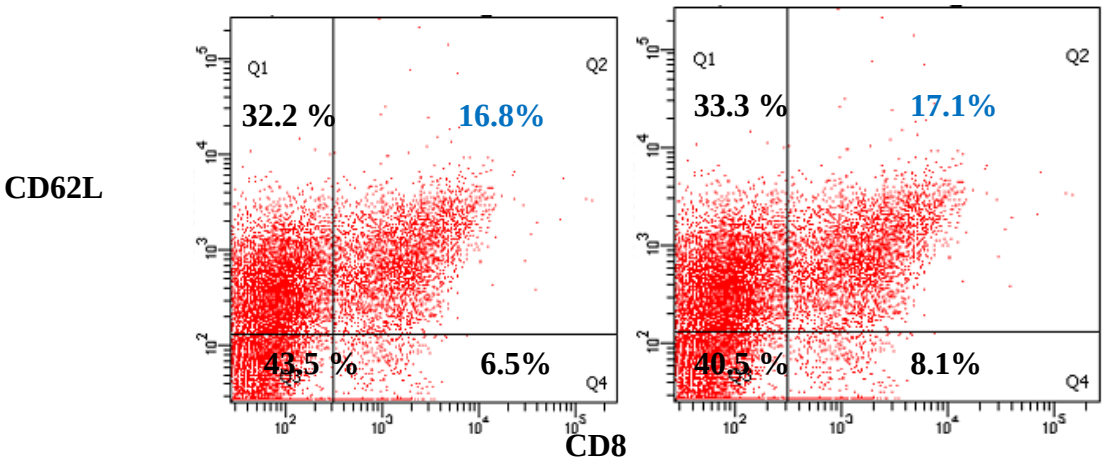

Un transduced IL2 cells **Transduced IL2 cells**
Stained for CD8/CD62L

Figure 46 flow cytometry of IL2 and IL7/15 cells phenotype before and after transduction stained for CD8/CD69 or CD8/CD62L. No significant difference between transduced and untransduced cells for both cell groups (the % population of positive staining for CD8/CD69 or CD8/CD62L indicated in blue color).

5.2.2.6.5. [^{124}I] FIAU uptake by T lymphocytes

To test the HSV1TK activity, transduced T cells (at MOI of 1 at day 3 post transduction) were incubated for 1,4, and 18 hours with [^{124}I]-FIAU at activity of 1µci/ml. Figure 45 showed the uptake result. Transduced Jurkat cells were test along with transduced T cells. The uptake of IL2 and IL7/15 cells looks comparable but less than transduced Jurkat cells. The reason is that the transduction efficiency of Jurkat cells is 100% as they were incubated with Blasticidin for selection more than one month as described previously (they are 100% transduced). While the transduction efficiency of T cells is lower than 40% compared to Jurkat cells as demonstrated in the uptake result (figure 47). The HSV1TK protein concentration was assessed after ^{124}I [FIAU] uptake by lysate cells and calculate the total protein concentration using protein assay kit as described previously. Figure 48 showed the result, Jurkat has a higher concentration than transduced T cells.

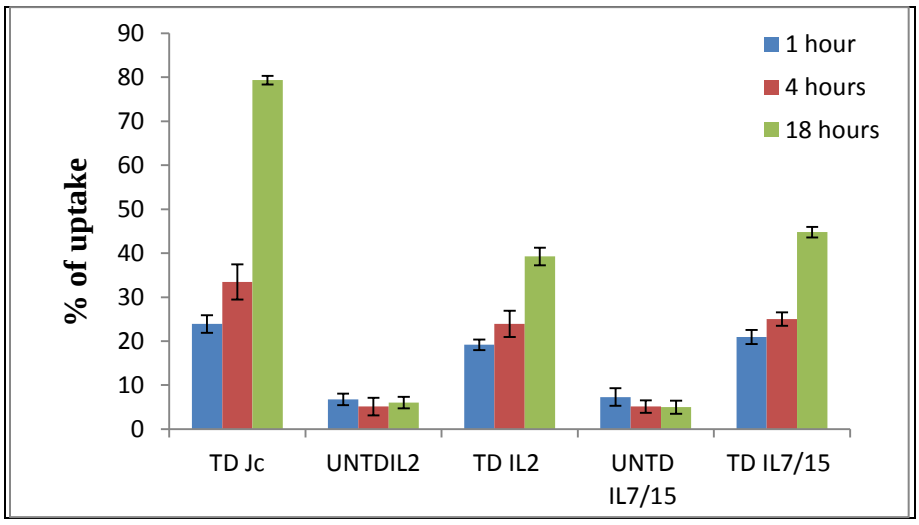

Figure 47 the % uptake of [^{124}I] FIAU by transduced T cells along with stable transduced jurkat cells. the transduction effecency of Jurkat cells is 100 % while T cells compared with Jurkat cells shwoed less the 40% of cells are transduced.

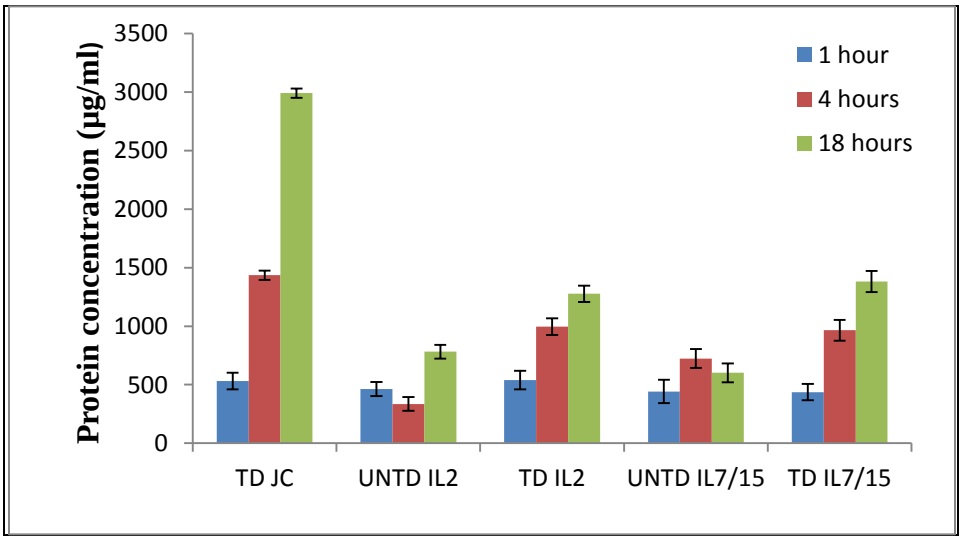

Figure 48 transduced cells protein (total cell protein including HSV1TK) concentration post [^{124}I] FIAU uptake. Jurkat cells (TDJC) showed higher protein concentration than T cells especially at 18 hours. There is significant differences ($p<0.05$) between protein concentration of Jurkat compared to T cells at 18 hours.

5.2.2.6.6 Biodistribution study

Transduced T cells were labeled with DiR and injected into 12 animals bearing 4T1 tumor (6 for IL2 cells and 6 for IL7/15). Another two groups of animals (4 in each) were injected with DiR labeled T cells to be used as controls for PET imaging and biodistribution study. Fluorescent and PET imaging were carried out for two weeks. Animals were dissected for biodistribution study on day 3 and day 10 post ^{124}I [FIAU] (i.v. injections at activity of 200-300 µci / animal). All tissues were taken for counting by gamma counting system. On day 3 both IL2 and IL7/15 cells showed similar % injected dose/tissue (%ID/tissue); spleen was the highest then liver, lymph nodes, tumor, and bone/bone marrow (femur + sternum) (figure 49 panel A). The DiR animal groups were dissected for counting (panels B and C). In both DiR groups (IL2 or IL7/15) % ID/tissue was very low compared to transduced (TD) IL2 or IL7/15 groups. This was expected, because DiR groups are animals were injected with untransduced DiR cell.

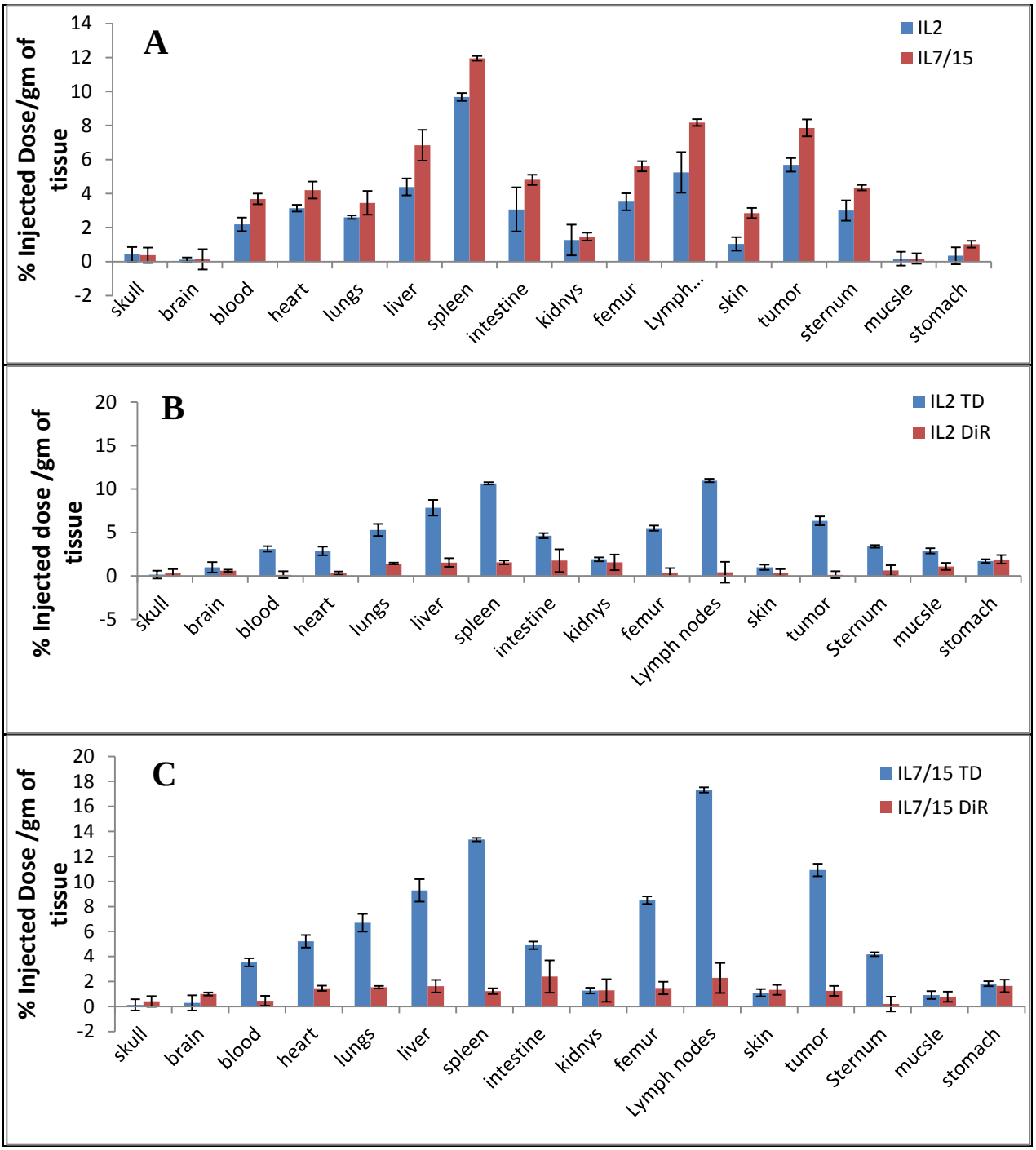

Figure 49 biodistribution study of transduced IL2 and IL7/15 animals on day 3 post ^{124}I [FIAU] injections (panel A). Both groups show similar %ID/tissue in all tissues. Panel B and C both groups were compared to DiR group. There are significant differences between TD groups and DiR groups ($p < 0.05$) in %ID/tissue in all tissues. Values expressed as %ID/gm ± SEM (n=3).

5.2.2.6.7 Detection of HSV1TK at different organs by western blot

To confirm the localization of transduced T cells at tumor site and other organs as shown in the Biodistribution study, western blot was performed to detect HSV1TK enzyme as shown in figure 50.

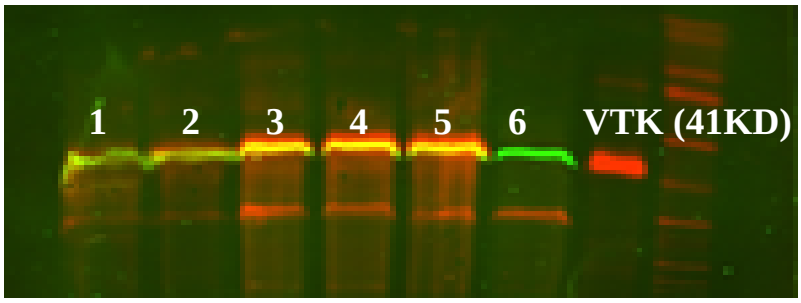

Figure 50 the western blot result of organs post transduced T cell injections.
1= lymph nodes, 2= 4T1 tumor, 3= lungs, 4= liver, 5= spleen and 6= control tumor (from animals not injected with untransduced T cell). HSV1TK enzyme is clearly shown at these organs beside the tumor which is consistent with the fluorescent data and Biodistribution study result. (green color is Beta Actin, and red is Viral Thymidin Kinase (VTK))

5.2.2.6.8 4T1 tumor metastasis and T cells trafficking study.

Our objective from this study is to compare the trafficking pattern of T cells to the primary tumors versus tumor metastasis. As explained previously, 4T1 tumor cells were transduced successfully with HSV1tk RG and implanted in number of animals at the abdominal mammary fat pad or in the right flank of the animal. Unfortunately tumors in the fat mammary pad did not grow well compared to untransduced cells implanted as a control into the left flank of the animals and most of the tumor was necrotic. Tumor volume measurements (figure 51) showed that fat mammary pad tumors (transduced 4T1 cells) did not grow well compared to the control tumor in the left flank of the animal consequently, no metastases were detected in PET imaging post [^{124}I] FIAU injections in the third and fourth weeks post tumor implantation. On the fourth week post tumor implantation and post 24 hours of [^{124}I] FIAU injections, Biodistribution study was conducted as shown in figure 52 (A and B). As explained before the activity at each organ expressed

in %ID/gm of tissue. Intestine showed the highest %ID/gm then liver and stomach due to the clearance of [^{124}I] FIAU from the body. Only the right flank tumor showed higher %ID/gm compared to the wild type tumor (left flank tumor) (figure 52 A) and also the mammary fat pad tumors showed about 2% of %ID/gm may some tumor cells are alive and still express HSV1TK protein (figure 52 B).

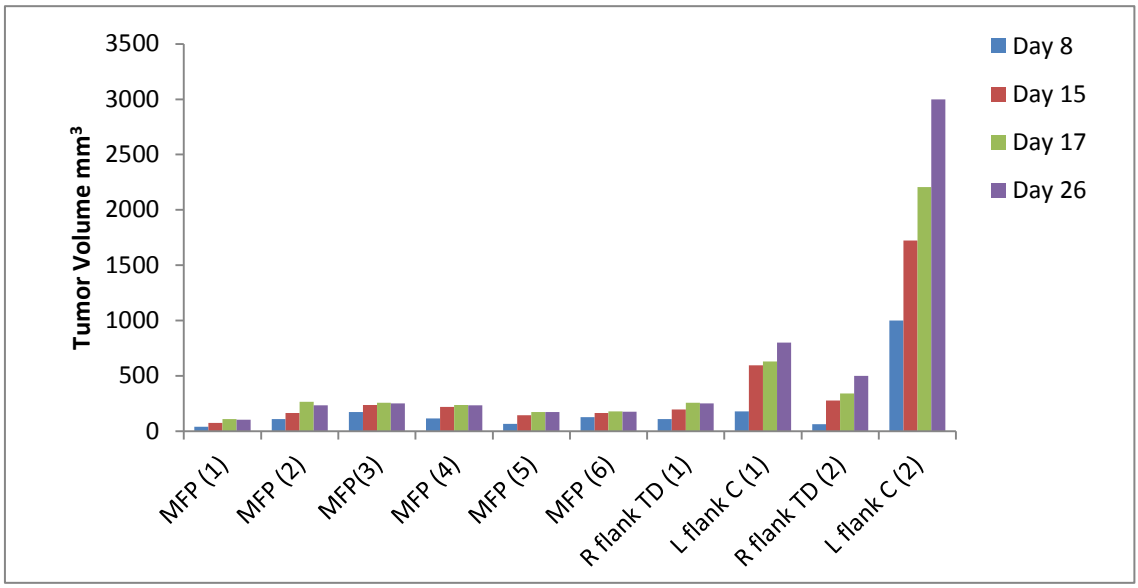

Figure 51 tumor volume measurements at different time post transduced and untransduced 4T1 tumor implantation. Abdominal mammary fat pad (MFP) did not grow
Well compared to left and right flank tumors.

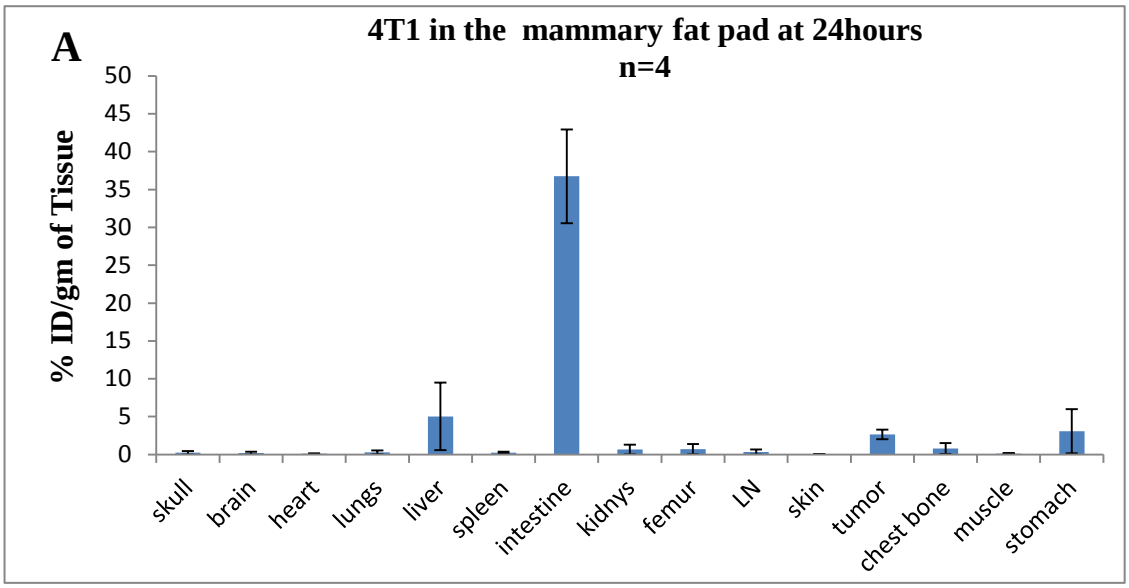

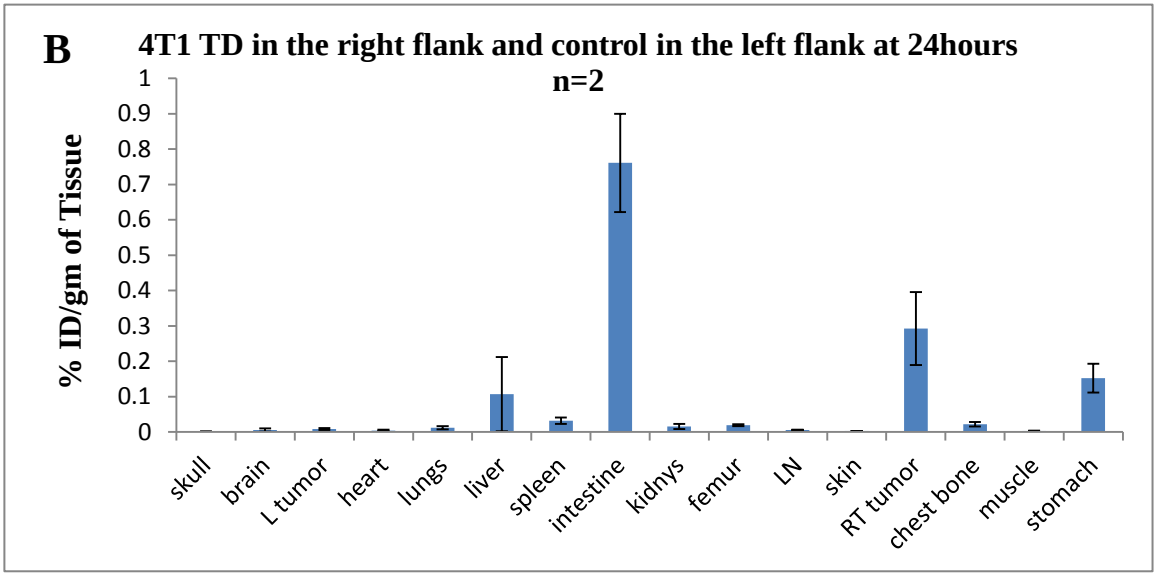

Figure 52 Biodistribution studies at 24 hours post ^{124}I FIAU injections. Panel A Biodistribution study from animals that had MFT tumors in the abdominal region. High % ID/gm was detected at the intestine, liver, stomach and tumor. Panel B Biodistribution study from animals implanted with flank tumors. The right flank tumor (transduced tumor) showed higher %ID/gm than the left flank tumor (wild type tumor). Values expressed in %ID± SEM.

Along with the Biodistribution study, western blot was performed from tumor, spleen, liver, lungs, brain and lymph nodes. The result (figure 53) showed HSV1TK protein only in the tumor

tissues and not in the other tissues, indicating, no TK 4T1 (transduced 4T1) cells localized at these organs.

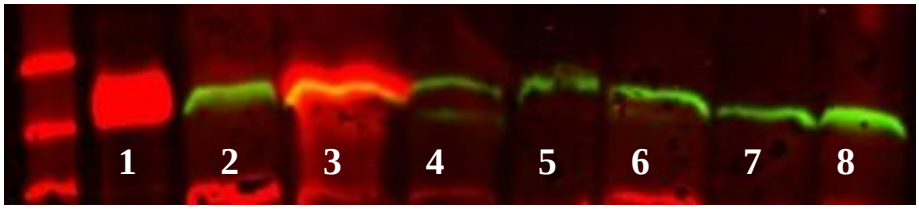

Figure 53 western blot result of tissues after 4 weeks of transduced 4T1 tumor implantation in the abdominal mammary fat pad. 1 is the purified HSV1TK protein, 2 is wild type 4T1 tumor, 3 is transduced 4T1 tumor, 4 to 8 are lungs, brain, lymph nodes, liver and spleen.

Chapter Six:Discussions

This study demonstrates two different labeling methods to monitor T lymphocytes that are sensitized to 4T1 breast carcinoma tumor, then activated and expanded *in vitro* and adoptively transferred to recipient mice. First method is direct labeling with NIR probe (DiR) for optical imaging. Although the use of DiR as a labeling probe for *in vivo* studies in AIT is still in its initial experimental stages; several studies have been successfully applied DiR to label cells and gather useful information about cell migration and localization *in vivo* in mice and rats. Kalchenko et al [64] successfully used DiR to label human leukemia G2L cells, mouse T lymphocytes, and rat red blood cells for *in vivo* studies, Granto et al [65] also used DiR to label fibroblast cells to target ovarian cancer. In another study by Jing Ruan et al [66], used DiR to label embryonic stem cells to target gastric cancer and they found that this labeling technique has great potential in molecular imaging application to track cells *in vivo*. The properties of NIR-DiR as lipophilic dye make it ideal for staining cytoplasmic membrane. The conclusion of these different studies and other studies used DiR to label and track different cells showed that DiR had no significant influence on the biological properties of cells.

In this study we have used DiR to label *ex vivo* activated T lymphocytes grown in different cytokines (IL2 or IL7 and IL15) and monitor their migration and trafficking in vivo at different time points as shown in our results. Cell viability, proliferation and the production of interferon-γ cytokine were assessed before and after labeling with DiR. The results of these assays showed that DiR is a compatible probe for cell labeling and in vivo monitoring and does not cause any changes in cell proliferation, viability or function.

Our *in vivo* studies showed that, the localization of 4T1 tumor specific T-lymphocytes occurred within 24 hours after intravenous administration of the activated cells. Although cells

grown in IL2 showed detectable signal starting from 2 hours (figure 21 A) while for cells grown in IL7/15, the signal was seen at 24 hours. Smironv and his colleagues [61] studied *in vivo* T cell trafficking by direct labeling with SPIONs for MRI imaging. Their results showed relatively lower signal in the spleen at 24 hours than at 48 hours. The signal at spleen and tumor then peaked at 72 hours. This result was consistent with our results, both IL2 and IL7/15 cells peaked at the tumor site at 72 hours. In another study done by Pittet and colleagues [67] it was shown that tumor specific cytotoxic T-lymphocytes directly labeled with [^{111}In]- Oxine (2.8 days half-life) for SPECT imaging, started localizing at the tumor site within the first 24 hours and continued to increase over time and were at peak when imaged at 72 hours post injection. Our results are consistent with these results; and moreover, the NIR signal from the T-cells at the tumor site persisted for nearly three weeks after labeling and administration. This demonstrates the suitability of this method for relatively long-term studies of cell trafficking in animal models of disease.

To confirm that the signal we observed at the tumor site is associated with DiR labeled T lymphocytes, cell lysate was prepared using freezing and thawing protocol following viability test to ensure all cells were lysed, then cell lysate was injected i.v. in number of animals at the same experiment viable cells were also injected i.v. to another group of animals. MSFI was carried out at different time points; the result showed that no signal was detected at the tumor site in the animal group injected with cell lysate. This confirms two important points: first the specificity and persistence of DiR as labeling probe for T cells, second, the specificity of viable 4T1 specific T cells to localize at the tumor site. Moreover, to test 4T1 specific T cells specificity toward 4T1 tumor, Meth A tumor was used as control tumor and from our results no localization of 4T1 specific T cells was observed at Meth A tumor. This specificity has been shown in a number of

studies that used different cytokines to activate *ex vivo* T cells isolated from tumor or draining lymph nodes (DLN) then adoptively transferred to tumor bearing hosts which cause regression of the tumor over specific period of time [68]. In our studies we used DLN T cells activated in Bryostatin 1 and Ionomycin (B/I) for 18 hours then grown in different cytokines (IL2 alone or combination of IL7 and IL15) for 10 to 12 days. This activation method has been shown by Esther Cha et al [26] for AIT in 4T1 breast tumor and by Hanh et al [23] for AIT in B16 melanoma tumor and their results showed significant regression of tumor depending on adoptively transferred cell number. Bryostatin 1 selectively activates protein kinase C and Ionomycin increases intracellular calcium with both mimicking cell signaling through CD3 T cell receptor (TCR) and leading to activation and proliferation of T cells. Chin et al [69] has shown that tumor sensitized draining lymph nodes (DLN) cells activated *ex vivo* with B/I are capable of inducing antigen-specific regression in murine mammary tumors. The same group demonstrated that B/I selectively stimulates and activates T cells expressing low levels of lymph node homing receptor (L-selectin^{low}) or (CD62L^{low}) which is a marker associated with sensitized T cells and promote their trafficking to other locations [70].

We also observed that the labeled T-cells home into lymphoid organs such as bone marrow and spleen, from *ex vivo* imaging of dissected organs. In order to examine whether these labeled T-cells are capable of moving out of these compartments and home into a tumor site at a subsequent tumor challenge, in one set of experiments, we first injected the labeled 4T1 specific T-cells in non-tumor bearing mice. One week later, these animals were imaged just before and then after the 4T1 tumor cells were implanted. DiR labeled 4T1 specific T-cells were detected in the tumor cell injection site as early as 2 hours after tumor cell implantation. The signal at the

tumor site persisted for another two weeks, confirming that the labeled T-cells can move out of the lymphoid organs to the site of a fresh antigen challenge.

Labeling of T-cells with near-infra red (NIR) fluorescent dyes for AIT has been reported in a few recently published studies. Du and coworkers [71] investigated the trafficking of DiR labeled human cytokine-induced killer (CIK) cells and cytotoxic T lymphocytes (CTLs) in a nude mouse model of orthotopic gastric carcinoma. In their study, the fluorescent signal peaked at 48 hours and was observed at the tumor site up to two weeks after infusion. The cell proliferation of labeled cells was comparable to unlabeled cells, similar to our observations. Moreover, after labeling the T-cells with a range of DiR concentrations (3.5, 14, 56, 224 and 320 μg/ml), we tested the cell viability using two different methods to ensure good cell tolerance to the dye before moving to the *in vivo* studies. T-cell function was also tested by measuring IFN-γ release in response to tumor antigen, and our results showed no significant detrimental effect of the labeling probe on cell proliferation, viability or function. Also, this allowed us to use a high DiR concentration (320 μg/ml) in the labeling solution. Our study also demonstrates signal persistence in the labeled T-cells even 3 weeks post labeling under the *in vivo* conditions of living mice.

The *in vivo* biodistribution of the labeled T-lymphocytes, in this study, was consistent with other studies. The signal was detected in lungs, spleen, liver, bone marrow and was observed at the tumor site at 24 hours and remained stable for up to 21 days when the labeled cells were infused into mice bearing established 4T1 breast carcinoma tumors. To ascertain whether the source of signal around the tumor was coming from labeled T-cells, double staining of tumor with CD69 (T cell activation marker) and F4/80 (macrophage marker), was performed. The confocal microscopy images revealed presence of activated T cells only in sections from mice bearing 4T1 tumor injected with *ex vivo* activated T cells and not in tumor sections from control 4T1 bearing

mice. On the other hand, the presence of macrophages was observed in tumor sections from both groups of animals as expected. Moreover, flow cytometry method was used to investigate whether DiR labeled T cells were engulfed *in vivo* by macrophages or DiR transferred to other immune cells. The result showed that no connection between DiR and macrophages or other immune cells, representing that DiR specifically labeled *ex vivo* activated T cells and the signal we detected is linked to only DiR labeled T cells.

In conclusion, this method shows that, labeling of 4T1 specific T lymphocytes with DiR, a NIR fluorescent cell membrane marker, provides an easy to use, stable and convenient tool for *in vivo* imaging of T-lymphocytes whilst retaining their inherent function. Use of DiR or similar cell membrane markers will be useful for investigating lymphocyte trafficking following their *ex vivo* sensitization, activation and proliferation. This method could also be used to non-invasively monitor the trafficking of other cell types.

The second method in this study was indirect labeling of T cells using PRG system (HSV1tk/ [^{124}I]-FIAU). Initially HSV1tk gene was used as therapeutic or suicide gene in the application of gene therapy studies for different types of cancer. The first approaches developed to introduce HSV1tk as therapeutic gene was by Moolten at al [72]. In this approached they used Ganciclovir (GCV) as substrate for HSV1tk gene which was transduced to a number of tumors. The result of phosphorylation showed cell toxcicity and death to transduced tumor cells. Since that time more studies were developed to image HSV1tk/GCV as reporter system for gene therapy [73]. The principle of *in vivo* imaging using HSV1tk as reporter gene for imaging was first demonstrated using ^{14}C 2- fluoro-5-methyl-1-ß-D- arabinofuranosylluracil ([^{14}C]-FMAU) by Saito et al in 1982 [74]. Later in 1995, Tjuvajev et al employed ([$^{123/124}$I]-FIAU) as reporter probe for HSV1-tk reporter gene for brain tumors [75]. Subsequently they demonstrated for the

first time that (HSV1tk/ [^{124}I]- FIAU) system is highly specific as noninvasive imaging system for clinical PET imaging due to its ability to image the distribution and the level of gene expression [76].

FIAU is a thymidine nucleoside has been used as an antiviral agent against hepatitis viruses [77]. FIAU has advantages of being imaged by different imaging modalities such as SPECT and PET due the ability of radiolabeling with $^{123/125/131}$ I or ^{124}I. Moreover, it is a specific substrate for viral thymidine kinase (VTK) enzyme that is expressed by HSV1tk gene, mammalian TK has no ability to phsphorylate FIAU. In comparison to other reporter probes such as FHBG or FHPG it has greater sensitivity and lower abdominal background radioactivity [78]. In this study we used HSV1tk/ [^{124}I]- FIAU system for the indirect labeling method of T cells due its mentioned advantages .

Our results demonstrate successful transduction in Jurkat, HEK293, 4T1 and T cells. This was confirmed by RT-PCR, western blot and uptake studies. One problem we faced is that the HSV1tk lentivirus we used showed some toxicity to T cells. This lead us to reduce the ratio of virus particles to cells number during the transduction; consequently the transduction efficiency was low and couldn't be detected by PET imaging. Toxicity of reporter gene imaging has been shown in a number of studies [79] and it is one of the limitations of this method. Another limitation is that, the level and persistence of gene expression was not enough to monitor our transduced T cells. Even though our ex vivo data showed successful transduction of T cells, but the scenario in vivo was different. Only few cells were transduced and the percentage of cells at each organ including tumor site was lower than 5% (this was shown in flow cytometry data) from the total 10 million cells were injected into each animal. Also our reporter gene promoter was an ubiquitin promoter which has limited amount of gene expression compared to other promoters

like cytomegalovirus (CMV) promoter. The rationale of using ubiquitin promoter is that it doesn't have a silencing problem with time, and our goal was to monitor T lymphocytes for long periods of time. However our biodistribution data showed results consistent with optical imaging data, the %ID/gm was higher at spleen, lungs, liver and tumor. Also Western blot assay from these tissues showed the presence of HSV1TK enzyme at each tissue.

In conclusions, to improve our reporter gene method, more effective HSV1tk lentivirus has to be constructed. The new constructed reporter gene should include GFP protein as a marker to accurately estimate cell transduction efficiency. This estimation method is more common and precise to know the exact percentage of transduced cells using flow cytometry or fluorescent microscopy. The promoter has to be chosen to result in a sufficient level of gene expression to successfully obtain good detection of signal for imaging.

The last objective in this study was to monitor the localization of T cells at 4T1 tumor metastases. To achieve this objective, 4T1 cells were successfully transduced with HSV1tk and implanted in number of animals at the abdominal mammary fat pad. PET imaging was performed at third and fourth week post tumor implantation, but no metastases were detected. From previous studies [80], abdominal mammary fat pad tumors more likely to spread in the abdominal region and do not show metastases at other regions of the animal body. Omar Rashid et al [80] has shown successful 4T1 tumor metastases model by implanting 4T1-luc2 (4T1 transduced tumor with luciferase reporter gene) orthotopically into chest mammary fat pad of Balb/C mice under direct vision. After 10 days resection of the primary tumor was done and the tumor metastases were detected by biolumencent imaging at lymph nodes by day 8 after tumor implantation then to the lungs by day 12. This method improves animal survival by decreasing the overall tumor burden, rapid increase in the metastases proliferation; decrease splenocyte

myeloid-derived suppressor cells (MDSCs) and increasing in CD8 and CD4 cells, suggesting potential improvement in the immunologic response against the tumor.

Chapter Seven Conclusion and Future Work

This study was done to develop multi-modality molecular imaging to monitor *in vivo* 4T1 specific T cells, for adoptive immune cell therapy. Direct and indirect labeling methods were employed and studied.

Direct labeling method using NIR DiR florescent probe showed good results compared to the indirect labeling method using (HSV1tk/ [^{124}I] FIAU) system.

The following points can be highlighted from the indirect labeling method:

- This method showed higher labeling efficiency (> 90%) compared to the indirect labeling method (≤ 30%).
- No transfer of the DiR to other cells in vivo and *ex vivo* was observed.
- DiR provides an easy to use, stable and convenient tool for *in vivo* imaging of T-lymphocytes whilst retaining their inherent function *in vivo* and *ex vivo*.
- In comparison to the indirect labeling method, direct labeling method showed valuable information about the trafficking and localizations of T cells grown in different cytokines
- Indirect labeling method is limited by targeting or delivery of the reporter gene (RG) to cell under transduction, integration, activation, amount or level of RG (transduction efficiency), RG expression and persistence over time.

Recommendations and future directions

As the direct labeling method with DiR provides valuable data about the trafficking and localizations of DiR labeled T cells without any changes in cell proliferation, viability, and function, it is worthwhile to label DiR with ^{124}I for PET imaging, or ^{131}I for SPECT imaging over prolonged period of time. To achieve this, the radio-iodination strategy of DiR has to be robust

and must resist dehalogination *in vivo.* Furthermore, the effect of radioactivity, per se, on cell proliferation and viability must be carefully addressed.

To improve the indirect labeling method, more effective HSV1tk lentivirus should be constructed with GFP to accurately estimate the transduction efficiency. Furthermore, the new construction should not be toxic at the adequate level for the gene to be detected in the *in vivo* imaging.

To develop successful breast cancer metastatic model, for the purpose of studying the migration pattern of labeled T cells to the metastases, it is highly recommended to follow Omer Rashid et al model [80]. This model as discussed previously improves animal survival by decreasing the overall tumor burden, rapid increase in the metastases proliferation; decrease splenocyte myeloid-derived suppressor cells (MDSCs) and increasing in CD8 and CD4 cells, suggesting potential improvement in the immunologic response against the tumor.

Appendix

Research publications and conference presentations

Youniss F, Gobalakrishnan S., Purnima Jose, Laura Graham, Collin Berry, Harry D Bear, Zweit J. (2011, 2012 and 2013) Multi-spectral fluorescence imaging of adoptive immune cell therapy using cell membrane probe (presented at the Massey Cancer retreat meetings with adding more data)

Youniss F, Gobalakrishnan S., Purnima Jose, Laura Graham, Collin Berry, Harry D Bear, Zweit J. (2013) Multi-spectral fluorescence imaging of adoptive immune cell therapy . J. Molecular Imaging (submitted)

Youniss F, Gobalakrishnan S., Purnima Jose, Laura Graham, Collin Berry, Harry D Bear, Zweit J. (2011) Multi-spectral fluorescence imaging of adoptive immune cell therapy using cell membrane probe .Journal of Nuclear Medicine.52:pp1557.2011(presented at the SNM-2011 meeting).

Georgi Gurli, Gobalakrishnan S., Youniss F, Ekaterine Goliadze , Li Wang, Sammuel P .R obison, Zweit (2012) Molecular Imaging of dendritic cell tracking in vivo in a murine prostate cancer model (presented to AUA 2012 meeting)

Youniss F, Ekaterine Goliadze, Gobalakrishnan Sundaresan, Li Wang, Georgi Gurili, Jamal Zweit. (2013) Non-invasive near-infrared imaging of dendritic cell trafficking in living mice. (presented to WMIC 2013 meeting as oral presentation)

Submitted predoctoral molecular imaging scholar program application to SNMMI 2012(not funded)

References

1. Michael O'Connor et al, Molecular breast imaging. *Expert Rev Anticancer Ther*. 2009 ; 9(8): 1073–1080.
2. www.breastcancer.org.
3. Andrew E Place et al. The microenvironment in breast cancer progression: biology and implications for treatment. *Breast Cancer Research.* .2011; 13:227-238.
4. Muaiad Kittaneh et al, Molecular profiling for breast cancer: comprehensive review. *Biomarkers Cancer*.2013; 5:61-69.
5. K.A.Cadoo et al, Biological subtypes of breast cancer: current concepts and implications for recurrence patterns. *QJ NUCLMED MOL IMAGING* 2013; 57:312-321.
6. Lin NU, Clinicopatholgic features,patterns of recurrence and survival amoung women with triple negative breast cancer in the national comprehensive cancer. *Cancer network.*2012; 118:5463-5472.
7. Den R et al. Pattern of metastatic spread in triple-negative breast cancer. *Breast cancer Res Treatment.* 2009; 115:423-428.
8. Ross JS et al. The HER-2 receptor and breast cancer: ten years of targeted anti-HER2 therapy and personalized medicine. *Oncologist*. 2009;14: 320-368
9. Salmon DJ et al. Use of chemotherapy plus monoclonal antibody against HER-2 for metastatic breast cancer that overexpress HER2. *NewEngl*. 2001;344:783-792.
10. Hudis CA et al Trastuzumab mechanism of action and use in clinical practice. *New Engl med*.2007;357:39-51.
11. Michail Lgnatiadis et al, Luminal breast cancer: from biology to treatment. *Nature*.2013;10:494-506.
12. Creighton C J et al. The molecular profile of Luminal B breast cancer.*Biologic*.2012; 6:289-297.
13. Valentina Guarner et al. The curability of breast cancer and the treatment of advanced disease. *European Journal of Nuclear Medicine and Molecular Imaging.*2004;31:149-161.
14. Stephen E Wright et al. Immunotherapy of breast cancer**.** *Expert Opin. Biol. Ther*. 2012; 12(4):479-490.
15. Shannon Puhalla et al, Hormonal therapy in breast cancer: A model disease for the personalization of cancer care. *Molecular oncology*. 2012:1-15.
16. William Coley et al. A commotion in the blood: life,deth,and the immune system.New work: Henry Holt.544pp.
17. Korngold R et al. Lethal graft-versus-host diseas after bone marrow transplantation across minor histocompatibility barrier in mice. Prevention by removing mature T cells from marrow. *Exp. Med*.1978; 148:1687-1698.
18. Bernhard H, et al. Adoptive transfer of autologous HER2-specific cytotoxic T lymphocytes for the treatment of HER2-overexpressing breast cancer. *Cancer Immunol Immunother*. 2008;57: 271-280.
19. Alan B. Frey, Ngozi Monu. Signaling defects in anti-tumor T cells. *Immunological reviews*. 2008; 222: 192-205.
20. Robert A Weinberg. The biology of cancer. *Published by Garland Science, Taylor& Francis Group, LLC UK* 2007.
21. Janeway's. Immunobiology. *Garland Science*, 2012.

22. Mark E Dudly and Steven A. Rosenberg. Adoptive-cell-transfer therapy for the treatment of patient with cancer. *Nature review*.2003; 3:666-675.
23. Hahn K.Le. Laura Graham. Catriona H.T. Miller. Maciej Kmieciak. Massoud H. Manjili. Harry Douglas Bear. Incubation of antigen-sensitized T lymphocytes activated with bryostatin 1 + ionomycin in IL-7+IL-15 increase yield of cells capable of inducing regression of melanoma metastases compared to culture in IL-2. *Cancer Immunol Immunother*.2009; 58:1565-1576.
24. Davies C et al. Relevance of breast cancer hormone receptors and other factors. *Lancet*. 2011; 378;771-784.
25. Fisher B et al. Reanalysis and results after 12years of follow-up in a randomized clinical trial in the treatment of breast cancer. N Engl J Med 1995;333:1456-1461.
26. Esther Cha. Laura Graham. Masoud H. Manjili. Harry D.Bear. IL-7+ IL-15 are superior to IL-2 for ex vivo expansion of 4T1 mammary carcinoma-specific T cells with greater efficacy against tumor in vivo. *Breast Cancer Res Treat*.2009.
27. C. Yee, J.A. Thompson, D. Byrd, S,R, Riddell, P. Roche, E. Celis, P.D.Greenberg. Adoptive T cell therapy using antigen- specific CD 8^+ T cell clones for treatment of patients with metastatic melanoma: in vivo persistence, migration, and antitumor effect of transferred T cells. *Mayo Clinic*. 2002; 99: 16168-16173.
28. Morgan RA, et al. Cancer regression in patients after transfer of genetically engineered lymphocytes. *Science*. 2006; 314: 126-129.
29. Qin Wang, Moshe Ornstein and Howard L Kaufman. Imaging the immune response to monitor tumor immunotherapy. *Expert Rev.Vaccines*. 2009; 8(10): 1427-1437.
30. Christoph Domscke et al. Long-term survival after adoptive bone marrow T cell therapy of adavanced metastasized breast cancer: follow-up analysis of a clinical pilot trial. *Cancer Immunol Immunother*. 2013; 62: 1053-1060.
31. Stefan Stefanovic et al. Adoptive immunotherapy of metastatic breast cancer: present and future. *Cancer Metastasis Rev*. 2013;13:9452-9456.
32. Michel Modo et al. Noninvasive imaging of transplanted cells. *Curr Opin Organ Transplant* . 2008,13:654–658.
33. Mankoff DA. A definition of molecular imaging. *J. Nucl. Med* 2007;48:18N, 21N.
34. Hang Hong, Yunan Yang, Yin Zhang and Weibo Cai. Non-Invasive cell tracking in cancer and cancer therapy. *Curr Top Med Chem*. 2010; 10 (12): 1237-1248.
35. Marybeth A. Pysz, et al. Molecular Imaging: Current Status and Emerging Strategies. *Clin Radiol*. 2010; 65(7): 500–516.
36. Adrian Taruttise et al.Fast Multispectral Optoacoustic Tomography (MSOT) for Dynamic Imaging of Pharmacokinetics and Biodistribution in Multiple Organs. Plos One. 2012;7:30491-30496.
37. M. Srinivas et al. Imaging of cellular therapies. *Advanced Drug Delivery Reviews*. 2010; 62:1080–1093.
38. Giovannni Lucignani et al. Molecular imaging of cell-mediated cancer immunotherapy. *Trends in Biotechnology*. 2006; 24: 410-418.
39. Elizabeth J Akins and Purnima Dubey. Noninvasive imaging of cell- mediated therapy for treatment of cancer. *Journal of Nuclear Medicine*. 2008; 49: 180-195.
40. Inna Serganova et al. Reporter gene imaging: potential impact on therapy. Nuclear Medicine and Biology.2005; 32: 763-780.

41. Christopher R Parich et al. Fluorscent dyes for lymphocyte migration and proliferation studies. *Immunology and Cell biology*.1999; 77:499-508.
42. Hirotatsu Kojima et al . Development of near-infrared fluorescent probes for in vivo imaging. *The pharmaceutical society of Japan* 2008;128:1653-1663.
43. Giovannni Lucignani et al. Molecular imaging of cell-mediated cancer immunotherapy. *Trends in Biotechnology*. 2006; 24: 410-418.
44. Vasilis Ntziachristos et al. Fluorscence imaging with near-infrared light: new technological advances that enable in vivo molecular imaging. Eur Radiol. 2003; 13: 195-208.
45. Foster AE et al. In vivo fluorescent optical imaging of cytotoxic T lymphocyte migration using IRDye800CW near-infrared dye. *Appl. Opt* 2008; 47:5944–5952.
46. Inna Serganova et al. Human receptor genes: potential use in clinical studies. *Nuclear Medicine and Biology.* 2007;34:791-807.
47. Dw Townsend. Physical principles and technology of clinical PET Imaging. *Ann Acad Med Singapore* 2004;33:133-145.
48. Simon R Cherry Jamwes A Sorenson. Physics in nuclear medicine, third edition. *Elsevier Science* 2003.
49. Swirski FK, et al. A near-infrared cell tracker reagent for multiscopic in vivo imaging and quantification of leukocyte immune responses. *PLoS ONE* 2007; 2: 1075.
50. Mandl S, et al.. Understanding immune cell trafficking patterns via in vivo bioluminescence imaging. J. Cell. *Biochem. Suppl* 2002; 39:239–248.
51. Jonathan Hardy, et al. Bioluminescence imaging of lymphocyte trafficking in vivo. *Experimental Hematology*. 2001; 29: 1353-1360.
52. Matthias T Stephan et al. Theraputic cell engineering with surface-conjugated synthetic nanoparticles. *Nature medicine*. 2010; 16:1035-1041.
53. Mathew L.Thakur, Antony W.et al. Indium-111-Labeled cellular blood components: mechanism of labeling and Intracellular location in human neutrophils. *J Nucl Med* 1977; 18: 1020-1024.
54. Elizabeth J. Read, Andrew M. Keenan, et al. In vivo traffic of Indium-111-oxine labeled human lymphocytes collected by automated apheresis. J Nucl Med 1990; 31:999-1006.
55. Simon R. Cherry, James A. Sorenson, Michael E. Phelps. Physics in nuclear medicine, third edition. *Elsevier Science* USA 2003.
56. Carlo Botti, Donatella RM. Negri, Ettore Seregni et al. Comparison of radiolabeled human activated T lymphocytes. Eur J Nucl Med 1997; 24: 497-504.
57. Adona N et al. Ex vivo cell labeling with ^{64}Cu- pyruvaledhyde-bis(N^4-methylthiosemicarbazone) for imaging cell trafficking in mice with positron-emission tomography. *Proc Natl Acad Sci.* 2002; 99: 3030-3035.
58. Dubey,P et al. Quantitative imaging of the T cell antitumor response by positron-emission tomography. *Proc. Natl. Acad.Sci*. 2003;100: 1232-1237.
59. Su,H. et al. Quantitation of cell number by a positron emission tomography reporter gene strategy. *Mol.Imaging* Biol. 2004; 6: 139-148.
60. Agger R, Petersen MS, Petersen CC, et al. T cell homing to tumors detected by 3D-coordinated positron emission tomography and magnetic resonance imaging. *J Immunother*. 2007;30:29–39.

61. Smirnov P, Lavergne E, Gazeau F, et al. In vivo cellular imaging of lymphocyte trafficking by MRI: a tumor model approach to cell-based anticancer therapy. *Magn Reson Med*. 2006;56:498–508.
62. Elazabeth J. Noninvasive imaging of cell-mediated therapy for treatment of cancer. J Nucl Med. 2008; 49:180-195.
63. Sumitaka Hasegawa et al. Molecular MR imaging of cancer therapy: Ferritin transgene reporter takes the stage. *Magn Reson Med Sci*. 2010; 9: 37-47.
64. Kalchenko V et al. Use of lipophilic near-infrared dye in whole-body optical imaging of hematopoitic cell homing. *J Biomed Opt*.2006; 11:050507.
65. Granto D et al. In vivo imaging of the systemic recruitment of fibroblasts to the angiogenic rim of ovarian carcinoma tumors. *Cancer Res*.2007; 67:9180-9189.
66. Jing Ruan et al. DiR-labeled embryonic stem cells for targeting imaging of in vivo gastric cancer cells. *Theranostics* 2012;2: 618-628.
67. Pittet MJ, Grimm J, Berger CR, et al. In vivo imaging of T cell delivery to tumors after adoptive transfer therapy. *Proc Natl Acad Sci U S A*. 2007;104:12457-61.
68. Johanna K. et al. Adoptive transfer of HER2/neu-specific T cells expanded with alternating gamma chain cytokines mediate tumor regression when combined with the depletion of myeloid-derived suppressor cells. Cancer *Immunol Immunother* 2008.
69. Cynthia S Chin et al. Bryostatin /Ionomycin-Activated T cells mediated regression of established tumors. *Jurnal of surgical research* 2001;98: 108-115.
70. Tuttle T M et al Activation and growth of murine tumor-specific T-cells have in vivo activity with bryostatin 1.*Cancer Res,*1992;52:548.
71. Du X, Wang X, Ning N, et al. Dynamic tracing of immune cells in an orthotopic gastric carcinoma mouse model using near-infrared fluorescence live imaging. *Exp Ther Med*. 2012;4:221-25.
72. Moolten FL et al. Curability of tumors bearing herpes thymidine kinase genes transferred by retrovirus vectors. *J Natl Cancer Inst*.1990;82:297-300.
73. Ronald Blasberg. PET imaging of gene expression. *European Journal of cancer* 2002;38:2137-2146.
74. Saito Y et al. Quantitative autoradiographic mapping of herpes simplex virus encephalitis with radiolabeled antiviral drug. *Sciences.* 1982;217:1151-1153.
75. Juri G Tajuvajev et al. Imaging the expression of Transfected Genes in vivo. *American Association for cancer research.* 1995;55:6126-6132.
76. Juri G Tjuvajev. Imaging virus thymidine kinase transfer and expression by positron emission tomography. *Cancer research*. 1998;58:4333-4341.
77. Andreas Jacobs et al. Quantitative Kinetics of [^{124}I] -FIAU in Cat and Man. *J Nucl Med* 2001; 42:467–475.
78. Juri Gelovani Tajuvajev et al. Comparison of radiolabeled nucleoside probes (FIAU,FHBG,and FHPG) for PET imaging of HSV1-tk gene expression. *The Journal of Nuclear Medicine*.2002;43:1072-1083.
79. Kenneth Lundstrom. Latest development in viral vectors for gene therapy. *Trends in biotechnology*. 2003; 21:117-122
80. Omar M Rashid et al. Resection of the primary tumor improves survival in metastatic breast cancer by reducing overall tumor burden. *Surgery* .2013; 153:771-778.

Vita

Fatma Mousa Youniss was born on May 21th, 1973, in Elmarj, Libya, and she is a Libyan citizen. She graduated from Elhurya High School, Elmarj, Libya in 1990. She received her Bachelor degree in Medical Technology from University of Derna, Libya in 1994. Subsequently she worked as teaching assistant (TI) in the same university up to December 2000. In January 2001 she was awarded scholarship from the high education ministry of Libya to study for master degree in Medical Physics in Malaysia. She obtained her master in 2004. From January 2004 to July 2008 she was working as faculty member in the University of Derna teaching undergraduate students in Medical Technology School/ Radiology department. In 2008 she was awarded another scholarship for PhD in Medical Physics in USA. In August, 2009, she entered graduate school at Virginia Commonwealth University.